Bulletin 134

New Mexico Bureau of Mines & Mineral Resources

A DIVISION OF
NEW MEXICO INSTITUTE OF MINING & TECHNOLOGY

Field excursions to the Jemez Mountains, New Mexico

by Stephen Self[1], Grant Heiken[2], Martha L. Sykes1, Kenneth Wohletz[2], Richard V. Fisher', and David P. Dethier[4]

'School of Ocean and Earth Science and Technology, University of Hawaii (Manoa), Honolulu, HI 96822
'Earth and Environmental Sciences Division, Los Alamos National Laboratory, Los Alamos, NM 87454
'Department of Geological Sciences, University of California, Santa Barbara, CA 93106
'Department of Geology, Williams College, Williamstown, MA 01267

SOCORRO 1996

Original Printing

Published by Authority of State of New Mexico, NMSA 1953 Sec. 63-1-4 Printed by University of New Mexico Printing Services, April 1996

Available from New Mexico Bureau of Mines & Mineral Resources, Socorro, NM 87801

Preface

This bulletin has been compiled from the field guides for two complementary and somewhat unconventional trips offered as part of the International Association of Volcanology and Chemistry of the Earth's Interior (IAVCEI) General Assembly in Santa Fe, New Mexico, in June, 1989. One, a Field Workshop of the IAVCEI Commission on Explosive Volcanism, was pre-assembly trip 11WA to study ignimbrites and calderas of the Jemez Mountains, New Mexico, and the San Juan Mountains, Colorado. Only the New Mexico part of the original Field Workshop Handbook has been rewritten and updated here for this publication. The original Workshop Handbook was not prepared as a standard geologic road guide but more as a series of volcanologic explanations of individual outcrops, showing how each contributes to the overall picture of ignimbrite eruption and caldera evolution in the Jemez Mountains. Some minor stop omissions, stop sequence changes, and simplifications from the original 11WA Workshop Handbook have been made in this version to improve the field guide's general appeal.

The field guide for White Rock Canyon was prepared for a 1-day-long trip to look at maar volcanoes along the Rio Grande. It is an unusual trip in that travel is by rubber raft. There are no odometer readings or road signs—descriptions are linked to side canyons along the Rio Grande. If you have your own raft, kayak, or canoe and know how to use it, you are ready to take this trip, which begins at Otowi Bridge along NM-4 (a permit is required from the main office of San Ildefonso Pueblo) or from Buckman Crossing, which is reached from Santa Fe (no permit required). Most rafters continue through White Rock Canyon to the boat docks at Cochiti Reservoir, where you leave the river. Plan for a very long day or camp along the river overnight. If you want to take the trip and have no way to float down the river, several of the northern New Mexican rafting companies occasionally have float trips through White Rock Canyon.

On the raft trip, if you leave White Rock Canyon via the Frijoles (Upper Falls) trail, you are in Bandelier National Monument. Take no samples and pay an entry fee at Monument Headquarters (if someone is picking you up, they will have already paid the fee at the entrance).

A few points should be borne in mind when following these field guides. Both trips present some degree of physical challenge, as the rafting and scaling of ignimbrite cliffs, while not requiring special preparation or equipment, are perhaps a little more demanding than usual field trip routes. Weather is another consideration for these trips, especially in the higher elevations of the Jemez Mountains. Unless it is an exceptionally precipitation-free winter, snow and harsh weather conditions are likely to prevail between November and March at many of the stops in the multi-day field guide, and bad snow storms can close much of the area as late as May.

Access for the geologist on foot and/or by vehicle in the Jemez Mountains, which encompass a patchwork of Indian lands, private tracts, Department of Energy land, and National Forest and National Monument areas, is ever changing. Obtaining permission to enter these lands can be a frustrating experience. Virtually the whole of the center of the Valles caldera, including the resurgent block, is owned by the Baca Land and Cattle Company and has been off limits in recent years, especially to large groups (although sometimes permits for small parties can be obtained), which is why it is not visited in this guide. An exception is the forest access road to Sulphur Springs at the Springs area itself, which is again private land held by another individual, but permission to visit can usually be obtained by contacting the owner.

These two field trips represent, in markedly different ways, alternative approaches to understanding the geology of this remarkable volcanic region. Both will take the reader to parts of the Jemez Mountains rarely seen by geologists on regular road trips through the Valles caldera and its environs. If you follow these guides we urge you to make adequate preparations for the trips and to leave the Jemez Mountains and their natural and anthropological treasures in as good a state as you find them.

Grant

Heiken[1]

Stephen Self[2]

[1]Earth and Environmental Sciences
Division Los Alamos National Laboratory
Los Alamos, NM 87545

[2]Hawaii Center for Volcanology and Dept. of Geology and Geophysics
School of Ocean and Earth Science Technology
University of Hawaii (Manoa)
Honolulu, HI 96822

Contents

Part I: Field guide to the Bandelier Tuff and Valles caldera

ACKNOWLEDGMENTS 7
INTRODUCTION 7
JEMEZ MOUNTAINS STRATIGRAPHY 7
TECTONIC AND VOLCANIC HISTORY OF THE JEMEZ MOUNTAINS 8
TEWA GROUP VOLCANISM: THE BANDELIER TUFFS AND VALLES CALDERA 11
San Diego Canyon ignimbrites **11**
Lower (Otowi) Bandelier Tuff 12
Cerro Toledo Rhyolites and associated pyroclastic deposits **12**
Upper (Tshirege) Bandelier Tuff 13
Valles Grande Rhyolite and associated deposits **14**
GEOCHEMISTRY OF THE BANDELIER TUFF 14
FIELD GUIDE
DAY **1:** GENERAL CHARACTERISTICS OF THE BANDELIER IGNIMBRITES AND RELATED UNITS 17
Stop 1 Upper and lower Bandelier ignimbrite, near edge of outflow sheet, Otowi Mesa 17
Stop 2 Puye Formation—pre-Bandelier volcanism and sedimentation from the Tschicoma volcanic complex. 20
Stop 3 Upper Bandelier Tuff (Guaje) pumice-fall deposit and Bandelier ignimbrites 22
Stop 3A Pre-Bandelier high-silica rhyolite Plinian deposit at the top of the Puye Formation 24
Stop 4 Upper Bandelier Tuff surge deposits and Cerro Toledo pumice-fall deposits 25
Stop 5 Proximal upper Bandelier Tuff 28
Stop 5A Late upper Bandelier ignimbrite and ground-surge deposits 28
DAY 2: LOWER BANDELIER TUFF IN DISTAL AND PROXIMAL LOCATIONS AND PRODUCTS OF THE YOUNGEST ERUPTIONS (-0.3-02 MA) FROM THE VALLES CALDERA 29
Stop 6 Welded upper Bandelier ignimbrite 30
Stop 7 Lower Bandelier fall units, Cochiti Canyon 30
Stop 8 Intra-Plinian lower Bandelier ignimbrite and general character of ignimbrites, Cochiti Canyon 30
Stop 9 Lateral margin of upper Bandelier ignimbrite sheet near Cochiti Canyon 31
Stop 10 Proximal lower Bandelier ignimbrite, Cat Mesa 33
Stop 10A Vapor phase pipes in the upper Bandelier ignimbrite 34
Stop 11 Main section of El Cajete pumice deposits and Banco Bonito lava flow 35
Stop 12 Valles caldera overview 35
DAY 3: PROXIMAL FACIES OF BANDELIER IGNIMBRITES AND SAN DIEGO CANYON IGNIMBRITES 35
Stop 13 Caldera rim section (La Cueva) exposing four ignimbrites 36
Stop 14 San Diego Canyon ignimbrite and lower Bandelier Tuff 38
Stop 15A Soda Dam and Jemez fault zone 38
Stop 15 Battleship Rock ignimbrite 38
DAY 4: BANDELIER TUFF IN THE NORTHERN JEMEZ MOUNTAINS AND INTRACALDERA GEOLOGY 42
Stop 16 Pueblo Mesa, Canoñes 43
Stop 17 Upper Bandelier Plinian deposit 45
Stop 18 Welded lower Bandelier ignimbrite, Cebolla Canyon 46
Stop 19 Sulphur Springs and intracaldera geology 46
DAY 5: BANDELIER OUTFLOW SHEET AND BASALTS OF CERROS DEL RIO VOLCANIC FIELD 50
Stop 20 Topographic control of upper Bandelier ignimbrite and ash cloud surges, Ancho Canyon 51
Stop 21 Upper Bandelier Tuff interflow unit surges and possible secondary explosion deposits, Ancho Canyon wall 51
Stop 22 Lower Bandelier Tuff and upper Bandelier Tuff with basal pumice-rich flow units, Ancho Canyon 52
Stop 23 Frijoles Canyon 52
Stop 24 Frijoles Canyon: Topographic controls on upper Bandelier Tuff thickness and entrainment of surface lithic clasts 53
Stop 25 Thin Bandelier ignimbrite on basalt of western part of Cerros del Rio volcanic field 53
REFERENCES 54

Part II: Field guide to **the** maar volcanoes **of White Rock Canyon**

ACKNOWLEDGMENTS 56
INTRODUCTION 56
GEOLOGIC SETTING AND HISTORY OF THE RIO GRANDE RIFT 56
WHITE ROCK CANYON 60
HYDROLOGY OF WHITE ROCK CANYON AND EFFECTS ON ERUPTION PROCESSES 61
FIELD GUIDE 62
REACHING THE HEAD OF WHITE ROCK CANYON 62
Entering from the north 62
Entering from the east 62
Entering from the west 63
LA MESITA MAAR 63
Introduction 63
Stratigraphy 64
Description of the eruption sequence 65
Conclusions regarding the origin of La Mesita maar 66
BUCKMAN MAAR 67
BEGINNING OF FLOAT TRIP 67
MORTANDAD CANYON **67**
NORTH END OF SAGEBRUSH FLATS 68
SOUTHWEST SAGEBRUSH FLATS 68
CHINO MESA AND MONTOSO MAAR 68
CHAQUEHUI AND FRIJOLES CANYONS 68
Side trip to Bandelier National Monument 69
FRIJOLES CANYON TO Lummis AND ALAMO CANYONS **70** ALAMO CANYON TO SANCHEZ CANYON **70**
BETWEEN SANCHEZ CANYON AND Rio CHIQUITO **71**
BOAT RAMP, COCHITI RESERVOIR **71**
REFERENCES 71

Tables

Part I: Field guide to the Bandelier Tuff and Valles caldera

V1—Ages of stratigraphic units in the Jemez Mountains 12
V2—Representative major and trace element compositions of the Valles caldera 15
V3—Stops where stratigraphic units and features of the Jemez Mountains are visited. 18

Part II: Field guide to the maar volcanoes of White Rock Canyon

W1—Geochronology of volcanic events along the Rio Grande 60

Figures

Part I: Field guide to the Bandelier Tuff and Valles caldera

V1—Location map showing Jemez Mountains volcanic field and basins of the north-central Rio Grande rift 8
V2—a) Generalized geologic map of the Jemez Mountains and Rio Grande rift; b) simplified structure map of the Jemez Mountains 9, 10
V3—Chronostratigraphic chart of major units in the Jemez Mountains 11
V4—Standard schematic section through Bandelier Tuff 13
V5—Simplified map of distribution of the Bandelier Tuff 13
V6—A) Lava domes and flows of Cerro Toledo age; and B) lava domes and flows postdating Valles caldera 13
V7—Schematic cross section through the Valles caldera and Rio Grande rift 14
V8—Enrichment diagram for lower Bandelier Tuff and Bishop Tuff 16
V9—Typical incompatible element ratios for lower Bandelier Tuff high-silica rhyolite, upper Bandelier Tuff high-silica rhyolites, and dacite 16
V10—Stops for Jemez Mountains field guide 17
V11—Lower Bandelier Tuff stratigraphy and deposit characteristics 19
V12—Distribution of components in the Bandelier ignimbrites 20
V13—Downflow changes in number of flow units, lithic size, and crystal content in the lower and upper Bandelier ignimbrites of the eastern Jemez Mountains 21
V14—Measured section through upper Bandelier Tuff 22
V15—Map showing distribution of Puye Formation alluvial fan 23
V16—Profile through the Puye ignimbrite and associated pumice and ash falls showing changes in median grain size (MO) and sorting of deposits (0) 24
V17—Lower Bandelier Plinian deposit and ignimbrite at Copar pumice quarries 25
V18—Pumice-fall units of the lower Bandelier Plinian deposit at Copar pumice quarries 25
V19—Isopach and isopleth maps of selected lower Bandelier Plinian fall units. 26
V20—Plot of unit thickness versus the square root of isopleth area for Plinian and co-ignimbrite ashes 27
V21—Pumice-fall deposit near Copar pumice quarries 27
V22—Section of upper Bandelier Tuff 27
V23—Plot of wave height and wave length versus distance from vent for pyroclastic-surge bedforms from various pyroclastic deposits taken largely from the literature 28
V24—Section through upper Bandelier Tuff showing flow units, welding and vapor-phase alteration zones, and the three depositional packages 29
V25—Surge deposit between welded, thin flow units in upper part of upper Bandelier Tuff 29
V26—Lower Bandelier Plinian fall units B-E and base of lower Bandelier Tuff ignimbrite 30
V27—Left, section through lower Bandelier Plinian deposit and ignimbrite section; right, section through upper Bandelier ignimbrite 31
V28—Upper Bandelier ignimbrite flow units 32
V29—Left, schematic diagram of contact zone between upper Bandelier Tuff and Cochiti Formation; right, Nb content (ppm) of whole pumice clasts from upper Bandelier Tuff plotted against stratigraphic height for three locations 32
V30—View looking north-northwest from edge of Valles caldera wall 33
V31—Section through the lower Bandelier Tuff at Cat Mesa 34
V32—Proximal lithic breccias in the lower Bandelier Tuff 35
V33—Left, composite schematic section through lower Bandelier Tuff showing major zones; right, phases in the lower Bandelier Tuff eruption 37
V34—Pipes in the upper Bandelier Tuff 38
V35—El Cajete section showing unit designations 38
V36—Section through the El Cajete and Banco Bonito units **39**
V37—Sketch of view from Valle Grande 40
V38—Sketch of the caldera wall near La Cueva 40
V39—Grain size profile through 3 flow units of San Diego Canyon ignimbrite B 40
V40—Fall units A-F of the upper Bandelier Plinian deposit on the caldera wall near La Cueva **40**
V41—Section through upper Bandelier Plinian deposit 41
V42—Seven sections at intervals shown along western wall of San Diego Canyon from La Cueva 41 V43—Soda Dam from the south side 42
V44—Map of Banco Bonito lava flow, Battleship Rock ig-

nimbrite, and part of South Mountain rhyolite lava flow 42
V45—Schematic stratigraphic section of the Battleship Rock type location 43
V46—Sections and correlation of young (post 0.5 Ma) Valles caldera units 44
V47—Sketch of relationships near steeply dipping contact between lower Bandelier Tuff and upper Bandelier Tuff at Pueblo Mesa 45
V48—Section through the upper Bandelier Plinian deposit and base of upper Bandelier ignimbrite 46
V49—Isopachs and isopleths of selected fall units of the upper Bandelier Plinian deposit 47
V50—Logs of VC-2A (1986) and VC-2B (1988) core holes drilled in the Sulphur Springs area 48, 49
V51—Schematic cross section northwest-southeast across the Valles caldera 50
V52—Averaged maximum thickness of ash cloud lenses at top of upper Bandelier Tuff flow unit 1 51
V53—Top, illustration of actual dimensions of ash cloud lenses; bottom, illustration of lateral thickness changes of the pyroclastic flow and the ash cloud surge developing above it 52
V54—Bedded secondary deposits around a possible explosion crater between flow units of upper Bandelier Tuff 52
V55—View of northeast face of Frijoles Canyon wall **53**

Part II: Field guide to the maar volcanoes of White Rock Canyon

W1—Generalized geologic map of the central Rio Grande rift 57
W2—Map of White Rock Canyon 58
W3—Geologic map of the Española Basin 59
W4—Schematic cross section of the Pajarito Plateau of the eastern Jemez Mountains volcanic field, the canyon of the Rio Grande, and Cerros del Rio 61
W5—Sketch geologic map of the Cerros del Rio volcanic field 62
W6—Access to White Rock Canyon 63 W7—Geologic sketch map of La Mesita maar 64 W8—Bedding sets within the La Mesita maar deposits 64
W9—Close-up of bedding sets within the La Mesita maar deposits 65
W10—Sorting versus median diameter plot for hydroclastic surge deposits and scoria-fall deposits of the La Mesita maar 65
W11—Model of hydroclastic eruption 66
W12—Variables that can be used to relate maar deposits to the model shown in Figure W11 66
W13—Four fields for hydroclastic deposits 66
W14—Stratigraphic section, Mortandad Canyon 67
W15—Stratigraphic section, north end of Sagebrush Flats 68
W16—Stratigraphic section, southwest end of Sagebrush Flats 68
W17—Stratigraphic section, northeast Chino Mesa 69
W18—Stratigraphic section, immediately south of Chaquehui Canyon 69
W19—Exposures and reconstruction of the maar volcano at Upper Frijoles Falls, Frijoles Canyon 70
W20—Stratigraphic section through the maar volcano at Upper Frijoles Falls, Frijoles Canyon 70

Part I: Field guide to the Bandelier Tuff and Valles caldera

Acknowledgments

Many colleagues have contributed to the study of the Jemez Mountains and to this field guide. Much of the early work by S. Self in the Jemez Mountains was done in collaboration with J. V. Wright and W. M. Kite, Jr., who made major contributions to the concepts discussed. Grant Heiken has always been a valuable source of information on the Valles caldera. J. N. Gardner, F. Goff, and R. V. Fisher are thanked for their encouragement of our work in the Jemez Mountains and for the liberal sharing of ideas and data. J. A. Wolff and J. McPhie similarly provided much data and have been instrumental in shaping the geological picture represented in this guide. For help with access to various parts of the Jemez Mountains we are grateful to Wayne Brown (Copar Pumice Co.), John Corbin (Sulphur Springs), and Noel Bennett and Jim Wakeman (La Cueva).

We thank Nancy Gilson of the New Mexico Bureau of Mines and Mineral Resources for editorial assistance and help in producing the final version of this field guide.

Stephen Self and Martha L. Sykes
Honolulu, HI 96822

Introduction

This field guide provides five days of trips through the volcanic Jemez Mountains of north-central New Mexico. Its main purpose is to guide the reader in examining the 1.2-1.6 Ma Bandelier Tuffs, extensive ignimbrites emplaced during collapse of the Valles caldera, and related pyroclastic deposits. The guide provides a detailed overview of an ignimbrite and caldera complex of moderate to large size. The Bandelier Tuff, consisting of the products of two major eruptions (circa 1.6 and 1.2 Ma; Spell, McDougall, and Doulgeris submitted) that yielded a combined magma (dense rock) volume of up to 650 km^3, and the Valles caldera, 22 km in diameter, have most of the characteristics of the largest volume silicic volcanic systems found on Earth.

The predominantly calc-alkaline Jemez Mountains volcanic field, located on the western edge of the Rio Grande rift in north-central New Mexico (Figs. V1, V2), has evolved over the past 13 m.y. It is best known for the eruptions of the Bandelier Tuff, which caused the formation of the Valles caldera complex (Smith and Bailey, 1966, 1968). Products of contemporaneous effusive and explosive basaltic volcanism in the Rio Grande rift can be seen interstratified with Jemez Mountains volcanic deposits on the eastern margin of the field (Gardner et al., 1986). The presence of rift-filling sedimentary sequences containing many primary pyroclastic units and a wide range of volcaniclastic sediments allow further interpretation of the tectonic and eruptive history of the field (e.g., Turbeville et al., 1989).

Examination of the complex, intracontinental Jemez Mountain volcanic field presents an opportunity to gain insight into the volcanologic, petrologic, and structural events involved in the development of a major rhyolitic volcanic center. The aims of this guide are to demonstrate evidence for the way in which large silicic eruptive systems evolve, stressing the following points:

How do large ignimbrite eruptions start?
How are the outflow sheets deposited?
When and how does caldera collapse begin?
Where are the vents in such eruptions?
Do vent sites switch during the eruption?
What is the nature of intracaldera ignimbrites?
What are the relationships between outflow and intracaldera ignimbrites?

Because of the geographic distribution of the critical exposures and travel distances involved, this guide does not demonstrate all major parts of the stratigraphic sequence in order. Geological details in the road log between stops are kept at a minimum. Further details on the roadside geology for many of the same routes are obtainable in an earlier Geological Society of America field guide (Self et al., 1987) and in another IAVCEI Santa Fe Assembly field guide (Goff et al., 1989).

Jemez Mountains stratigraphy

The stratigraphy of the Jemez volcanic field consists of the Keres, Polvadera, and Tewa groups (Fig. V3). The Keres Group is volumetrically dominated by the Paliza Canyon Formation (13-7 Ma), which is mainly andesite with subordinate basalt and dacite, but includes two high-silica rhyolite formations (Canvas Canyon and Bearhead Rhyolites). Volcaniclastic rift-basin fill deposits of the Cochiti Formation are intimately related to, and commonly interbedded with, the volcanic rocks of the Keres Group.

The Polvadera Group includes the Lobato Basalt, Tschicoma Formation (dacitic and andesitic), and El Rechuelos Rhyolite, which includes pre-caldera high-silica rhyolites (Loeffler et al., 1988). As defined, units of the Polvadera Group cover an age span from 14 to 2 Ma. Distinctions between many Polvadera and Keres Group formations, given their petrologic similarities and temporal overlaps, are merely geographic. The Puye Formation, equivalent in age to the upper Polvadera and lower Tewa groups, represents a large alluvial fan that was built off the constructive highlands of the Tschicoma lava domes in the northeastern Jemez Mountains.

The Tewa Group is volumetrically dominated by the Bandelier Tuff, the products of two large-volume ignimbrite and caldera-forming eruptions. The Otowi (lower) and Tshirege (upper) members of the Bandelier Tuff were deposited at 1.6 and 1.2 Ma, respectively[1]. Both eruptions

[1]Where possible, the ages used throughout this guide are new $^{40}Ar/^{39}Ar$ dates of Spell et al., (1990), Spell and Harrison (1993), Izett and Obradovich (1994), and Spell et al. (submitted) which revise the original K-Ar ages given by Doell et al. (1968).

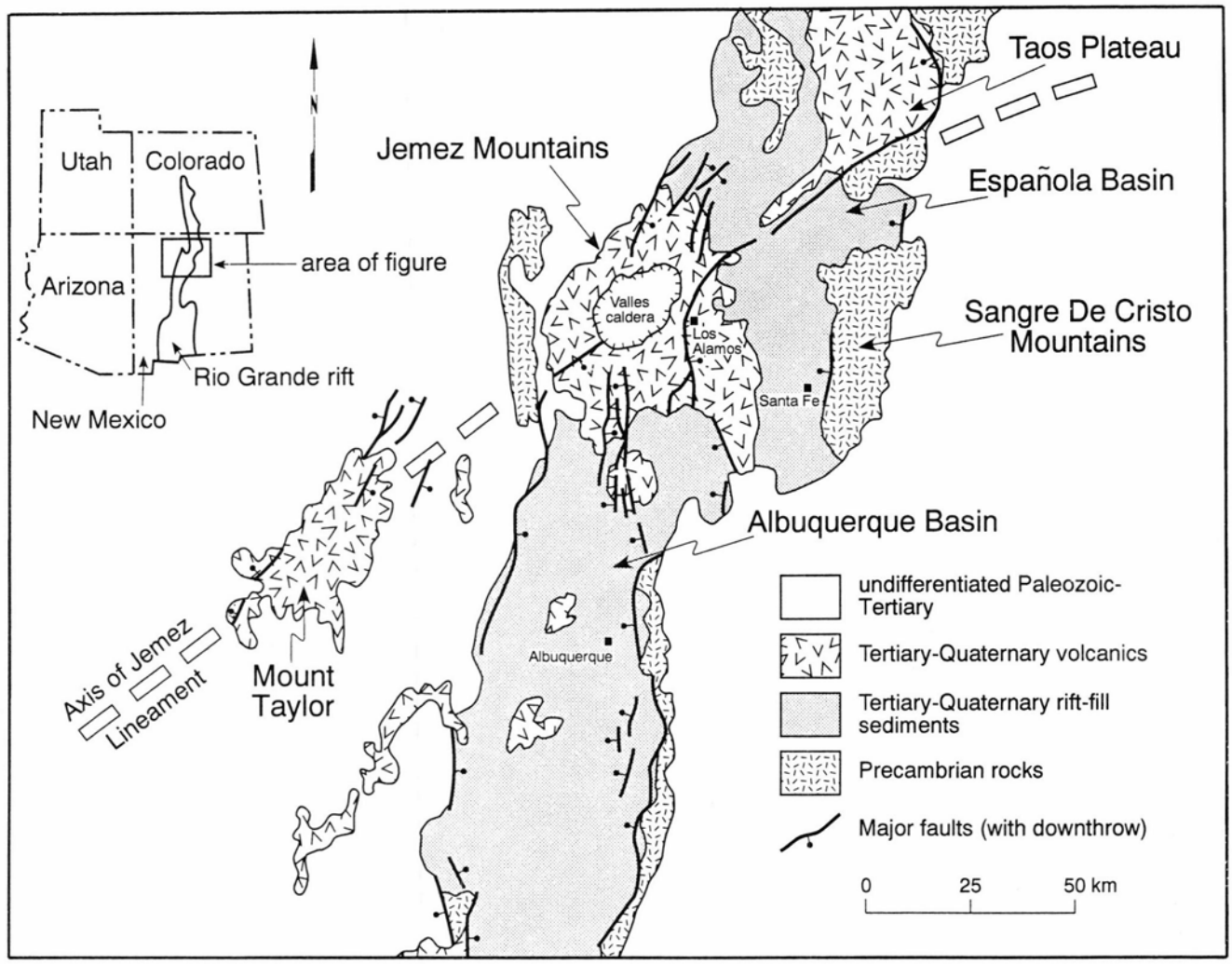

FIGURE V1—Location map showing relationship of the Jemez Mountains volcanic field to basins of the north-central Rio Grande rift. Valles caldera denotes Valles/Toledo caldera complex. Major fault zones of the region are shown; ball symbol on downthrown side.

led to the recognized episodes of caldera development, the earlier Toledo and later Valles stages, producing the nested caldera complex collapses seen today. Evidence summarized by Goff et al. (1989) suggests that only the 1.14 Ma event led to structural and magmatic resurgence. Eruptions of tephra and rhyolite domes in the caldera moat last occurred at about 0.2 Ma (Self et al., 1991; Spell and Harrison, 1993), or perhaps as young as 60 ka (Wolff and Gardner, 1995); hydrothermal activity persists to the present day. The system must still be considered active.

Tectonic and volcanic history of the Jemez Mountains

The Jemez Mountains volcanic field lies at the intersection of the Jemez lineament with the western boundary faults of the Rio Grande rift. Thin (35 km) crust and late Cenozoic basaltic volcanism characterize this Miocene to Recent age rift. The rift contains several en echelon sedimentary basins; volcanic rocks of the Jemez Mountains overlie and interfinger with sediments of the western Española Basin. The Jemez lineament was originally recognized as a northeast-trending alignment of young volcanic fields stretching from eastern Arizona to southeastern Colorado, following the southeast margin of the Colorado Plateau. Recent work (Aldrich and Laughlin, 1984) has shown that regionally it represents a complex zone of concentrated tectonic activity. Within the Jemez volcanic field the lineament is a structural entity possibly inherited from a fault zone originating in the Precambrian basement. It is expressed as the Jemez fault zone in San Diego Canyon, as the structure within the resurgent dome of Valles caldera (Gardner and Goff, 1984), and as faults occurring further to the northeast (Aldrich, 1986). The contiguous depression in the northeast Valles caldera that is filled by post-Toledo age Cerro Toledo rhyolites was previously known as the Toledo caldera (Smith et al., 1970) but is now referred to as the Toledo embayment (Fig. V2b). The origin of this structure is not yet resolved, but it may have developed in the Tschicoma volcanic complex prior to formation of the Toledo stage caldera (Heiken et al., 1986; Self et al., 1986).

Volcanic activity in the Jemez region began with mantle-derived alkaline basalts at about 16.5 Ma (Gardner et al., 1986). Poor exposure and complex interbedding with basin-fill sediments of the Santa Fe Group prevent knowledge of the distribution and vent localities for these basalts. In the period from 13 to 10 Ma the Jemez Moun-

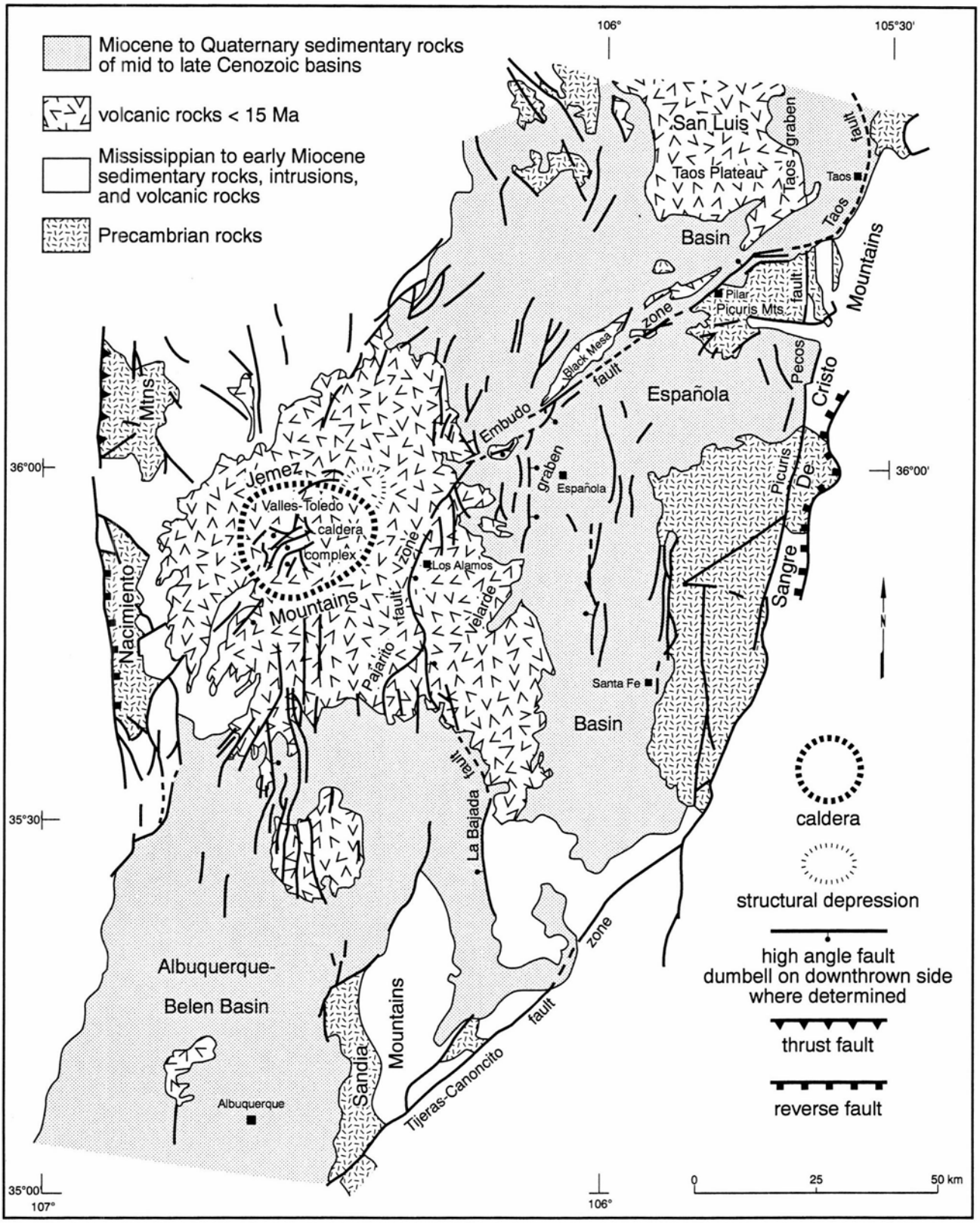

FIGURE V2a—Generalized geologic map of the Jemez Mountains and adjacent Rio Grande rift zone.

tains volcanic edifice began to build, with early Keres Group volcanism producing basaltic, rhyolitic, and minor intermediate products. Evolved basaltic lavas of this period are interbedded with coarse-grained debris-flow deposits and basin-fill gravels (Cochiti Formation). High-silica rhyolite lavas and pyroclastic deposits were erupted from vents aligned along north—south trending faults. These relations suggest that intense tectonic activity occurred during this period and that faults provided conduits for the magmas. Although exposures are sparse, it

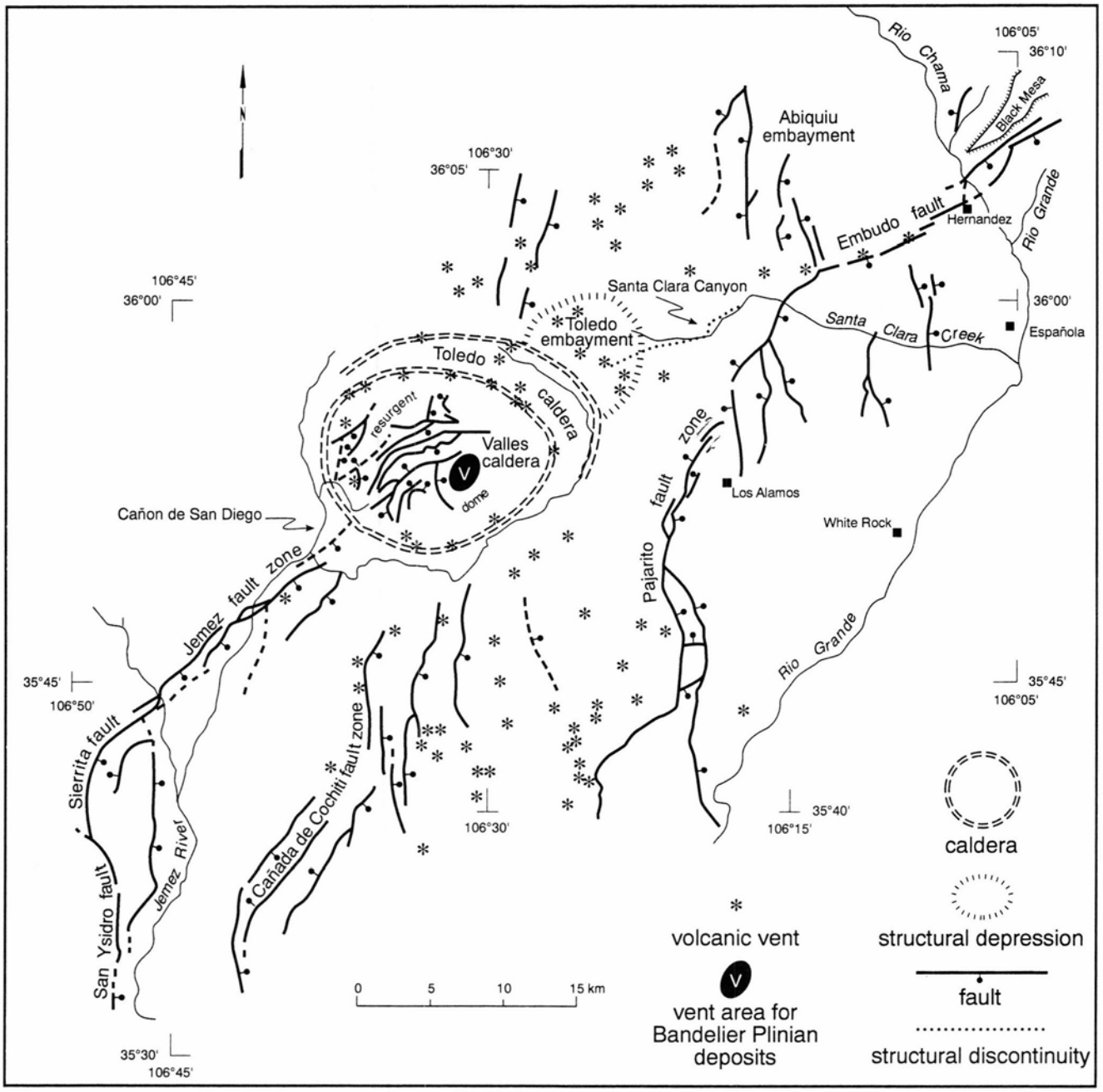

FIGURE V2b—Simplified structure map of the central and south Jemez Mountains (after Aldrich, 1989) showing the suspected vent area for the Bandelier Plenian deposits based on dispersal axes of fall units (see Figs. V19 and V45).

appears that the basalts were erupted in the vicinity of the Jemez lineament—Rio Grande rift intersection and flowed eastward into the rift.

Basalt and high-silica rhyolite continued to be erupted during the period from 10 to 7 Ma but were volumetrically overwhelmed by effusion of some 1000 km^3 of Paliza Canyon andesite and subordinate rhyodacite. This activity centered on the lineament—rift intersection even more strikingly than basaltic activity prior to 10 Ma. Half the volume of the entire Jemez volcanic field was erupted in this brief 3 m.y. period. The Paliza Canyon andesite volcanoes probably formed a major edifice before the Bandelier Tuff eruptions occurred.

A compilation of available age dates for predominant rock types from the Jemez Mountains region shows three noteworthy features (Gardner and Goff, 1984): (1) a probable 3 m.y. gap in basaltic volcanism occurred from 7 to 4 Ma; (2) at 7 to 6 Ma, coincident with the beginning of the lull in basaltic volcanism, there was a change in the composition of intermediate vulcanism from dominantly andesitic to dacitic; and (3) the revival of basaltic volcanism at about 4 Ma preceded the onset of the earliest eruption of Bandelier-type rhyolitic magma. Furthermore, at about 7 Ma a sharp reduction in the rate of volcanism occurred. Gardner and Goff (1984) suggest that these temporally coincident events indicate a lull in tectonic activity, and Gardner et al. (1986) point out that the geometry of the Puye Formation volcaniclastic alluvial fan, built largely in this period, also indicates tectonic stability.

The transition from predominantly andesitic to dacitic volcanism at about 7-6 Ma reflects a major change of mag-

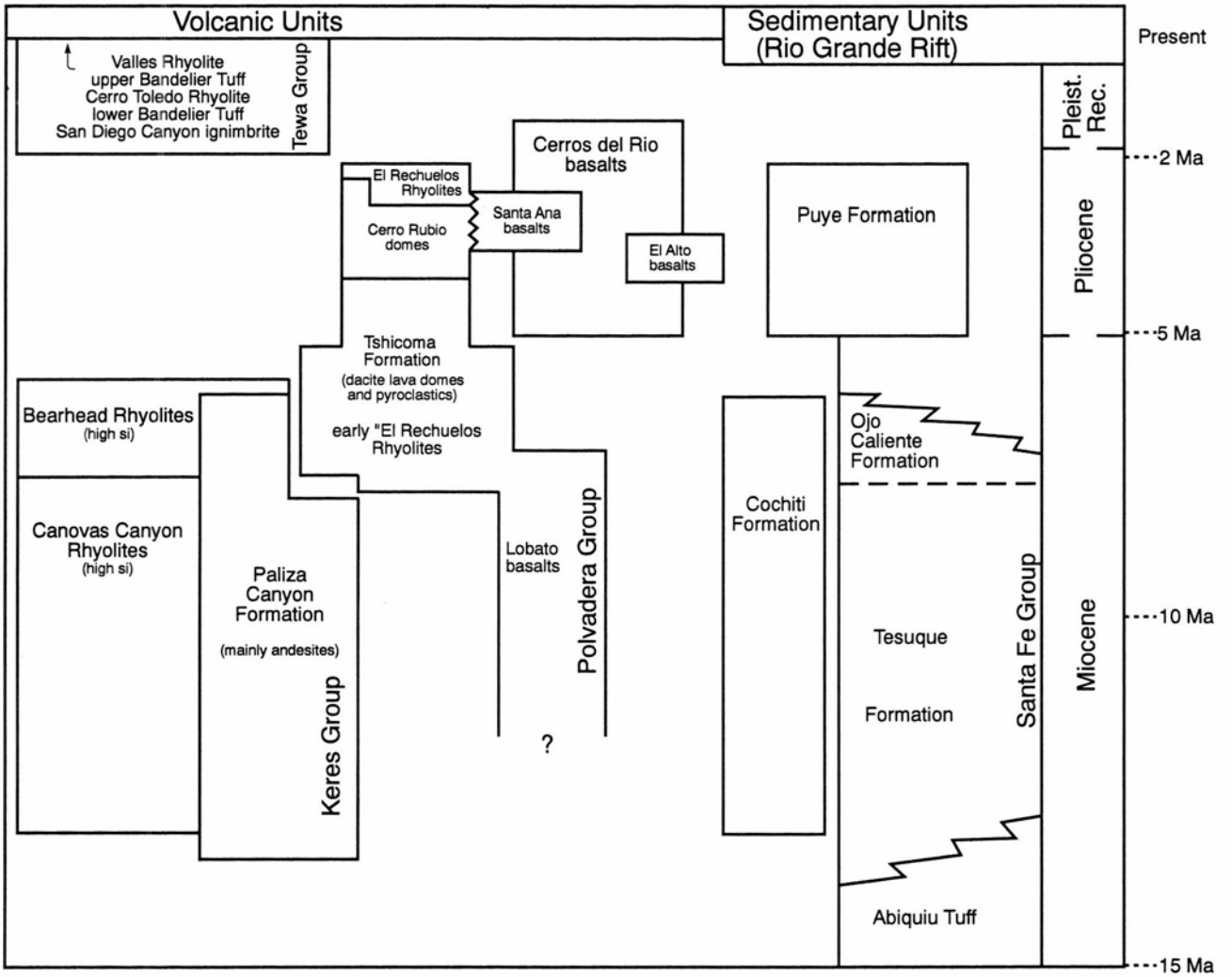

FIGURE V3—Chronostratigraphic chart of major units in the Jemez Mountains (information from Bailey et al., 1969; Smith et al., 1970; Gardner and Goff, 1984; McPherson et al., 1984; Self et al., unpublished data 1984). High Si denotes high silica rhyolite composition.

matic processes in response to the tectonic lull. Pockets of basalt and basaltic andesite began to coalesce with pods of high-silica rhyolite, yielding intermediate magma chambers, from which portions were erupted as the hybrid dacitic lavas of the Tschicoma Formation. The focus of volcanism in this period (7-4 Ma) was again centered on the lineament—rift intersection, and the Tschicoma volcanic complex grew to be a major edifice in the period immediately before the Bandelier eruptions. Further details on the pre-Bandelier history of the Jemez Mountains and a day of field stops examining the rock evidence can be found in another field guide (Self et al., 1987).

Since 4 Ma, with renewed tectonic activity in the rift, further basaltic volcanism occurred peripherally to the Jemez Mountains volcanic field, and rift-related faulting shifted eastward of its former position to the Pajarito fault zone. These events, together with later small-volume eruptions of Bandelier-type rhyolite magma (the San Diego Canyon ignimbrites; Turbeville and Self, 1988), and eruptions of dacitic lavas in the Tschicoma volcanic center (Doell et al., 1968; Smith et al., 1970; Smith, 1979; Gardner et al., 1986), indicate the presence of shallow silicic magma chambers centered beneath the lineament—rift intersection after about 4 Ma.

Tewa Group volcanism: the Bandelier Tuffs and Valles caldera

San Diego Canyon ignimbrites

Magmatic activity in the Jemez Mountains culminated in a series of rhyolitic explosive and effusive episodes, formally assembled as the Tewa group (Fig. V3). Radiometric age dating of the Jemez Mountains rhyolites has proven difficult due mainly to xenocrystic phases in the erupted magmas. The currently accepted ages based mainly on recent $^{40}Ar/^{39}Ar$ dating are shown in Table Vl. The earliest known rhyolitic pyroclastic units are two lithic-rich, nonwelded ignimbrites (designated A and B) exposed along the southwestern topographic wall of Valles caldera and in San Diego Canyon, informally called the San Diego Canyon ignimbrites (Turbeville and Self, 1988). The age of these units by $^{40}Ar/^{39}Ar$ dating is 1.78 Ma, determined on sanidine separated from pumice clasts of ignimbrites A and B (Spell et al., 1990). Both ignimbrites contain nearly aphyric, high-silica rhyolite pumice and have localized coarse pumice rafts; lag breccias in Valles caldera wall exposures indicate relative proximity to vents. Distinctive tube pumice within the ignimbrites and trace-element patterns allow correlation of ig-

TABLE V1—Present understanding of ages and stratigraphy of units in the Jemez Mountains.

Unit	Age (Ma)	Method*	Reference
Banco Bonito	≤0.20 ± 0.03	A	Self et al., 1991; Spell and Harrison, 1993
VC–1 rhyolite	0.36 ± 0.06	K	Goff et al., 1989
Battleship Rock	<0.52	A	Self et al., 1991; Spell and Harrison, 1993
El Cajete	<0.52	A	Self et al., 1991; Spell and Harrison, 1993
Valle Grande Rhyolite (Valles II domes)			
La Jara (LJ)	0.52 ± 0.01	A	Spell and Harrison, 1993
South Mountain (SM)	0.52 ± 0.01	A	Spell and Harrison, 1993
San Antonio I & II (SA)	0.56 ± 0.004	A	Spell and Harrison, 1993
Santa Rosa II (SR)	0.79 ± 0.02	A	Spell and Harrison, 1993
San Luis (SL)	0.80 ± 0.003	A	Spell and Harrison, 1993
Seco (S)	0.80 ± 0.005	A	Spell and Harrison, 1993
Santa Rosa I	0.91 ± 0.004	A	Spell and Harrison, 1993
Del Abrigo I–III (DA)	0.97 ± 0.10	A	Spell and Harrison, 1993
Del Medio I (DM)	1.09 ± 0.12	A	Spell and Harrison, 1993
Del Medio II & III	1.13 ± 0.11	A	Spell and Harrison, 1993
Redondo Creek	undated		
Deer Canyon	?undated		Spell et al., 1990; Izett and Oberdovich, 1994;
Upper Bandelier Tuff (Tshirge Member)	1.23 ± 0.08	A	Spell et al., submitted
Cerro Toledo Rhyolite			
Fall unit D	1.21 ± 0.009	A	Spell and Harrison, 1993; Spell et al., submitted
Fall unit C	1.48 ± 0.02	A	Spell and Harrison, 1993; Spell et al., submitted
Fall unit B	1.43 ± 0.11	FT	Izett et al., 1981
Toledo embayment domes			
Pinnacle Peak	1.20 ± 0.02	K	Tamanyu and Goff, 1985
Turkey Ridge (TR)	1.24 ± 0.03	K	Stix et al., 1988
Unnamed dome	1.33 ± 0.02	K	Tamanyu and Goff, 1985
Cerro Toledo (CTO)	1.38 ± 0.05	K	Stix et al., 1988
Cerro Toledo	1.62 ± 0.02	K	Tamanyu and Goff, 1985
Valles I (Toledo) moat domes			
Warm Springs (WS)	1.25 ± 0.04	K	Doell et al., 1968
Rabbit Mountain (RM)	1.43 ± 0.04	K	Stix et al., 1988
Rabbit Mountain	1.52 ± 0.06	K	Stix et al., 1988
Cerro Trasquilar (CT)	1.27 ± 0.03	K	Tamanyu and Goff, 1985
East Los Posos (ELP)	1.47 ± 0.05	K	Stix et al., 1988
West Los Posos (WLP)	1.50 ± 0.05	K	Stix et al., 1988
Lower Bandelier Tuff (Otowi Member)	1.61 ± 0.01	A	Spell et al., 1990; Izett and Oberdovich, 1994;
San Diego Canyon Ignimbrite			Spell et al., submitted
Ignimbrite B	1.78 ± 0.07	A	Spell et al., 1990
Ignimbrite A	1.79 ± 0.04	A	Spell et al., 1990
Cerro Rubio Quartz Latite			
Dome N. of Cerro Rubio	2.18 ± 0.09	K	Heiken et al., 1986
Cerro Rubio Dome	3.59 ± 0.36	K	Heiken et al., 1986

*A $^{40}Ar/^{39}Ar$
K K/Ar
FT Fission track

nimbrite B with a pumice-fall deposit in the upper part of the Puye Formation (Turbeville and Self, 1988). Eruption of these early ignimbrites may have led to the formation of small calderas.

Lower Bandelier Tuff (Otowi Member) (1.61 ± 0.01 Ma)

The Bandelier Tuff consists of two rhyolitic ignimbrites and associated deposits (Fig. V4). The older Otowi Member (or lower Bandelier Tuff, LBT) attains a maximum thickness of 180 m and occurs in all parts of the Jemez Mountains (Fig. V5). It originally had an estimated volume of about 400 km^3 dense rock equivalent (DRE) of nonwelded to densely welded ignimbrite and Plinian deposits.

The initial Guaje Plinian pumice-fall deposit has a maximum thickness of about 10 m and an estimated volume of 20 km^3 DRE. Tephra fall from the Bandelier eruptions has been correlated as far as Lubbock, Texas (Izett et al., 1972), but probably fell well to the east of that area. The LBT eruption was accompanied by the engulfment of a large area of country overlying the magma chamber and formation of the 22-km-diameter Toledo caldera (Smith and Bailey, 1966, 1968). A semi-circular, 9-km-diameter depression in the northeastern Jemez Mountains, initially identified as part of the Toledo caldera (Smith and Bailey, 1968), may be an older feature as it contains older lava domes as well as the inter-Bandelier Cerro Toledo Rhyolite lavas (Goff et al., 1984). It is now usually referred to as the Toledo embayment (Fig. V6). Several lines of evidence summarized in Heiken et al. (1986) and Self et al. (1986) suggest that the first major (Toledo) collapse caldera was roughly coincident with the later Valles structure.

Cerro Toledo rhyolites and associated pyroclastic deposits

Following the eruption of the LBT, a series of rhyolitic lava domes and flows, the Cerro Toledo rhyolites, were emplaced along the northern moat of the Toledo caldera and in the Toledo embayment (Bailey et al., 1969; Heiken et al., 1986; Table V1). These domes include Rabbit Mountain, Los Posos, Cerro Toledo, and several other small domes that predate the onset of Tshirege volcanism and possibly mark the outline of the Toledo collapse ring fracture (Fig. V6). Extracaldera Plinian pumice deposits as-

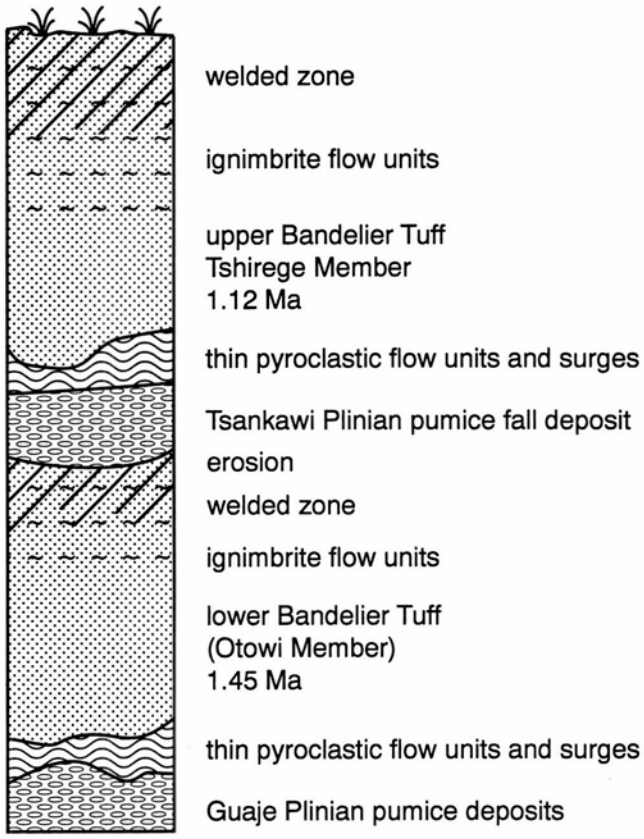

FIGURE V4—Standard schematic section through Bandelrier Tuff showing major eruptive units.

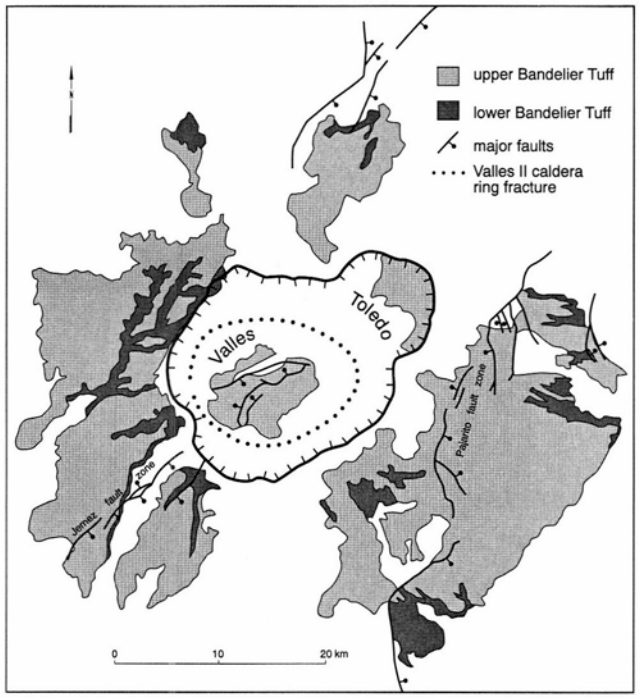

FIGURE V5—Simplified map of distribution of the Bandelier Tuff (after Smith et al, 1970) with minor changes from S. Self, unpublished data.

sociated with these lava domes, the Cerro Toledo Rhyolite tuffs, occur interbedded with epiclastic sediments and phreatomagmatic ash. Activity associated with the Cerro Toledo Rhyolite persisted until about 1.2 Ma (Izett et al., 1981; Spell, et al, in preparation).

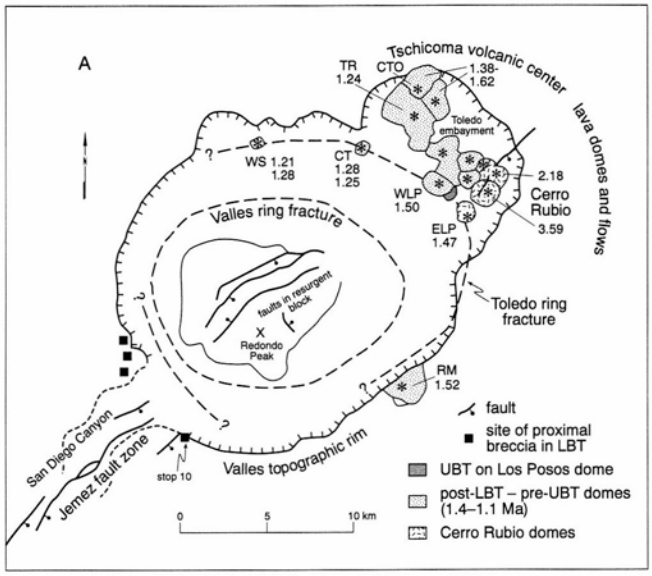

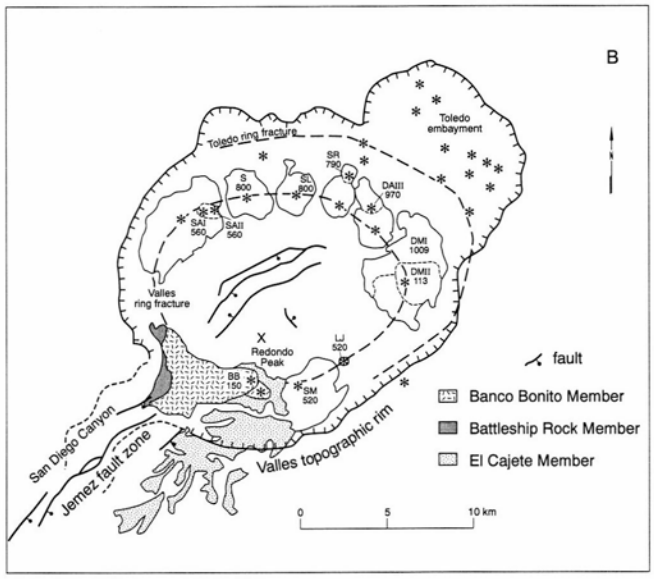

FIGURE V6—A) Lava domes and flows of Cerro Toledo age (post-Toledo). Numbers are K–Ar ages in Ma for domes (see Table 1). B) Lava domes and flows postdating Valles caldera. Numbers are $^{40}Ar/^{39}Ar$ ages in ka (see Table 1). Abbreviations of dome names given in Table 1; stars are vent locations.

Upper (Tshirege Member) Bandelier Tuff (1.23 ± 0.01 Ma)

The second Bandelier eruption produced the Tshirege Member (or upper Bandelier Tuff, UBT), which consists of a basal Plinian deposit (Tsankawi Pumice) totaling about 15 km^3 (DRE) and an overlying sequence of ignimbrite flow units (Smith and Bailey, 1966; Kite, 1985). The ignimbrite has a maximum thickness of 275 m and an estimated original volume of 250 km^3 (DRE). The initial pumice-fall unit associated with UBT activity may be phreatomagmatic in origin, in accord with the existence of a caldera lake at that time. Eruption of the **UBT** initiated the collapse of the Valles caldera, nested within the Toledo caldera. Both calderas may have collapsed in a predominantly trap-door fashion about a westward hinge. This interpretation, suggested by gravity and drill-hole data (see Nielson and Hulen, 1984), is also consistent with the past existence of an intracaldera lake; lacus-

trine deposits thicken dramatically to the east within the caldera (Heiken et al., 1986). Lava domes were emplaced within the Valles caldera in the period following formation and have continued to perhaps 100,000 years ago (Fig. V6B; Table V1).

Resurgence of the Valles caldera involving uplift of the intracaldera ignimbrites by more than 1000 m occurred less than 70 ka after collapse (Spell et al., 1990). In recent years advances have been made in understanding the structural details of the intracaldera sequence (Nielson and Hulen, 1984; Heiken et al., 1986; Wilt and Vonder Haar, 1986). Much of the interpretation relies on gravity data (e.g., Segar, 1974) and shows that fault patterns parallel the Jemez fault zones and Rio Grande rift faults. (For details, see Stop 19.)

The deeper structure of the Jemez Mountains region has been investigated by various seismic methods. Ankeny et al. (1986) suggest a possible model based on a three dimensional inversion interpretation (Fig. V7). The depth to and presence of the basaltic intrusion are unknown, but this model provides a plausible, overall picture of the Valles caldera and its subsurface structure.

Valles rhyolites and associated deposits

The later stages of Jemez Mountains volcanism consist of the eruption of rhyolitic domes and lava flows moat zone of the Valles caldera (Table V1; Fig. V6b). Thick (300400 m) intracaldera ignimbrites younger than the UBT are found in drill cores, the "Upper Tuffs" of Nielson and Hulen (1984) and Hulen et al. (1988). As recent as 0.5 Ma these were of high-silica rhyolite composition (Spell 1987; Spell and Kyle, 1989). Erupted magma composition changed from high-silica rhyolite to low-silica rhyolite after 0.5 Ma (Table V2).

One of the latest eruptive episodes in the Jemez Mountains was thought to have occurred about 0.3 Ma, and resulted in the El Cajete pumice fall and associated Battleship Rock ignimbrite, together with a lava flow known only from drill core (VC-1 Rhyolite Lava of Goff et al., 1986). This complex sequence is capped by the product of the last eruption from the Valles caldera, the Banco Bonito obsidian flow. Determination of the age of these units has proved difficult; the published $^{40}Ar/^{39}Ar$ ages on the El Cajete, Battleship Rock, and Banco Bonito units range from 0.5 to 0.2 Ma (Spell and Harrison, 1993). Self et al. (1991) suggest that an eruption at about 300 ka produced the El Cajete—Battleship Rock—VC1 rhyolite units, and that a slightly later eruption at about 200-150 ka yielded the Banco Bonito lava and associated pyroclastic rocks. This scenario is supported by $^{40}Ar/^{39}Ar$ ages of Spell and Harrison (1993), see Table V1, but a new study has suggested an age of about 60 ka for these units (Wolff and Gardner, 1995).

Geochemistry of the Bandelier Tuff

The two Bandelier ignimbrites and their associated Plinian deposits resulted from eruptions of zoned magma

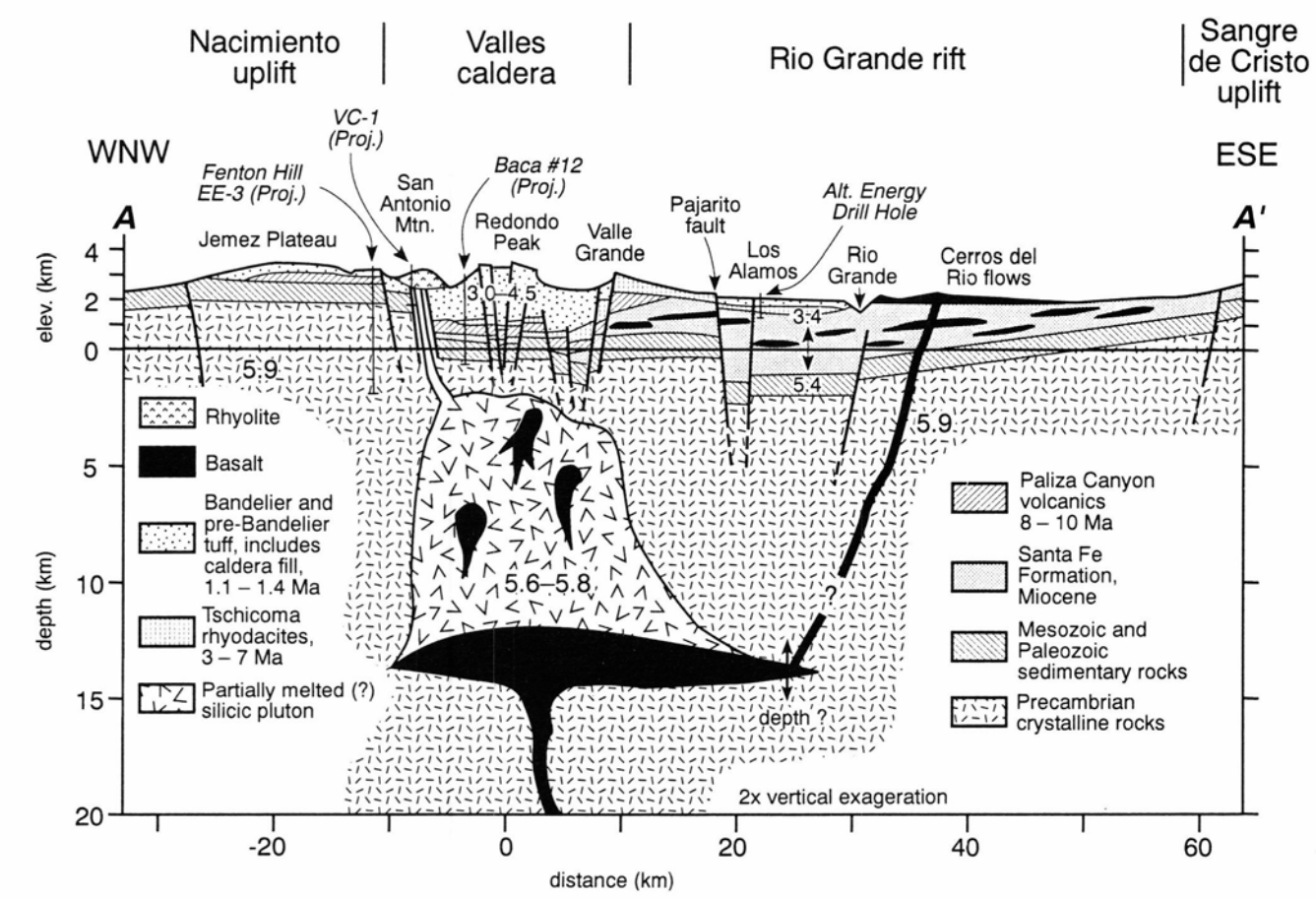

FIGURE V7—Schematic cross section through the Valles caldera and Rio Grande rift based on the three-dimensional seismic inversion interpretation of Ankeny et al. (1986). Velocity values (large numbers) in km/sec are averages determined from the inversion technique.

TABLE V2–Representative major and trace element compositions of main ignimbrite units from the Valles caldera. All analyses were performed at the New Mexico Bureau of Mines and Mineral Resources (Kuentz, 1986; Balsley, 1988).

A. Major elements analyzed by X-ray fluorescence in weight percent.

UNIT*	SDC A	SDC B	LBT HSR	LBT HSR	UBT HSR	UBT HSR	UBT LSR	Dacite
Sample No.	PBA-01	12–02A	27–63	11–14	20–53	8–38	20–51	22–70
SiO_2	—	76.67	77.94	76.95	78.03	76.97	72.11	68.05
TiO_2	—	0.09	0.11	0.05	0.08	0.05	0.27	0.42
Al_2O_3	—	12.33	11.67	12.33	12.16	12.13	14.75	14.96
Fe_2O_3	—	1.42	1.35	1.46	1.54	1.50	2.83	3.40
MnO	—	0.06	0.05	0.08	0.04	0.08	0.04	0.07
MgO	—	0.27	0.06	0.14	0.35	0.07	1.07	1.36
CaO	—	0.34	0.30	0.30	0.40	0.25	1.80	2.99
Na_2O	—	3.30	3.77	4.30	2.90	3.83	3.28	4.85
K_2O	—	5.50	4.74	4.39	4.48	5.09	3.78	3.29
LOI**	—	4.62	2.45	4.53	3.05	2.82	5.27	1.28

B. Trace elements analyzed by X-ray fluorescence in parts per million.

UNIT*	SDC A	SDC B	LBT HSR	LBT HSR	UBT HSR	UBT HSR	UBT LSR	Dacite
Sample No.	PBA-01	12–02A	27–63	11–14	20–53	8–38	20–51	22–70
Pb	—	25.79	17.54	47.38	53.00	51.23	85.94	36.90
Rb	—	173.25	110.98	358.49	158.35	336.12	108.83	177.51
Sr	—	6.80	5.30	4.58	15.16	5.94	210.13	432.78
Y	—	45.83	37.64	116.40	88.99	134.84	69.72	26.04
Zr	—	227.07	236.95	262.23	215.14	284.86	238.10	210.83
Nb	—	65.8	53.5	189.27	74.75	157.85	39.16	27.36
Ga	—	18.0	18.0	28.00	22.37	28.00	19.35	—
Zn	52	63.0	52.0	125.0	69.38	140.0	70.68	—

C. Trace elements analyzed by instrumental neutron activation analysis in parts per million.

UNIT	SDC A	SDC B	LBT HSR	LBT HSR	UBT HSR	UBT HSR	UBT LSR	Dacite
Sample No.	PBA-01	12–02A	27–63	11–14	20–53	8–38	20–51	22–70
Sc	2.052	2	1	—	1	—	5	5
Cr	0.9	—	—	—	19.0	<0.5	13.0	1.3
As	1.4	1.7	—	3.1	9.6	3.5	10.9	—
Sb	0.188	0.42	0.13	0.5	0.25	0.48	0.25	0.12
Cs	3.91	8.3	2.3	10.38	4.1	12.7	4.0	3.9
Be	<60	65	16	<48	90	23	547	922
La	40	50	54.1	38.7	80.3	54.2	73.1	37.0
Ce	78.1	100.4	106.2	93.3	142.0	113.8	124.1	69.4
Nd	26.3	32.4	38.6	38.1	69.1	44.8	60.4	25.8
Sm	6.34	7.2	6.7	11.1	14.2	10.8	12.0	5.1
Eu	0.210	0.156	0.142	0.02	0.46	0.249	0.892	0.879
Tb	1.11	1.12	0.99	2.70	2.46	2.64	2.09	0.710
Yb	4.26	4.16	3.56	10.80	6.92	11.58	5.48	2.36
Lu	0.631	0.630	0.55	1.60	1.02	1.72	0.81	0.37
Hf	6.99	7.8	7.3	13.90	8.04	14.90	7.12	6.28
Ta	4.66	5.00	4.5	14.0	4.3	11.20	2.5	2.0
Th	19.7	18.8	15.1	42.2	18.3	35.2	12.0	7.7
U	7.3	6.4	4.9	17.8	5.3	12.6	2.9	2.2

* Unit abbreviations are as follows:
SDC A & B: San Diego Canyon ignimbrites A and B
LBT HSR: Lower Bandelier Tuff high silica rhyolite. Sample 27–63 is least evolved; sample 11–14 is the most evolved composition (from Plinian pumice).
UBT HSR: Upper Bandelier Tuff high silica rhyolite. Sample 20–53 is representative of the dominant composition. Sample 8–38 is the most evolved composition (from Plinian pumice).
UBT LSR: Upper Bandelier Tuff low silica rhyolite.
Dacite: A minor dacitic juvenile component found in the Upper Bandelier Tuff.
**LOI Loss on ignition
—not determined

systems (Smith and Bailey, 1966), with compositions from high- to low-silica rhyolite. Detailed descriptions of their geochemistry can be found in Self et al. (1991) and Dunbar and Hervig (1992).

The LBT consists almost entirely of high-silica rhyolite of constant major element composition with pronounced variations in minor and trace elements (Table V2), accompanied by phenocryst contents from 7.5 to 19.5% (Self et al., 1991). In proximal sections, these variations are systematic from first-erupted to last-erupted units, and closely mimic element zoning patterns seen in the Bishop Tuff (Hildreth, 1979) and other high-silica rhyolites (Fig. V8). The chemical profiles are fully consistent with fractionation of the observed phenocryst assemblage of quartz

+ alkali feldspar + ferrohedenbergite + orthopyroxene + fayalite + magnetite + zircon + allanite + apatite (as inclusions in other phases) + chevkinite. Only sanidine and quartz are present in amounts greater than 1%. Incompatible element plots exhibit very little scatter (Fig. V9) attributed to fractionation from an initially homogeneous starting composition. In distal sections, the variation is more chaotic and a range of pumice compositions is observed within any one flow unit. However, the Guaje basal Plinian deposit predominantly consists of the most highly fractionated materials and represents tapping of the uppermost layer of the zoned magma chamber. Concentrations of H_20 and F in melt inclusions found in quartz, sanidine, and pyroxene phenocrysts also indicate enrichment of the Plinian tephra in these volatiles relative to the ignimbrite (Dunbar and Hervig, 1992). Mafic pumice occurs as a trace component in the LBT; it is most abundant in banded pumice clasts found in pumice swarms at the base of the lowest flow unit at Stop 3. Neodymium and strontium isotopic data indicate these pumice clasts originate by mixing of the LBT high-silica rhyolite with basement Proterozoic granite and by assimilation and melting of Precambrian country rock into the LBT magma shortly before or during the eruption (Self et al., 1991).

The UBT is more heterogeneous petrographically and more chaotic geochemically. As well as the dominant high-silica rhyolite, low-silica (about 73% $Si0_2$) rhyolite and dacite (69% $Si0_2$) pumice occur in trace to minor amounts (Fig. V9). The dacite first appears about halfway up the Tsankawi Plinian layer and is found throughout the ignimbrite. A wide range of pumice compositions (dacite, low-silica rhyolite, and high-silica rhyolite of varying trace element abundances) may be found within individual flow units, particularly in the late-erupted units at Stop 9. However, as with the LBT, the Plinian layer appears to consist of the most fractionated material. The UBT shows a range in, and a systematic variation of, crystal contents similar to the LBT. The phenocryst assemblage is quartz + alkali feldspar + ferrohedenbergite + orthopyroxene + magnetite + ilmenite + fayalite + chevkinite + apatite + hornblende + biotite in high-silica rhyolite. Low-silica rhyolite is similar with increased abundances of mafic phases, especially hornblende and biotite, and plagioclase.

The distinctive grey dacite pumice consists of phenocrysts of plagioclase + two pyroxenes + Fe—Ti oxides + biotite + hornblende set in a microvesicular groundmass containing up to 80% microlites; the texture indicates vesiculation after microlite growth, which therefore must have preceded eruption. Close inspection of clasts frequently reveals a jacket of highly vesicular high-silica rhyolite glass that is largely abraded during transport, and many clasts may have originally been erupted as "cored bombs." Shapes vary from orthogonal tabular to spindles. The dacite pumice represents a small quantity of more mafic magma mixed into, and quenched by, the dominant rhyolite shortly prior to the eruption. These data suggest that the dacite was injected into and chilled against the dominant rhyolite melt (Self et al., 1991). Geochemically the dacite is unrelated to the rest of the Tewa Group magmas. A second type of banded pumice is texturally similar to those in the Otowi and is considered to have a similar origin, i.e., melted country rock granite.

Although trace-element variations in UBT high-silica rhyolite and low-silica rhyolite are generally similar to those in the LBT, there is much more scatter in incompatible-element ratios (Fig. V9) suggesting fractionation of the observed assemblage from heterogeneous parent material. The UBT heterogeneous parent can be modeled as a mixture of the LBT high-silica rhyolite and mafic components (Balsley et al., 1987; Skuba et al., 1989). Mixing of these components into the system therefore did not proceed to completion before renewed fractionation began to re-zone the system following the LBT eruption. The dacite pumice has trace element characteristics inappropriate for a UBT parent and seems to represent a magma unrelated to the Bandelier system.

Each Bandelier Plinian-ignimbrite sequence contains several distinct pumice types with variable crystal contents (aphyric to 30 wt%) depending partly on composition. The Plinian deposits have rhyolitic pumice from 1 to 5 wt% phenocrysts, while the rhyolitic ignimbrite pumice clasts possess from 8 to 20 wt% phenocrysts. When crystal concentration in the pyroclastic deposits is noted in this guide, it is calculated relative to the average crystal content of the most common pumice type in the Plinian deposit or ignimbrite being discussed.

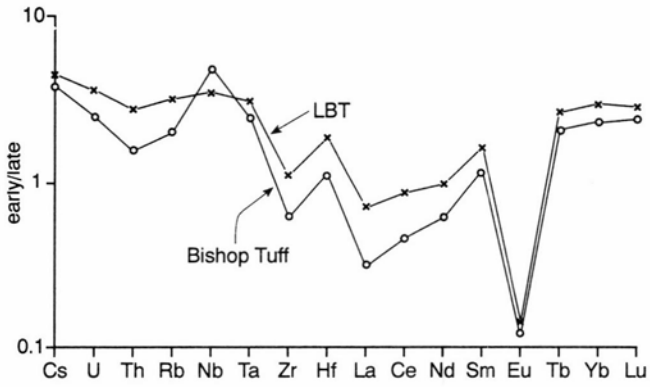

FIGURE V8—Enrichment diagram for lower Bandelier Tuff (lower Bandelier Tuff, +'s) and Bishop Tuff (o's), consistent with fractionation of phenocryst assemblage.

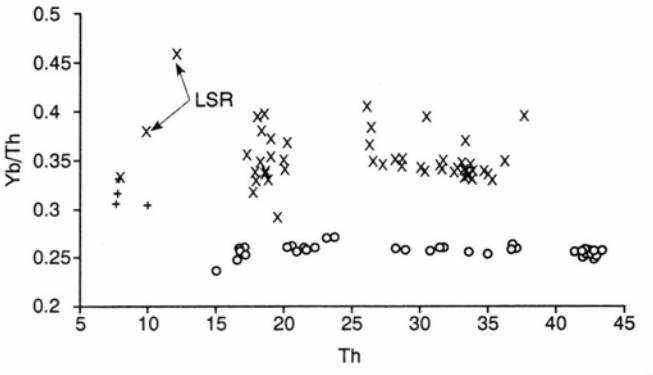

FIGURE V9—Typical incompatible element ratios for lower Bandelier Tuff (LB T) high silica rhyolite (o's), upper Bandelier Tuff (UBT) high silica rhyolites (x's) and dacite (+'s), and upper Bandelier Tuff low silica rhyolites as labeled. The UBT fractionated from a more heterogeneous parent than the LBT.

Field guide

Field guide stops in the Jemez Mountains are shown in Figure V10. The day-by-day accounts give routes from the intersection of NM-502/4 and Overlook Drive in White Rock, New Mexico (0 miles). Road distances are given in miles, but all other measurements in this guide use the metric scale.

Stops are designated by numbers. Those with the suffix "A" are alternate stops which can be made if time permits. After access information for each stop is given, a description will follow the order: significance to the theme of the field guide, description of the outcrop, and summary.

Days 1 and 2 will give the reader with less time to spare a general overview of the silicic, caldera-related volcanism of the Jemez Mountains. Days 3 to 5 fill in the details. Table V3 shows which units, arranged stratigraphically, can be seen at which stops on this field guide.

Day 1: General characteristics of the Bandelier ignimbrites and related units

Drive northeast from White Rock on NM-4 until the other part of the NM-502/4 loop (through Los Alamos town) is reached at the Y-junction (4.3 mi). Veer right (east) and proceed downhill for about 4 miles until it is possible to safely make a U-turn and start back up the hill in the westbound lanes of NM-4. After you have reached the base of the Bandelier Tuff (massive pumice fall unit), pull onto the wide shoulder, well out of traffic. The outcrop is in the cliffs on the north side of the road. Do not attempt to walk across this busy highway!

Stop 1: Upper and lower Bandelier ignimbrite near edge of outflow sheet, Otowi Mesa

Significance: This outcrop provides a good introduc-

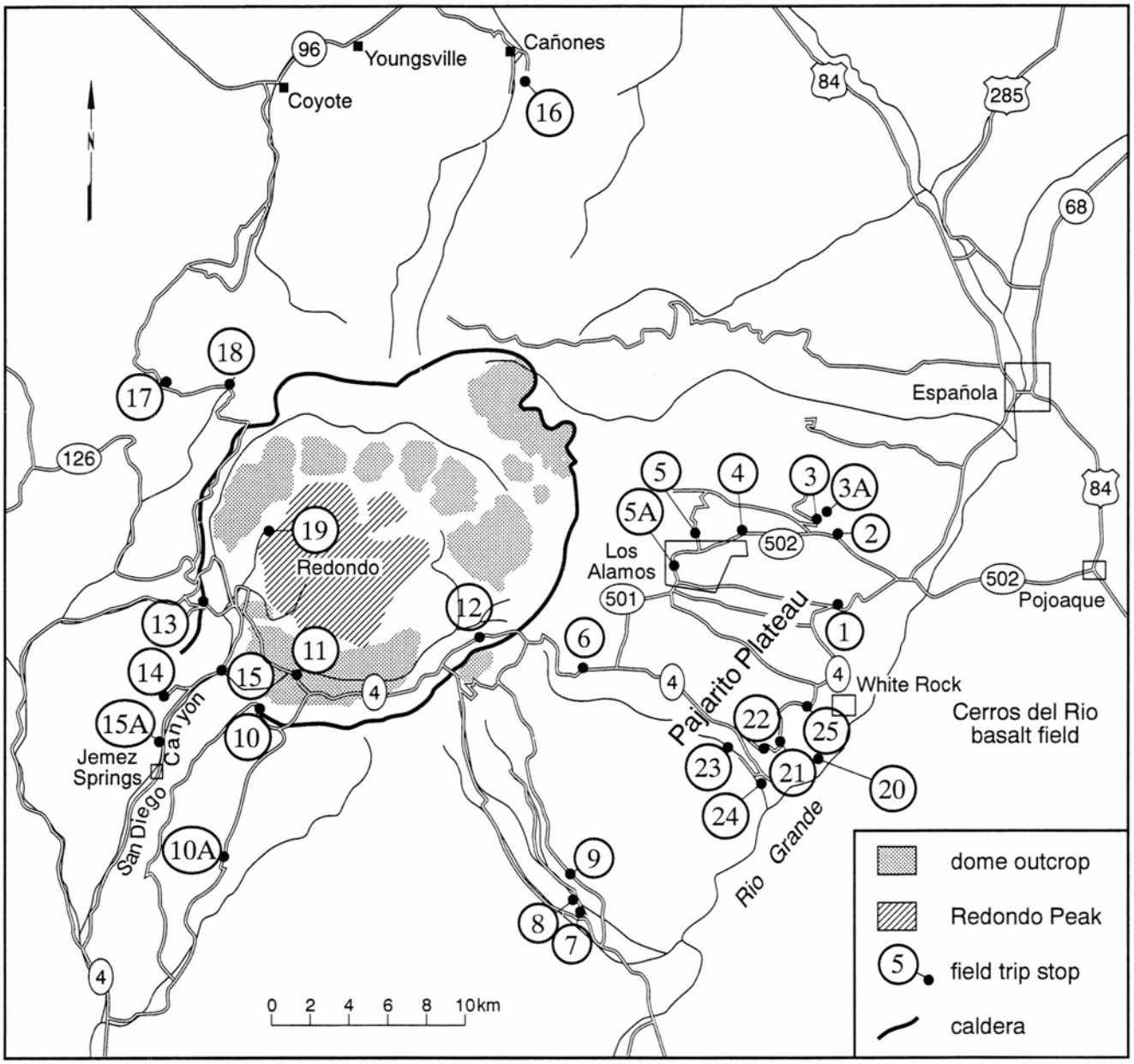

FIGURE V10—Stops for Jemez Mountains field guide. Dotted patterns—dome outcrop; hatched pattern—Redondo Peak resurgent block.

TABLE V3—Stratigraphic units and features of the Jemez Mountains and stops where they are visited. X = hands-on exposures, O = overview of the exposure.

Surface exposed units and features	1	2	3 & 3A	4	5 & 5A	6	7	8	9	10	10A	11	12	13	14	15	15A	16	17	18	19	20	21	22	23	24	25
Pleistocene-Recent hot spring deposits																	X				X						
Banco Bonito												X				O											
Battleship Rock												X			O	X											
El Cajete												X															
Valles caldera and resurgent blocks										O			O	O	O						X						
Valles Grande Rhyolite													O														
South Mountain												X	O														
San Antonio I and II														O													
Redondo Creek																					O						
Upper Bandelier Ignimbrite	X		X	X	X	X		X	X		X			X	O			X	X			X	X	X	X	X	X
Upper Bandelier Plinian	X	O		X	X			X						X	O			X	X			X		X	X	X	
Cerro Toledo Rhyolite																											
Fall units				X	X																						
Toledo caldera moat domes													O														
Lower Bandelier Ignimbrite	X		X				X	X		O				X	X									X	X		
Lower Bandelier Plinian	X		X				X	X							X												
San Diego Canyon Ignimbrite														X	X												
Puye & Totavi Formations	X	X																									
Basalts of Cerros del Rio	O																					X			X	X	
Paliza Canyon andesites														X	X												
Paleozoic sediments															X	X											
Precambrian basement rocks																	X										

tion to the stratigraphy of the outflow sheet of the two Bandelier ignimbrites.

Description: Only parts of the sequence of the Bandelier ignimbrites are seen here on the edge of the Pajarito Plateau (the gently sloping surface formed by the Bandelier ignimbrite sheet east of the Jemez Mountains). The exposure is 23 km from the Valles caldera ring fracture and about 28 km from the proposed early vent sites for these eruptions (Self et al., 1986) and thus is medial to distal. The original distal margins of the ignimbrites must have extended further downslope but have been eroded away. The two Bandelier ignimbrites, LBT (Otowi) and UBT (Tshirege), are disconformable (Fig. V11); the LBT rests on soil and lacustrine silts, which in turn overlie a basalt dated at 2.4 Ma (Bachman and Mehnert, 1978). In the Bandelier ignimbrites, flow units, i.e., depositional aspects, of the deposits, are not always easy to relate to the more obvious (in the field) cooling unit boundaries of Smith and Bailey (1966).

Guaje pumice deposit: The lower Bandelier Plinian de-

posit (to be examined in detail at Stop 3) is 7 m thick at this site. The group of bedded fall units at the top is thicker than at Stop 3, showing that this upper group of fall units thickens towards the south. These are best seen in a small pumice borrow pit some 200 m east of the main cliff (Fig. V11, bottom right).

Lower Bandelier Tuff: Above the thick Plinian deposit are two ignimbrite flow units totaling 40 m in thickness. The flow unit boundary is a cryptic pumice concentration zone. These units are typical of the lower LBT; most exposures show homogeneous nonwelded ignimbrite that is more lithic-rich than the UBT (Fig. V12), a general characteristic of the LBT. Here, in the medial to distal part of the sheet, lithic contents are generally low (LBT, 10.3 wt%; UBT, 2.7 wt%), whereas crystal contents are high (LBT, 21.8 wt%; UBT, 23.6 wt%), representing crystal enrichment factors (Walker, 1972) of 2.2 in the LBT and 1.8 in the UBT. Enrichment factors are the amount by which an ignimbrite or fall deposit is enriched in loose crystals over the abundance of crystal (phenocrysts) in the juvenile material (pumice). Higher enrichment factors indicate more violent eruptions.

Toward the source, the LBT (and UBT) has a basal set of thin flow units (Fig. V13) that are pumice-rich, but these pinch out before Stop 1 in the LBT. Little can be determined about the LBT eruption in this general area, other than the nature of the opening Plinian phases due to the high degree of dissection and erosion and lack of complete exposures of the ignimbrite.

Upper Bandelier Tuff: The most widespread Plinian layer

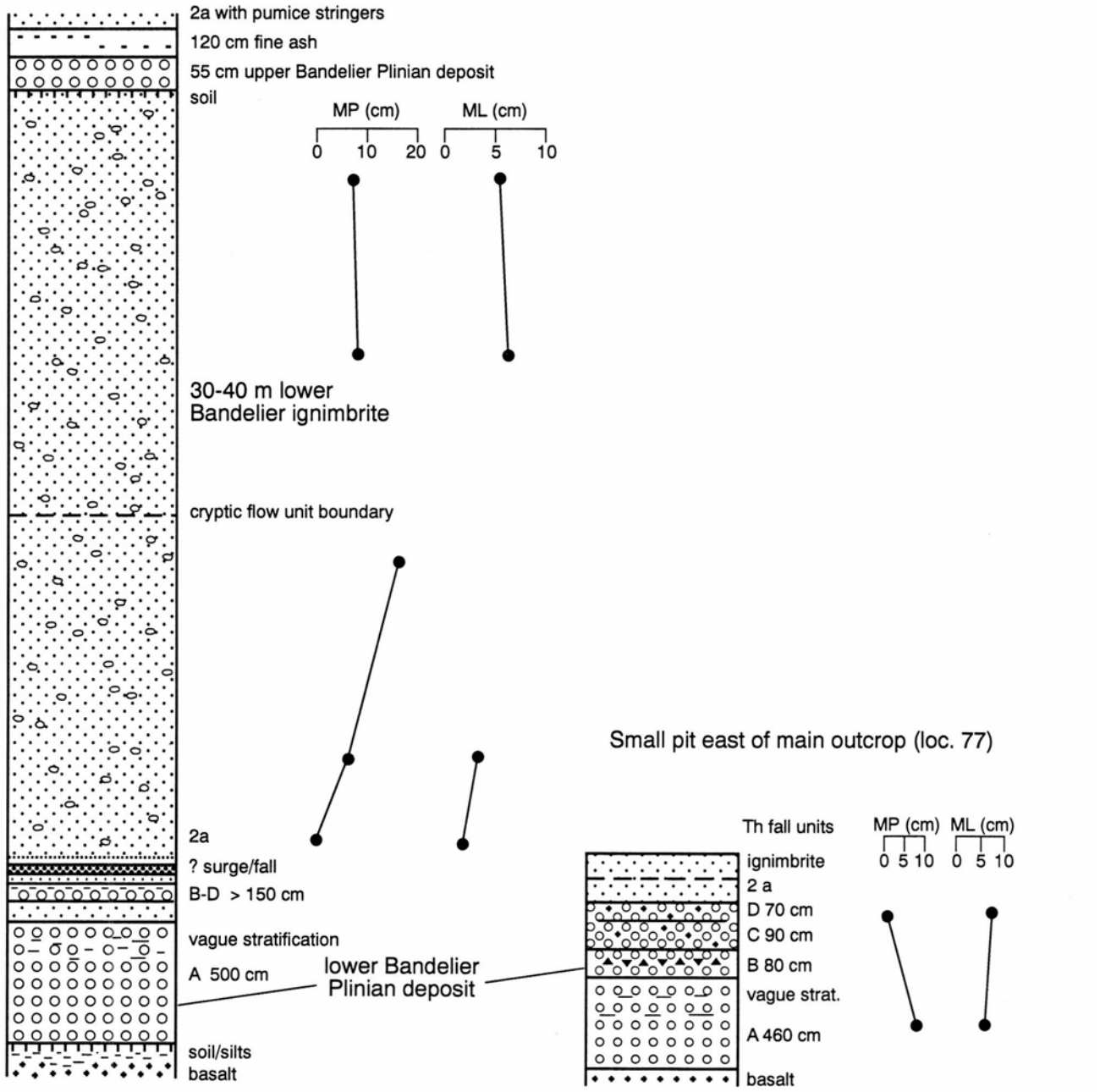

FIGURE V11—Lower Bandelier Tuff stratigraphy and deposit characteristics at Stop 1. Lower Bandelier ignimbrite is entirely nonwelded at this location. A, B, etc., are fall units; 2a refers to basal layer of ignimbrite (see text). Th is thickness; MP and ML are average maximum clast size of pumice (P) and lithics (L), respectively.

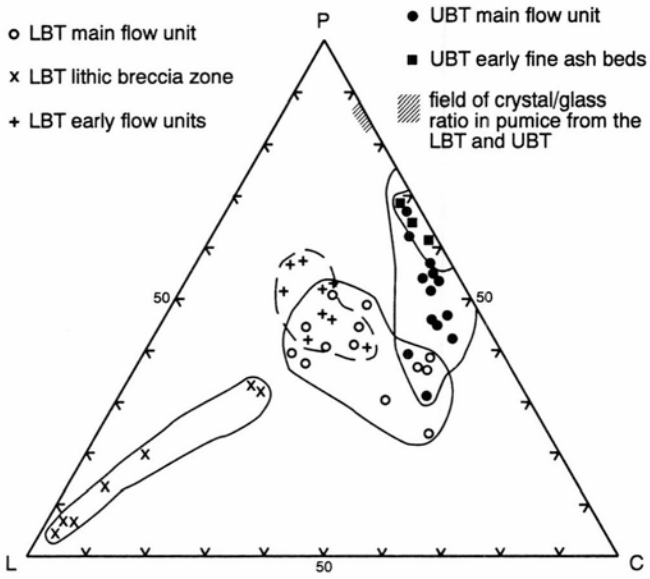

FIGURE V12—Distribution of the component pumice clasts (P), accessory lithic clasts (L), and free crystals (C) in samples the Bandelier ignimbrites. LBT, UBT, see Fig. 9.

of the Bandelier eruptions, upper Bandelier Plinian fall-unit B (part of the Tsankawi pumice deposits) forms the base of the UBT sequence (Fig. V14). Note the high crystal content (enrichment factor of 7) at this location, which is located on the upwind side of the dispersal area. This is one of the highest measured in any pyroclastic deposit anywhere. It is overlain by a group of bedded fine ashes (unit C) that are either fall or surge deposits or both. Unit C is part of the Plinian sequence, and a remnant of Plinian fall unit D or E can be found above it; the full UB Plinian sequence is best seen at Stop 13. Fall-units D and E, and usually part of C, were largely eroded during deposition of the ignimbrite in this eastern part of the Jemez Mountains.

Eleven or more flow units occur in the 38 m thickness of UB ignimbrite here. They are divisible into three groups or packages (Fig. V14), a lower thick group containing one or two flow units, a middle group of thin flow units showing strong pumice zonation, and an upper, incipiently welded unit (top of mesa). Thin ground (or ash cloud) surge layers are seen between flow units in the middle group (cf., Fisher, 1979).

The upper Bandelier ignimbrite shows an increasing number of flow units from more proximal to more distal exposures up to the area of Stop 1 (Fig. V13). The increasing number of thin units appearing in the upper and middle zones of the UBT reflects budding of units down flow. Beyond Stop 1, the number of flow units decreases towards more distal exposures. Samples of the main lower flow unit collected at intervals downflow from basal and middle horizons show no clear trend in content of crystals, save for a slight decrease in distal parts.

The UBT has a prominent bench (Figs. V13, V14) near the upper part of the lower zone. This can be attributed to the onset of vapor-phase alteration, which begins just below the bench, overprinting incipient welding (or thermally induced discoloration), as suggested by Crowe et al. (1978).

Summary: The main purpose of this stop is to present an overview of the Bandelier ignimbrite outflow sheets. Points to consider include: (1) the presence of "cryptic" flow unit boundaries, and the deposition of thick flow units, exemplified by the lower part of the LBT here and elsewhere (Fig. V13); and (2) the significance of the fine-grained deposits (unit C and/or surges at the base of the UBT; see also Stop 3). Are they the result of phreatomagmatic activity? Note that a distal exposure of upper Bandelier ignimbrite to the northeast of Stop 1, which cannot usually be visited as it is on Indian tribal grounds, has accretionary lapilli in the basal flow unit. These may have been picked up from unit C during the erosive passage of the lowermost flow unit, but to date unit C (in outcrop) has not been found to contain accretionary lapilli. The extreme crystal enrichment factor in the UB (Tsankawi) Plinian deposit indicates a very powerful ultraplinian eruption (Walker, 1981).

Continue west, taking the freeway back toward White Rock. Again, make a U-turn when it is safe and go east on NM-4 toward Santa Fe. Reset your mileage to zero when you are opposite the point where you were looking at the complete section of Bandelier Tuff Continue east on NM-4 for 2.6 mi, descending through Cerros del Rio basalts, Totavi and Puye formations, and Chamita Formation (sands and gravels filling Espanola Basin); turn left at metal gate onto Forest Service (FS) road 57/442; enter Guaje Canyon. Drive for 3.8 mi upcanyon, and turn right off road onto a gravel track, which in 50 meters makes a circle (6.4 mi). Park and walk to stream bed following unnamed arroyo (north). High on the west side of canyon is outcrop of LBT Plinian deposit with "tent rock" erosional forms. The outcrops for Stop 2 occur at the east side of the entrance of the small arroyo (Totavi deposits) and about 500 m to the north of the parking area, along the small arroyo where the channel becomes very narrow and winding (Puye ignimbrite and pumice-fall deposits).

Stop 2: Puye Formation—pre-Bandelier volcanism and sedimentation from the Tschicoma volcanic complex

Significance: The Puye and Totavi formations are coarse sedimentary and primary volcanic units that give evidence of the styles of volcanism and volcaniclastic sedimentation occurring before the onset of Bandelier volcanism, i.e., up to about 2.0 Ma. The Totavi Formation consists of axial stream gravels of the ancestral Rio Grande in this area, with some input from local volcanism (Waresback and Turbeville, 1990). The Puye Formation (Fig. V15) is a volcanogenic alluvial fan sequence with many primary fall and flow deposits, largely of dacite composition with subordinate andesite, derived mainly from explosive volcanism accompanying the effusion of Tschicoma lava domes in the period from 5.0 to 2.0 Ma (Turbeville et al., 1989).

Description: This stop explores an unnamed dry arroyo that gives an excellent strike section through the mid-fan Puye Formation. The Puye deposits consist of primary dacitic pumice-fall deposits derived from explosive eruptions in the Tschicoma volcanic center, small nonwelded dacitic ignimbrites (e.g., the Puye ignimbrite, 2.5 Ma; Fig. V16), and debris flows representing reworked ignimbrite, talus, and carapace rocks from associated lava domes and flows. Stream-channel and pumice-rich mudflow deposits are also common in this mid-fan section. This stop also includes an outcrop that was misinterpreted as fluvial deposits of the Totavi Formation as "wet surge" deposits (Nocita, 1988; corrected by McPherson et al., 1989).

Summary: The history of the Jemez Mountains prior to the onset of high-silica rhyolite-dominated Bandelier

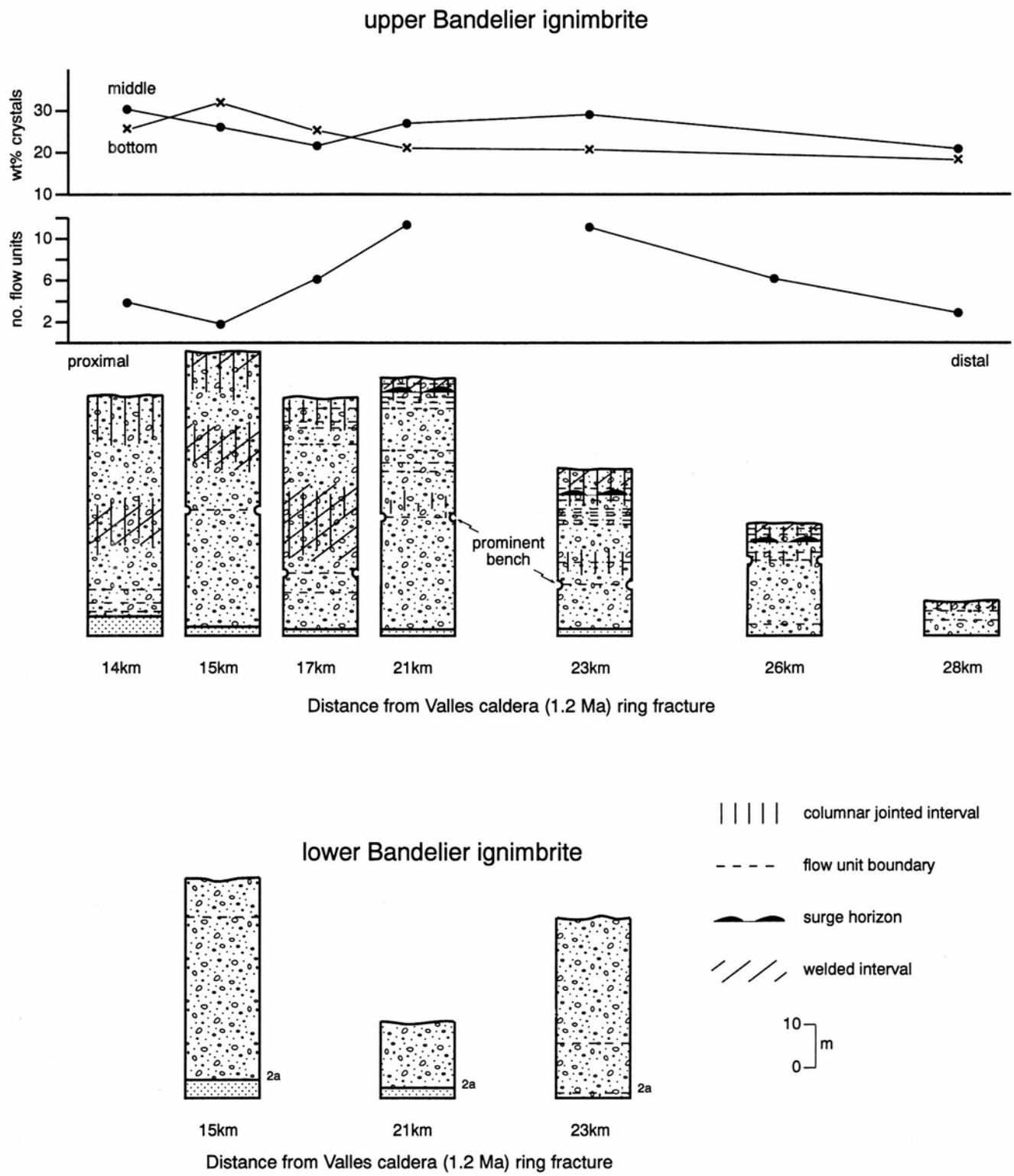

FIGURE V13—Down flow changes in number of flow units, lithic size, and crystal content in the lower and upper Bandelier ignimbrites (LTB, UBT) for the region of the eastern Jemez Mountains between Los Alamos and the edge of the ignimbrite sheet. Distances are given from the eastern part of the Valles caldera ring fracture; Plinian deposits not shown (J. McPhie and S. Self, unpublished data).

volcanism included many dacitic and andesitic explosive eruptions and led to the formation of the Puye fan.

Return to FS-57/422 and continue up Guaje Canyon to the junction with Rendija Canyon (FS-57 and 442), then continue ahead on FS-442 in Guaje Canyon. At the junction with FS-416, take the hairpin curve to the right uphill on FS-416. This road climbs through the Puye Formation. At the top of the mesa there is a good view down Guaje Canyon over the Bandelier/Puye surface. Continue on FS-416 and, when it bears left, continue to the Copar pumice quarries (9.0 mi). You must obtain permission to enter the quarry.

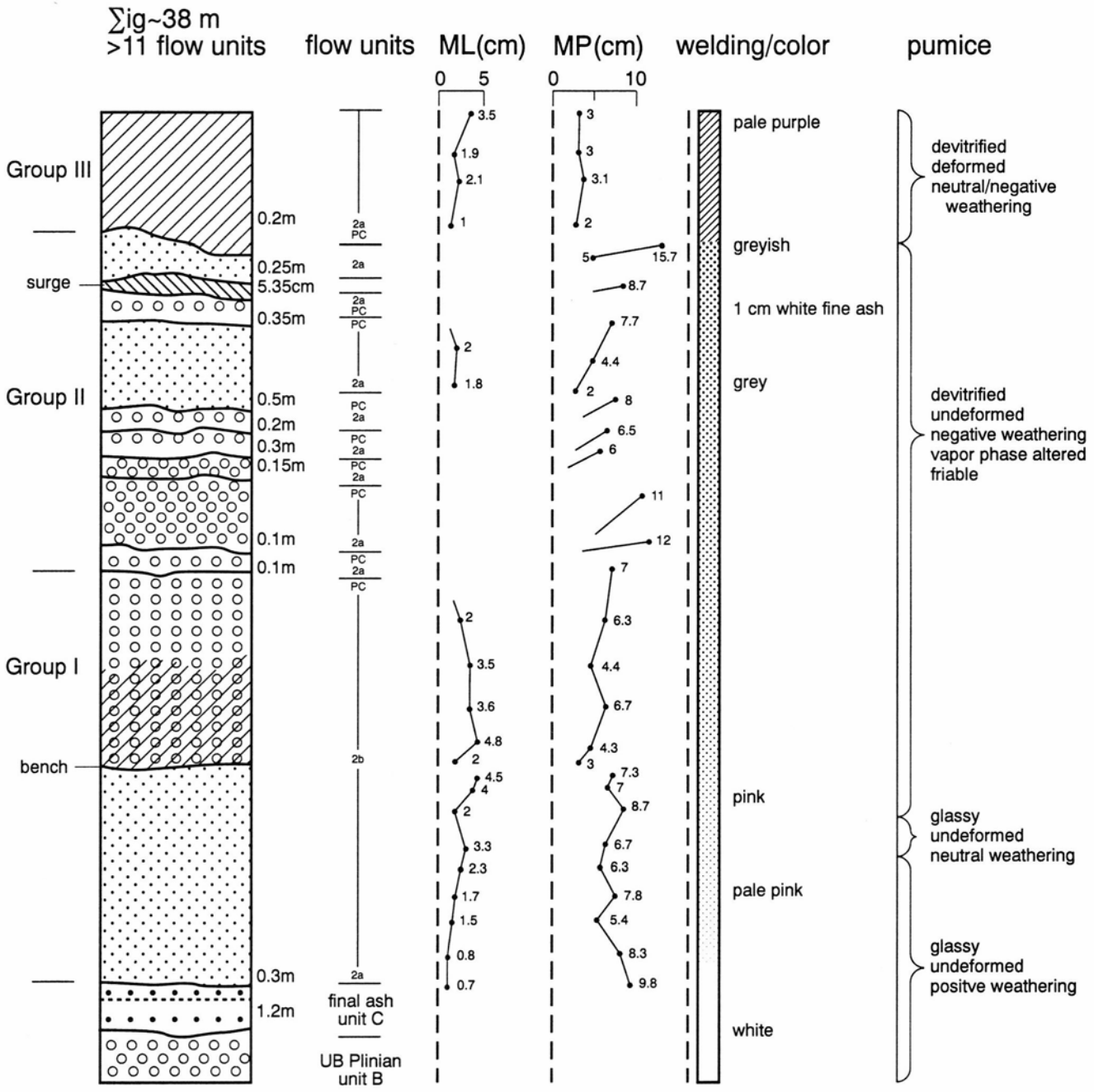

FIGURE V14—Measured section through upper Bandelier Tuff at Stop 1 showing deposit stratigraphy and characteristics. Diagonal shading indicates welding or induration. ML and MP = average maximum lithic and pumice clast size in centimeters, respectively, at level shown in deposits (J. McPhie and S. Self, unpublished data).

Stop 3: LBT **(Guaje) pumice-fall deposit and Bandelier ignimbrites**

Significance: At this location, 18 km from the Valles caldera ring fracture and 24 km from the middle of the caldera, the sequence of deposits produced during the opening phases of the LBT eruption is seen. An idea of the magnitude and dynamics of the Plinian eruption can be obtained from the evidence displayed here.

Description: The quarry workings expose more than 10 m of lower Bandelier Plinian pumice deposit (Guaje Pumice Bed of Bailey et al., 1969). A massive (9 m thick) graded fall unit, A, underlies bedded fall-units B to E (Fig. V17), which in turn are overlain by the nonwelded lower Bandelier (Otowi) ignimbrite with "pumice dunes" at the base.

Fall unit A has an extremely homogeneous lower part (Fig. V18) and an upper 3 m section that shows vague stratification. Maximum pumice and lithic diameters (here designated MP and ML, average diameter of five largest pumice clasts and lithic clasts, respectively) and median clast diameters (Md) do not change through the deposit; a very steady eruption column and constant depositional conditions are indicated. Stop 3 is about 20 km from the source vent for the LB Plinian eruption (Self et al., 1986), and the fall units show no ballistic lithic clasts consistent with this interpretation. The large thickness of pumice fall accumulated along a narrow dispersal axis. Several lines of evidence suggest a relatively low eruption column. These include the lack of crystal concentra-

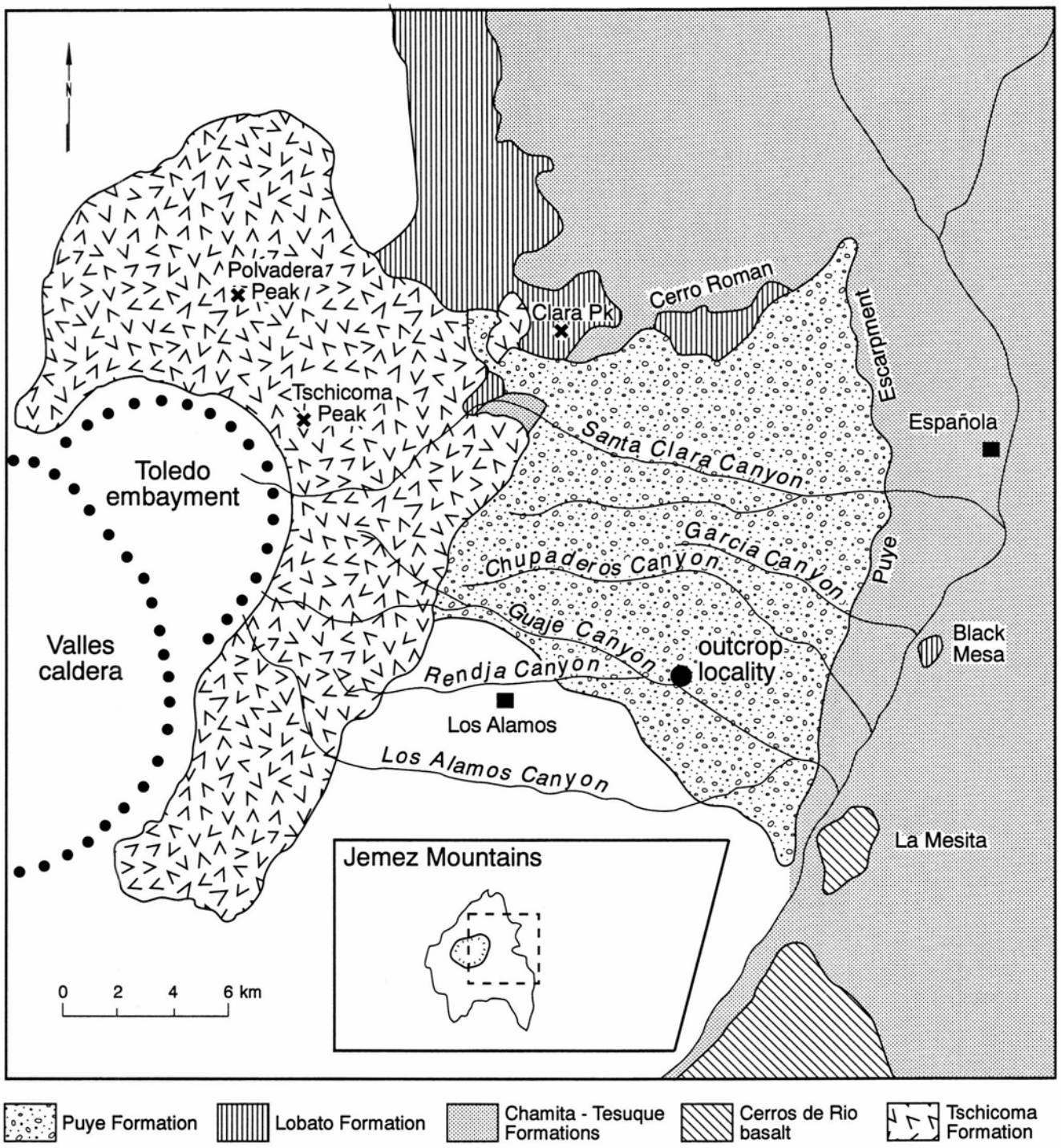

FIGURE V15—Map showing distribution of Puye Formation alluvial fan and location of Stop 2 outcrop locality (from McPherson et al., 1989).

tion (enrichment factor about 1.0), the comparatively small maximum grain sizes (MP = 8 cm and ML = 3 cm in the area of Stop 1), and modeling results. Using the fallout model of Carey and Sparks (1986), the dispersal of lithic clasts indicates an eruption column height on the order of 20 km or less (22 km altitude including the elevation of the vent region). However, there must have been a strong westerly wind blowing, as indicated by the elongate isopachs and isopleths; winds in excess of 50 m/s are plausible in jet stream conditions that occur in this region at altitudes below 20 km. Mixed pumice clasts of grey dacite intermingled with high-silica rhyolite can be found in unit A, which has the most evolved high-silica rhyolite composition in all the Bandelier Tuff.

This exposure occurs on the dispersal axis of fall unit A, which has an easterly distribution and elongate isopachs (Fig. V19). In our interpretation, unit A was not deposited in the southern Jemez Mountains, but units B to E occur there (Stop 7).

The interpretation that unit A is absent in the south, west, and north of the Jemez Mountains is based on the presence of more lithic-rich, strongly stratified fall units in these regions that strongly resemble fall units B to E at the Copar quarries. These units are apparently widely

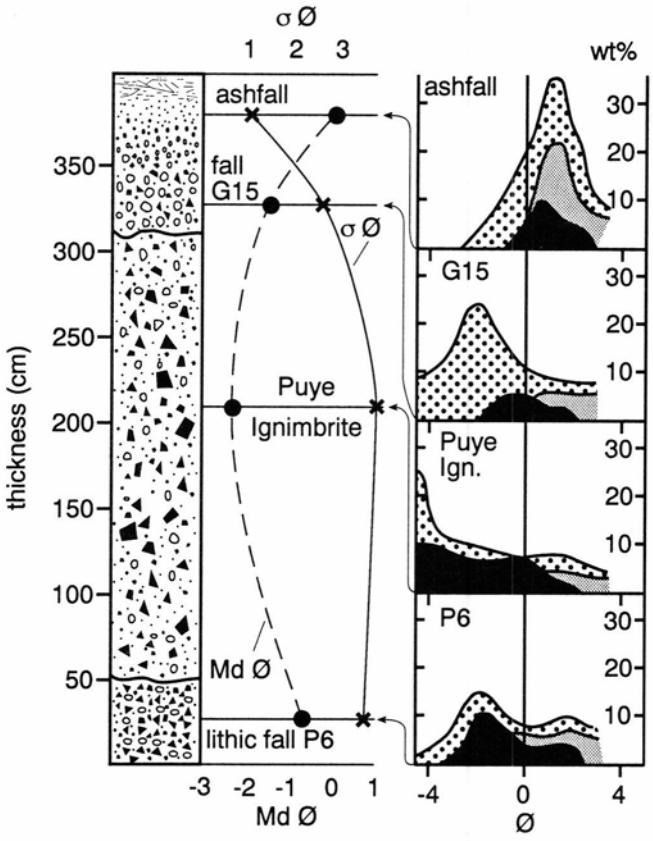

FIGURE V16—Profile through the informally-named Puye ignimbrite' and associated pumice and ash falls showing changes in median grain size (Mdϕ) and sorting of deposits (σϕ); values derived from cumulative frequency curves in the grain size range - 4ϕ to 4ϕ and frequency variation curves of individual component populations (pumice—stippled; lithic clasts—black; crystals—shaded). Samples taken from homogeneous (ungraded, massively bedded) portions of each unit. Shown at right are estimated percentages of accessory lithic types observed in pumice falls P6 and G15 (from Turbeville et al., 1989).

dispersed (Fig. V19) with a southeasterly dispersal axis, although correlation between the eastern sector and the south is made difficult by the absence of LBT exposures in the intervening region. Fall unit B is lithic-rich (up to 25 wt%) representing deposition during a vent-widening episode and is variably stratified. As represented on the isopach map, it may be a combination of several fall units with variable dispersal axes. Unit C is coarse and more homogeneous and probably represents the period of highest eruption columns and greatest mass flux during the LBT Plinian eruption. Units D and E are rarely exposed due to widespread erosion of the top of the pumice-fall deposits by early, violent pyroclastic flows. Units B, C, D, and E have traces of fine ash between them in this area, and, to the north of Stop 3, a fluvial erosion channel can be seen cut into unit D, indicating a slight pause in deposition at that point in time. The fine ash layers will be seen again at Stop 7.

Volumes of the LBT Plinian deposits are difficult to estimate because it is impossible to close all but the thickest isopachs due to lack of distal exposures. The bulk volume of unit A could be a little as 7 km^3 or as much as 30 km^3; volumes of units B to E over the present area of dispersal total 11 km^3 but originally must have been much larger. Up to 65 km^3 bulk volume can be reconstructed for units B to E using reasonable closures of the isopachs.

Distal equivalents are found in Texas, 550 km from source (Izett et al., 1971), and have been correlated compositionally to the LBT Plinian deposit (Izett, 1981). However, ash thicknesses in Texas suggest that these distal ash falls lie on different thinning curves than the Plinian deposits (Fig. V20), and they may be co-ignimbrite ashes.

The LBT in this area shows a similar sequence to that at Stop 1 and is examined only to view evidence of thin, violently emplaced flow units that possess dunelike lenses of coarse pumice clasts. The lowermost 1 to 1.5 m of the LBT is a flow unit that contains casts of trees felled during the eruption. The casts have been used to interpret flow directions of the pyroclastic flows (Potter and Oberthal, 1983); they occur just above the contact of the Plinian deposit and the ignimbrite.

Summary: The LBT eruption began with a very steady, moderate intensity Plinian phase (unit A) followed by successive Plinian phases indicative of column instabilities and increasing intensity interpreted on the basis of lithic content and lithic isopleth, reaching a climax during deposition of fall unit C. Some pauses in deposition may have occurred. The first pyroclastic flows to arrive in this area were violently emplaced, having formed basal pumice dunes (a type of layer 1P deposit) by some kind of turbulent mixing process at the flow head, perhaps analogous to processes envisaged to occur in the Taupo ignimbrite (Wilson, 1985).

To reach Stop 3A, walk or drive about 600 m (this mileage is not included in the log) to the northeast from the main Copar pumice pits following a jeep trail that passes trial pumice excavations. The trail enters a small, unnamed arroyo where you should turn right and walk downstream about 30 m until the arroyo makes a sharp right turn. The unit of interest lies in the east bank just above the stream bed.

Stop 3A: Pre-Bandelier high-silica rhyolite Plinian deposit at top of Puye Formation

Significance: The arroyo bank exposes a 2-m-thick Plinian deposit (Fig. V21) that correlates with the pre-Bandelier San Diego Canyon (SDC) ignimbrites exposed in the southwest part of the Jemez Mountains (Turbeville and Self, 1988). Such exposures of pre-Bandelier high-silica rhyolite pumice falls are rare in the Jemez field; only one other exposure of a similar deposit is known.

Description: The age of this Plinian deposit is considerably less than 2.5 Ma based on its position near the top of the Puye Formation above horizons giving 2.5-2.4 Ma K—Ar age dates. An $^{40}Ar/^{39}Ar$ age obtained on SDC ignimbrite B of 1.78 Ma (Table V1) fits well with the expected age of this deposit (Spell et al., 1990). This Plinian deposit shows a considerable crystal concentration (enrichment factor is 4-5) and was probably once widespread.

After returning to the Copar pumice quarry, retrace the route to the confluence of Rendija Canyon and Guaje Canyon, FS-57 and FS-442 (11.4 mi). Turn right up Rendija Canyon (FS-57). This road climbs gradually through spectacular Puye Formation exposures, including dacitic Puye ignimbrite and Plinian deposits. Past the Sportsmen's Club (14.7 mi) the road runs on the Puye surface with cliffs of Bandelier Tuff above to left. At 14.9 mi turn right onto a small, unmarked track and stop at edge of stream valley (15.0 mi). Walk northwards downslope and across the (usually dry) stream bed and continue for about 300 m, heading towards a prominent cliff. The outcrop for Stop 4 is exposed at base of the cliffs.

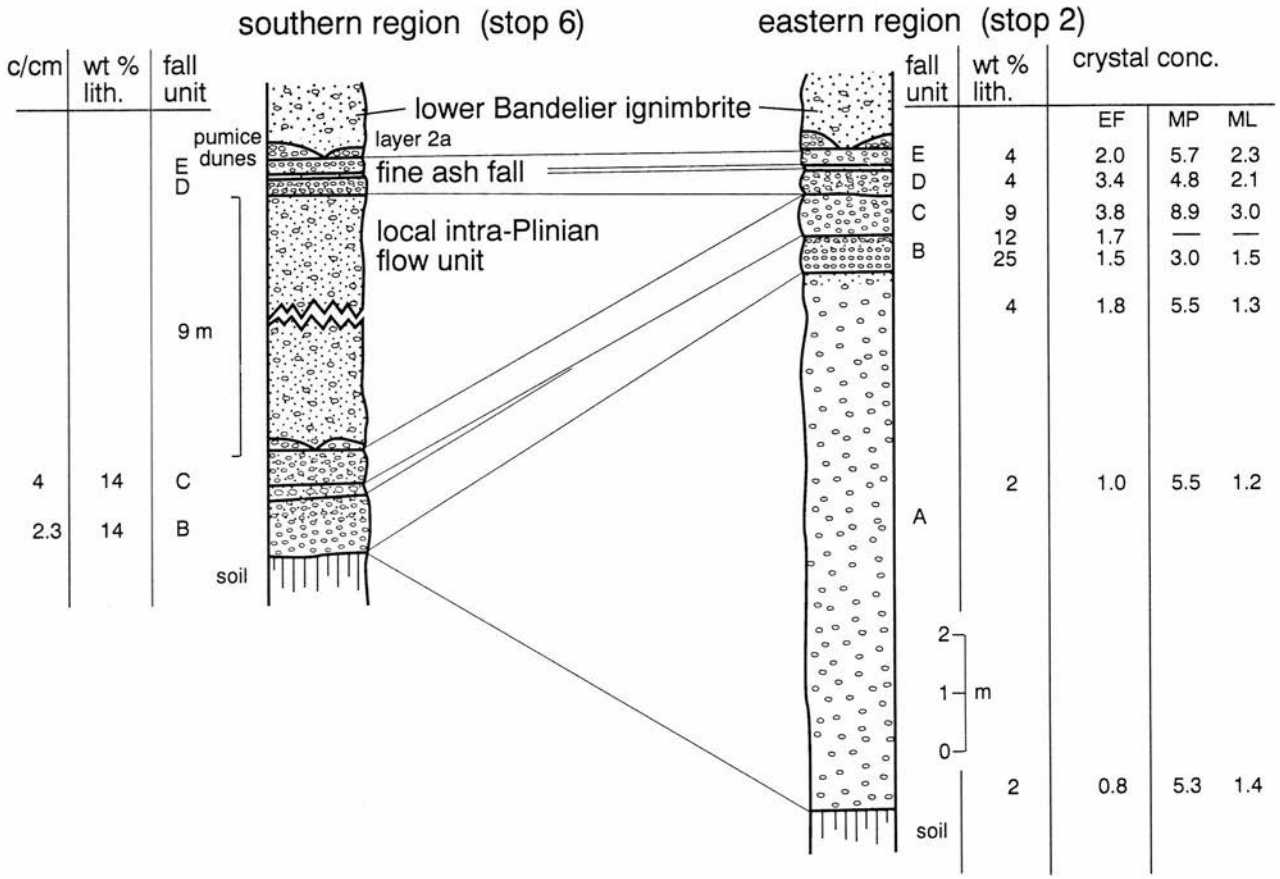

FIGURE V17—Lower Bandelier Plinian deposit and ignimbrite at Copar pumice quarries (Stop 3) showing proposed correlation of fall units between this area and the southeastern Jemez Mountains (area of Stops 7–8). ML and MP = average maximum lithic and pumice clast size in centimeters, respectively; EF = crystal enrichment factor.

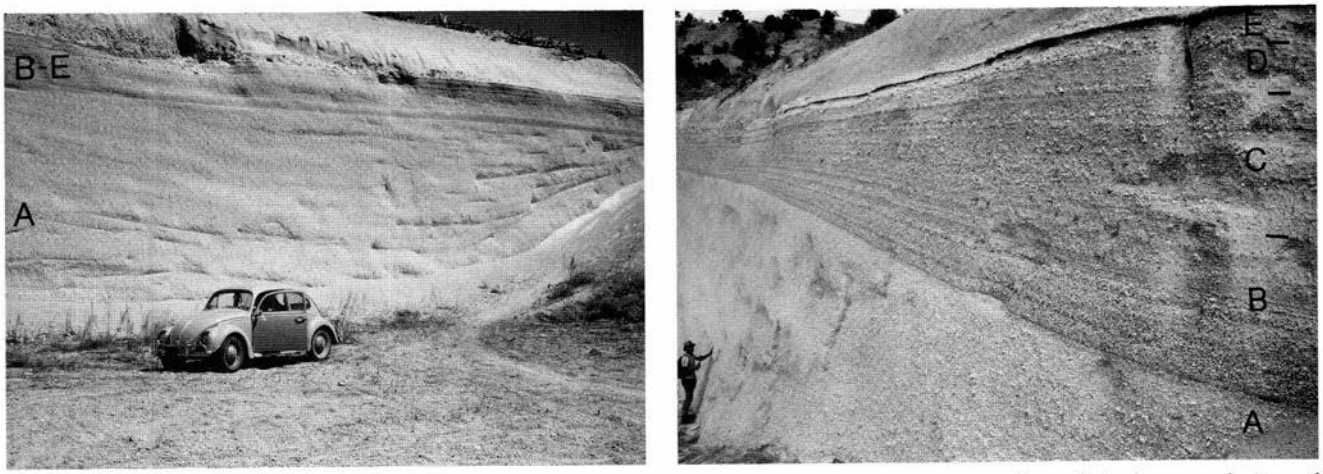

FIGURE V18—Pumice fall units of the lower Bandelier Plinian deposit at Copar pumice quarries (Stop 3). Left, general view of units; right, detail of upper bedded fall units B–E.

Stop 4: Upper Bandelier Tuff surge deposits and Cerro Toledo pumice-fall deposits.

Significance: This exposure of proximal to medial UBT contains a fine-grained set of basal surge deposits. The outcrops also show the Cerro Toledo pyroclastic-fall deposits which were deposited between the two Bandelier Tuff ignimbrites.

Description: The upper Bandelier Plinian fall unit is **the** widespread unit B (note high crystal concentration). The UBT ignimbrite is 55 m thick at this location and composed of at least 8 flow units (Fig. V22), showing the same three groups as at Stop 1. Other than a general similarity in sequence through the ignimbrite, including the presence of a thick (15 m) lower, nonwelded flow unit and a group of thinner flow units above, it is difficult to correlate in detail with the UBT at Stop 1. Fine-grained surge deposits at the base may be either very thick unit C or fine-grained surges preceding the main flow units. The latter interpretation is favored based on correlation with other nearby outcrops. These fine-grained surge depos-

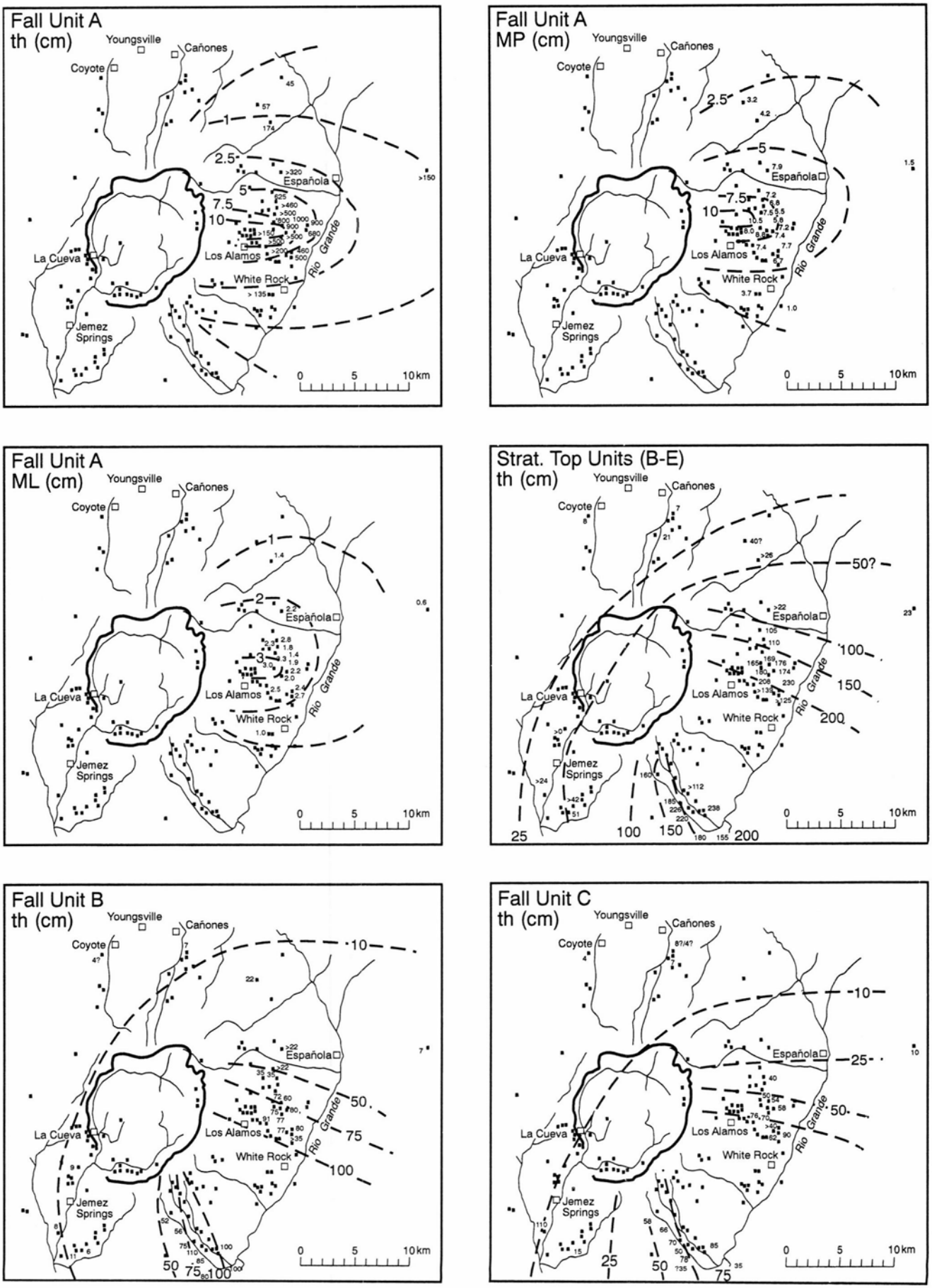

FIGURE V19—Isopach and isopleth maps of selected lower Bandelier Plinian fall units. In fall unit A isopach (th) map, the isopach values are in meters. Heavy line is Valles caldera topographic rim.

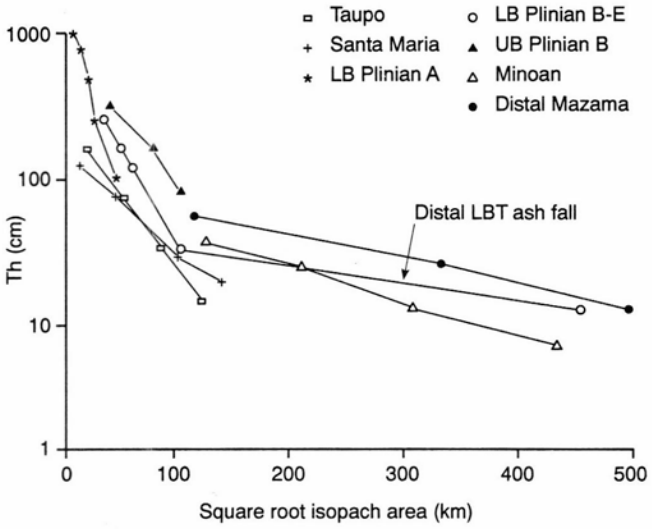

FIGURE V20—Plot of unit thickness versus the square root of isopleth area (after Pyle, 1989) for the Bandelier Plinian units, and other Plinian (Taupo and Santa Maria) and co-ignimbrite (Minoan and distal Mazama) ashes. Note similarity of slope of distal-fall lower Bandelier Tuff deposits and co-ignimbrite ashes.

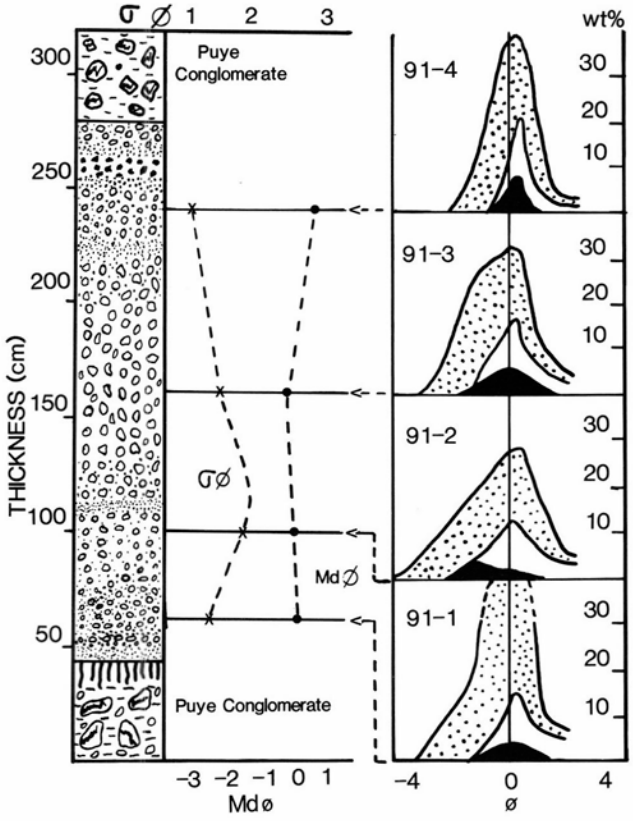

FIGURE V21—Pumice fall deposit G22 (high silica rhyolite) near Copar pumice quarries exposed in top of Puye Formation (high silica rhyolite) exposed in top of Puye Formation (from Turbeville and Self, 1988).

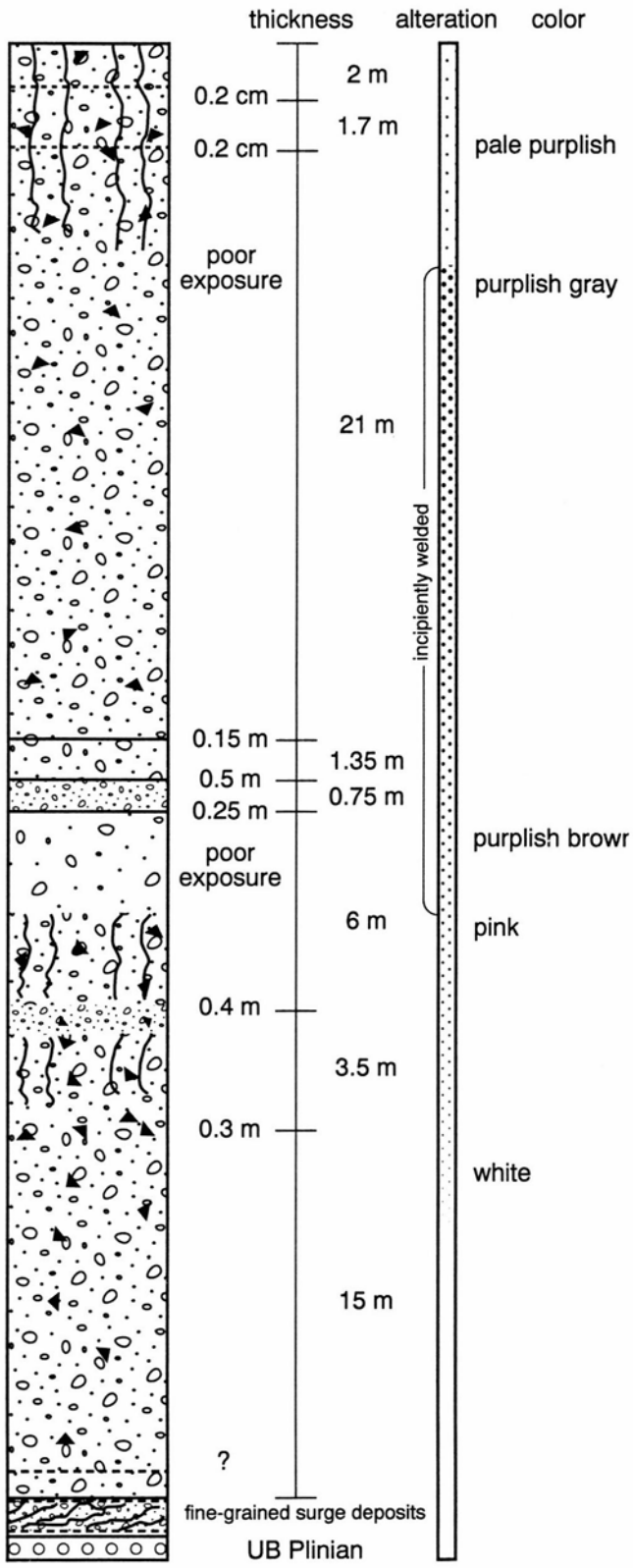

FIGURE V22—Section of upper Bandelier Tuff at Stop 4 showing basal fine-grained surge deposits, flow units, variations of welding and alteration, and the three depositional groups of units. Vertical lines show zones of crude columnar joints.

its are lithic-poor (less than 3 wt%) and are not quite as crystal-enriched as the ignimbrite. Bedform dimensions in the surge deposits at the base of the UBT show evidence of moderately violent emplacement (Fig. V23).

Cerro Toledo rhyolitic pumice deposits underlying the UB Plinian layer are also Plinian in nature and have ages in the 1.5-1.11 Ma range (Table V1; Spell et al., 1990; Spell, McDougall, and Doulgeris, submitted). Lava domes related to these fall units fill the Toledo embayment.

Summary: The transition between the Plinian and ignimbrite-forming phases of the UB eruption was characterized by the production of fine ash fall and surge deposits, both at the level of unit C and at the very base of

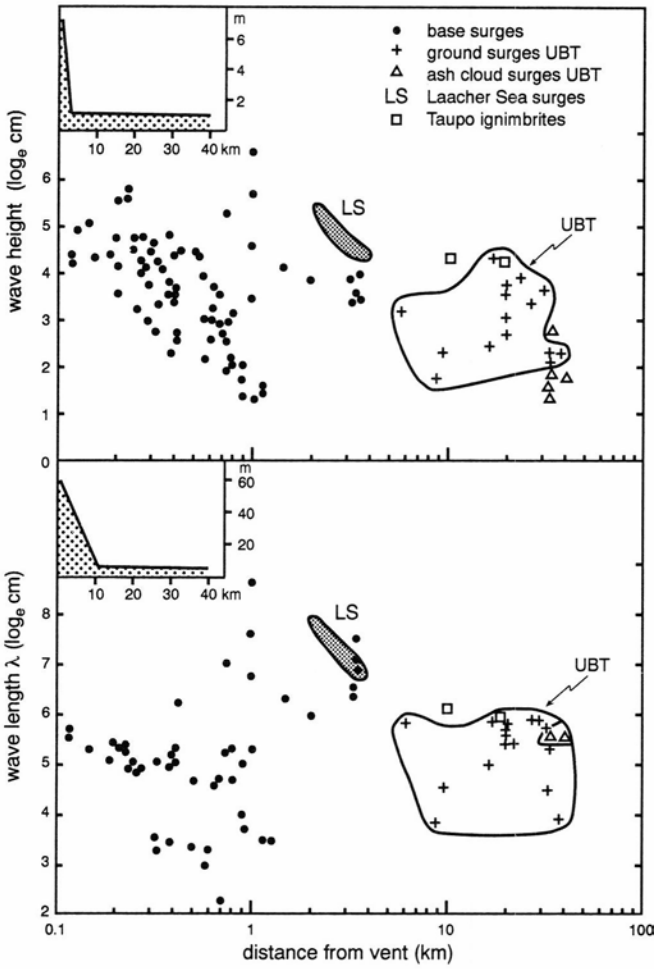

FIGURE V23—Plot of wave-height and wave length versus distance from vent for pyroclastic surge bedforms from various pyroclastic deposits taken largely from the literature. +'s are ground surge deposits at base and between upper flow units of the upper Bandelier Tuff (UBT) (J. V. Wright and S. Self, unpublished data); triangles are UBT ash cloud surges (R. V. Fisher, unpublished data).

the ignimbrite. Were these the result of phreatomagmatic activity at the transition? The fine-grained surges are broadly similar to the overlying ignimbrite in crystal and lithic content, but differ markedly in crystal content and sorting from the interflow unit surge deposits seen at Stop 1. Here, at Stop 4, surges are absent in the thin flow unit interval about 30 m up into the deposit.

Retrace the route to the road in Rendija Canyon and proceed upcanyon (to the right). The road crosses the Pajarito fault zone (Fig. V2). Turn right at the junction with Barranca Rd., Los Alamos (15.9 mi). Follow the main road to the four-way junction, then turn right onto Diamond Drive. Continue on Diamond Drive to the fire station, then take the right turn to Guaje Pines Cemetery. Follow this road as it curves right until it becomes dirt-surfaced (unnumbered FS road), and proceed into the upper reaches of Rendija Canyon where the road begins to climb through Bandelier ignimbrite. Stop and park near the metal gate (17.0 mi). The outcrop for Stop 5 occurs in the road cut both up and down slope from the gate.

Stop 5: Proximal upper Bandelier Tuff

Significance: A more proximal but thinner UBT sequence is exposed that shows multiple gas-escape pipes in the lower part of the ignimbrite. The **UBT** package of flow units is a condensed sequence containing representatives of each of the three main groups. Interflow unit surge deposits, related to the deposition of the middle and upper groups of flow units, are well developed.

Description: Fall-unit B of the UBT Plinian deposit rests on Cerro Toledo pumice-fall deposits. It is overlain by nonwelded ignimbrite with a surge deposit at the base (Fig. V24). The lower part of the ignimbrite contains two flow units and each shows prominent gas-escape (elutriation) pipes. In one case a pipe crosses a flow unit boundary. The upper flow unit becomes incipiently welded, and above this is a group of thin, variably welded flow units with prominent ground-surge deposits between them. The origin of these cross-stratified surge deposits is uncertain. The upper flow unit is poor in coarse clasts, including lithic clasts, and is purplish-grey and moderately welded.

Summary: Although located 13 km from the Valles caldera ring fracture, this exposure is one of the most proximal, giving a reasonably complete section through the UBT. The late (upper) welded flow unit(s) are proportionately thicker here and will be seen again at the next stop. The area around Los Alamos exposes some of these late, welded, coarse-clast-depleted flow units, with ground surge deposits at flow unit boundaries. These may have been outflows occurring during the period of intracaldera ignimbrite formation, if the lithic-rich ignimbrite units beneath (not seen at this stop) represent flows formed at the time of caldera-collapse. Beneath these late flow units, a significant gap in deposition occurs due perhaps to the position of this exposure on steep topography. The early flow units at this exposure show evidence of deposition in an environment of vigorous fluidization, due again to their position at the base of steep topography.

Retrace your route to Diamond Drive, and turn right, following the road past Los Alamos Golf Club and across one set of traffic lights. On the left is Los Alamos Baptist Church (18.8 mi); pull into the church parking lot. The exposure for Stop 5A is in the road cut on the other (north) side of Diamond Drive. EXERCISE EXTREME CAUTION; THIS IS A BUSY ROAD.

Stop 5A: Late upper Bandelier ignimbrite and ground surge deposits

Significance: This exposure of late, welded UBT flow units includes thick accumulations of surges, possibly in a paleo-topographic low at the head of a canyon cut into the LBT (equivalent to the present-day Pueblo Canyon).

Description: The proximal, welded, upper part of the UBT contains beds of pyroclastic surge material with prominent crossbedding at this exposure (Fig. V25). Surge unit thicknesses are approximately 0.5 m. Amplitude and wave lengths of dune forms are approximately 0.4 m and 2.0 m, respectively. Bedset angles vary up to 35°. These units occur in the upper group of flow units of the UBT, which has a grey color due to welding, and are closely related to welded flow units. Sparse lithic clasts of country rock (Madera Limestone of Carboniferous age) occur. They may be either ground surge deposits left by the passage of flow units or deposits at the edge of high concentration flows which were channeled down local drainages. Flow direction was roughly eastward (perpendicular to the outcrop face).

Summary: Late flow units of the UBT are welded, despite the thinness of such units. This is probably due not to compositional zonation preserved in the deposit (i.e., later units are not composed of more mafic, hotter juvenile material) but to the eruption mechanism forming these pyroclastic units. They were formed from lower

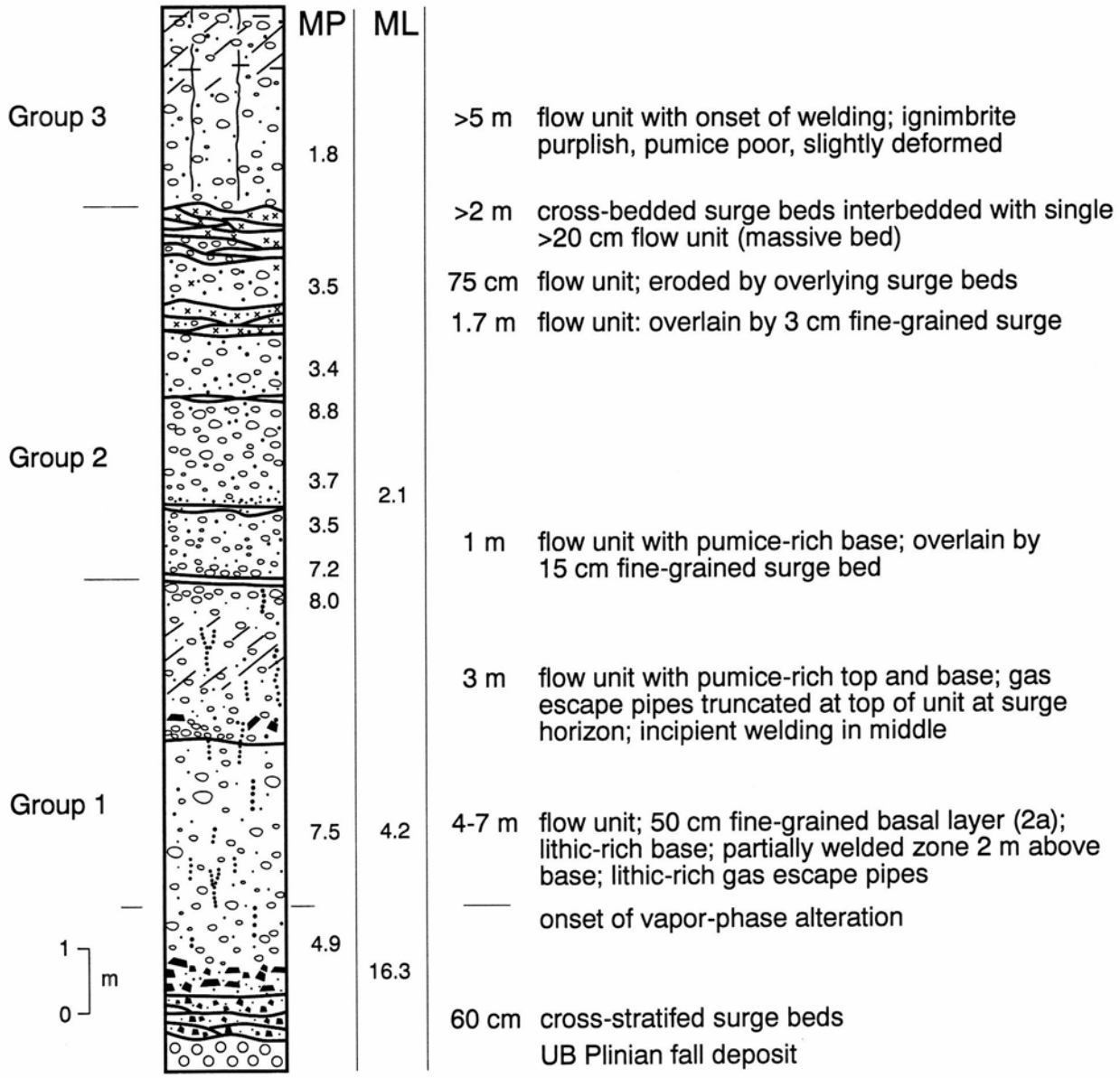

FIGURE V24—Section through upper Bandelier Tuff at Stop 5 showing flow units, welding and vapor phase alteration zones, and the three depositional packages. Note gas-escape pipes in the lower flow units. ML and MP = average maximum lithic and pumice clast size in centimeters, respectively.

eruption columns and thus retained a higher temperature, a conclusion supported by the apparently restricted dispersal of these units. They are rarely found in medial to distal locations in this sector of the outflow sheet. The precise origin of the surge deposits is under debate.

Return to White Rock via Los Alamos (about 12.5 miles depending on route taken). Total mileage for day should be about 31 miles.
END OF DAY 1.

Day 2: Lower Bandelier Tuff in distal and proximal locations and products of the youngest eruptions (~0.3-0.2 Ma) from the Valles caldera

From White Rock (0 miles), drive on NM-502/4 towards Bandelier National Monument and Jemez Springs. NM-502/4 passes through several canyons exposing UBT (to be examined on Days 4 and 5) and past the entrance to Bandelier National Monument (8.2 mi). Beyond this, for 6 miles, you are

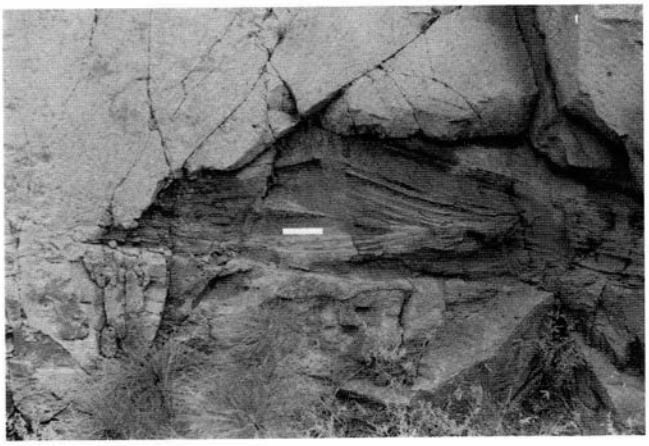

FIGURE V25—Surge deposit between welded, thin flow units in upper part of upper Bandelier Tuff at Stop 5A. The scale is 10 cm long.

traveling on the Bandelier ignimbrite surface, here known as the Pajarito Plateau. Just above the junction of this road with the Los Alamos loop NM-502(4A), a steep hill climbs the main, post-1.1 Ma scarp of the Pajarito fault which down drops the UBT by up to 200 m. The most recent movements on this fauli occurred about 20,000 years ago. At the top of this scarp, densely welded UBT flow units from late in the second Bandelier eruption are seen. The outcrop for Stop 6 occurs just above a sharp right-hand curve. Park in the limited space on the side of the road (15.9 mi). THIS STOP OCCURS NEAR A VERY DANGEROUS CURVE IN THE ROAD. PLEASE EXERCISE CAUTION.

Stop 6: Welded upper Bandelier ignimbrite

Description: The UBT exposed on the Pajarito fault scarp is one of the most densely welded found in the outflow ignimbrite with a density of 2.2-2.3 g/cm^3, compared to 1.1 g/cm^3 for nonwelded ignimbrite,and has flattening ratios of 6:1 in fiammé (deformed juvenile clasts). These are interpreted to be late-erupted flow units, perhaps hotter upon emplacement than lower units because of formation from collapse of lower eruption columns. Crystal-rich gas-escape pipes abound. The grey, pumice-poor ignimbrite is devitrifled and slightly vapor-phase altered. Lithic clasts are sparse. Thin surge beds can be found, indicating the presence of several flow units. The surge beds are not as intensely welded as the body of the ignimbrite flow unit.

Note also the vista from the top of the fault scarp over the Pajarito Plateau, the Bandelier Tuff surface sloping gently 5°) eastward to the Rio Grande rift, and to the Sangre de Cristo Mountains beyond.

To reach Stop 7, continue west on NM-502/4, crossing the head of Frijoles Canyon (21.1 mi), and turn left at the junction of FS-289 (21.9 mi). Follow FS-289 (sign posted Cochiti), taking the left fork at the junction with FS-36 (24.2 mi). At 29.6 mi, a photograph stop may be made along FS-289 at the overlook of Cochiti Canyon (to the right side of the road) where Bandelier Tuff overlies gravels of Cochiti Formation (Fig. V3) and andesite lavas of Paliza Canyon Formation (8.5-9.5 Ma). From this point until the next stop, FS-289 runs across andesite-rhyolite lavas and minor intrusives of the San Miguel Mountains (Keres Group, 13-6 Ma), which form a large "kipuka" (an area of older rocks surrounded by ignimbrite or lava), in the Bandelier ignimbrite sheet. The young surficial pumice deposit in this area is the El Cajete Plinian pumice (circa 200 ka). The road begins to descend the scarp of the Pajarito fault zone at 34.2 mi. Proceed on FS-289 until it meets FS-268 (37.9 mi). Turn right on FS-268 and continue to the junction with FS-89 (39.3 mi). Note: FS-268 bears left, but you should continue straight ahead on FS-89. Stop on the left side of the road at the bottom of the small hill, opposite an apple orchard (40.0 mi), where the outcrop for Stop 7 occurs in a low cut on the west (right) side of the road.

Stop 7: Lower Bandelier fall units, Cochiti Canyon

Significance: LBT Plinian fall units B—D are present here; the main fall unit A (seen at Stops 1 and 2) of the LBT (Guaje) pumice-fall deposit is missing. Thin, fine ash-fall units occur between pumice-fall units, and one of these contains accretionary lapilli.

Description: Coarse and lithic-rich fall units of the upper sequence of the lower Bandelier Plinian deposits (Fig. V26) correlate with the sequence in the eastern Jemez, seen at Stops 1 and 3. These deposits therefore demonstrate evidence of a wind shift during the LBT eruption from westerly during deposition of fall unit A to northwesterly during deposition of units B—D. They also have more widely dispersed coarse clasts than fall unit A. Fine ash falls between the pumice-fall units are well developed in the lower Bandelier Plinian deposit in the southern part of the Jemez Mountains and thicken towards the northwest. Occasionally accretionary lapilli can be found in these ash beds, as between B and C here, suggesting wet eruption clouds during these intervals.

Summary: Unit B is considerably more lithic-rich than unit A and possibly represents a period of vent widening, leading to an increased mass eruption rate. Pauses in the Plinian eruption are marked by fine ash beds, which may be co-ignimbrite ashes. At the next location (Stop 8) an intra-Plinian ignimbrite unit occurs between units C and D. The source of moisture needed to generate accretionary lapilli in these fine ash clouds may have come from secondary explosions as ignimbrite invaded local water courses.

FIGURE V26—Lower Bandelier Plinian fall units B–E and base of lower Bandelier Tuff ignimbrite, above D, at Stop 7.

To find Stop 8, turn around. It is located 300 m along FS-89 at the prominent cliffs on the left (west) side of the road (40.3 mi).

Stop 8: Intra-Plinian lower Bandelier ignimbrite and general character of ignimbrites, lower Cochiti Canyon

Significance: This edge of Horn Mesa exposes a complete section through both units of the Bandelier Tuff in the southern part of the Jemez Mountains. Intra-Plinian ignimbrite occurs between fall units C and D of the lower Bandelier Plinian deposit. The transition from Plinian to ignimbrite-forming activity was gradual and featured at least one partial column collapse phase giving sectorially distributed intra-Plinian ignimbrite.

Description: *Lower Bandelier Tuff:* The earliest record of major instability in the lower Bandelier Plinian eruption column is an intra-Plinian flow unit (Fig. V27, left), here exposed at a distance of 27 km from the center of the caldera. The flow unit was confined to paleo-Cochiti Canyon, and appears after the deposition of lithic-rich fall units B and C. This is the only such example found so far but others may exist. Above it are fall units D and E, which are rarely preserved elsewhere due to erosion of the top of the Plinian sequence by the early ignimbrite flow units. The intra-Plinian flow unit has pumice dunes (layer 1P

deposits) at the base and is lithic-poor (<10 wt%). At other nearby locations the horizon of the intra-Plinian ignimbrite is marked by fine ash fall.

The base of the main ignimbrite has a thin sequence of pumice-rich flow units (Fig. V27), distal representatives of a set of early flow units. Above this is 70 m of homogeneous ignimbrite incipiently welded in the middle. A pumice concentration zone at the top contains pumice clasts up to 90 cm diameter. This thick unit is capped by the remnant of another flow unit.

Upper Bandelier Tuff: Plinian fall unit B occurs above the soil on the LBT; and here unit B has a fine ash layer near the base, probably correlative to upper Bandolier Plinian unit A found in the western Jemez Mountains. Above this is a 40 cm thick pumice-rich, lithic-poor flow unit capped by thick ignimbrite that shows few signs of flow unit partings. The onset of welding is seen about 20 m above the base in this same unit. Note that the gully climbed at this location is fault-controlled, and this fault is, in fact, a splay of the young Pajarito fault zone down-dropping the ignimbrites by about 15 m to the east.

Summary: The significance of the LBT intra-Plinian ignimbrite has been discussed above. The LBT again shows a thick, homogeneous lower unit, seen throughout its dispersal area, and thin pumiceous basal flow units. The UBT shows a similar sequence but is welded in its upper part. A point to consider is the correlation, or lack thereof, between the internal ignimbrite flow unit stratigraphy of the southern and eastern Jemez Mountains.

For Stop 9, retrace the route on FS-289 to the crest of the steep climb with switchbacks out of Cochiti Canyon (46.2 mi). A small un-named canyon occurs on the left. The roadcut on the right contains exposures of coarse epiclastic deposits capped by Bandelier Tuff, which form the outcrop of interest.

Stop 9: Lateral margin of upper Bandelier ignimbrite sheet near Cochiti Canyon

Significance: This exposure shows the way in which upper Bandolier ignimbrite flow units lap against a paleo-

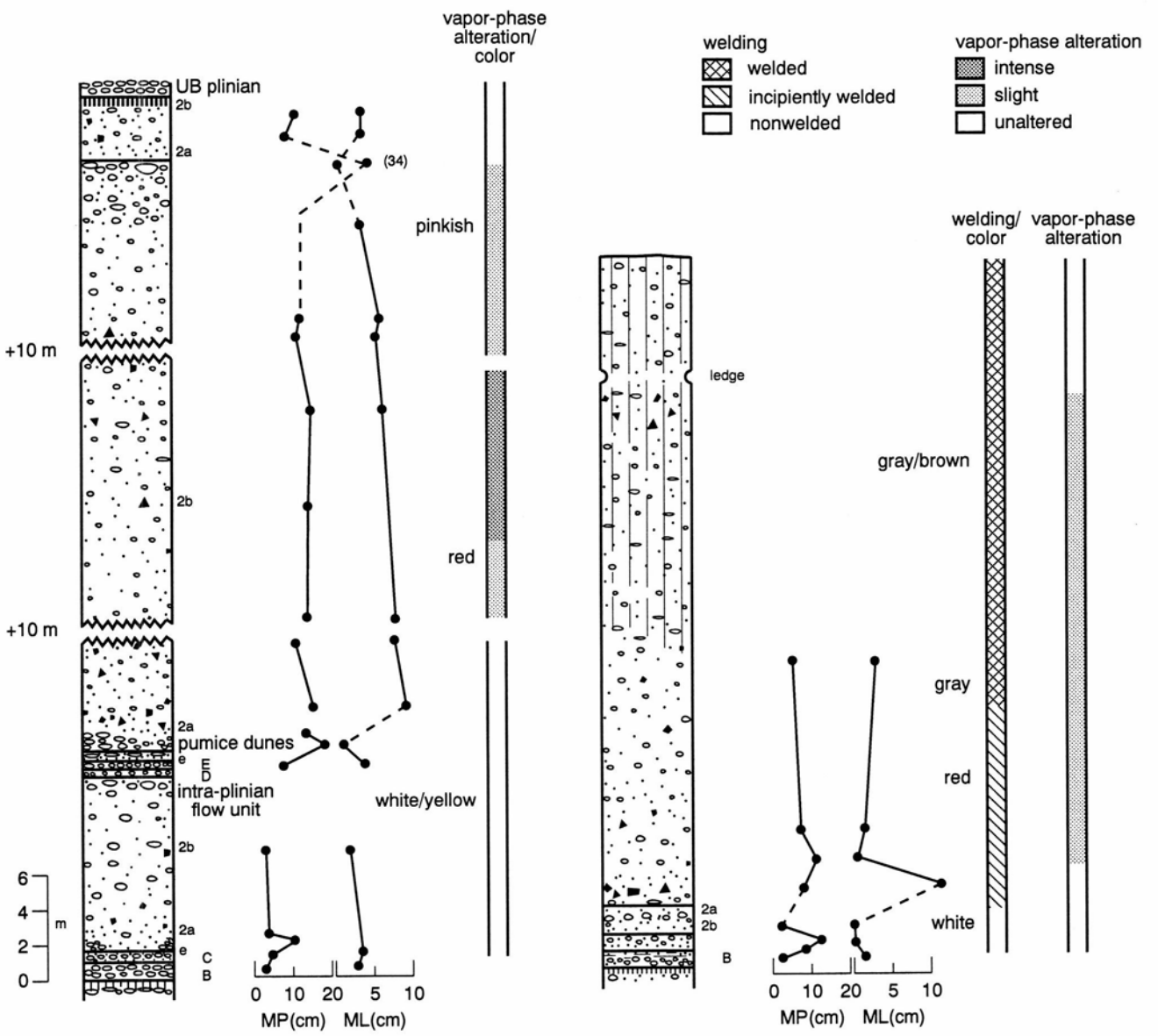

FIGURE V27—Left, section through lower Bandelier Plinian deposit and ignimbrite section at Stop 8, showing flow units and color zonation. Right, section through upper Bandelier section; note absence of obvious flow unit boundaries above basal region. ML and MP = average maximum lithic and pumice clast size in centimeters, respectively.

topographic high. The ignimbrite also contains a wide range of pumice clast types and compositions.

Description: UBT flow units bank up onto a preexisting high of Paliza Canyon age volcaniclastic deposits, part of the lower Cochiti Formation (Fig. V28). At the base are bedded deposits that may be thin ignimbrite veneer deposits (or surge deposits) which drape over the topographic high. Plinian fall units are absent. Above this a number of ignimbrite flow units pinch out, demonstrating gradual filling-in of the topography (Fig. V29); each has pumice concentrations at the base and margin.

Chemical analysis of samples from individual flow units through the sequence has shown that compositions of pumice clasts at this location cover almost the entire range found in the UBT (Balsley, 1988), except for the most evolved types (Nb > 150 ppm; Fig. V29, bottom). This indicates that pyroclastic flows arriving at this point carried pumice clasts from the magma body covering a wide range of compositions and that there is no trend stratigraphically towards selectively less-evolved compositions. Aggregate pumice clasts are found in several flow units; they are individual clasts of pumice breccia

FIGURE V28—Upper Bandelier ignimbrite flow units (left of contact) at Stop 9 can be seen to onlap an older valley wall or topographic high composed of Cochiti Formation gravels in front of person.

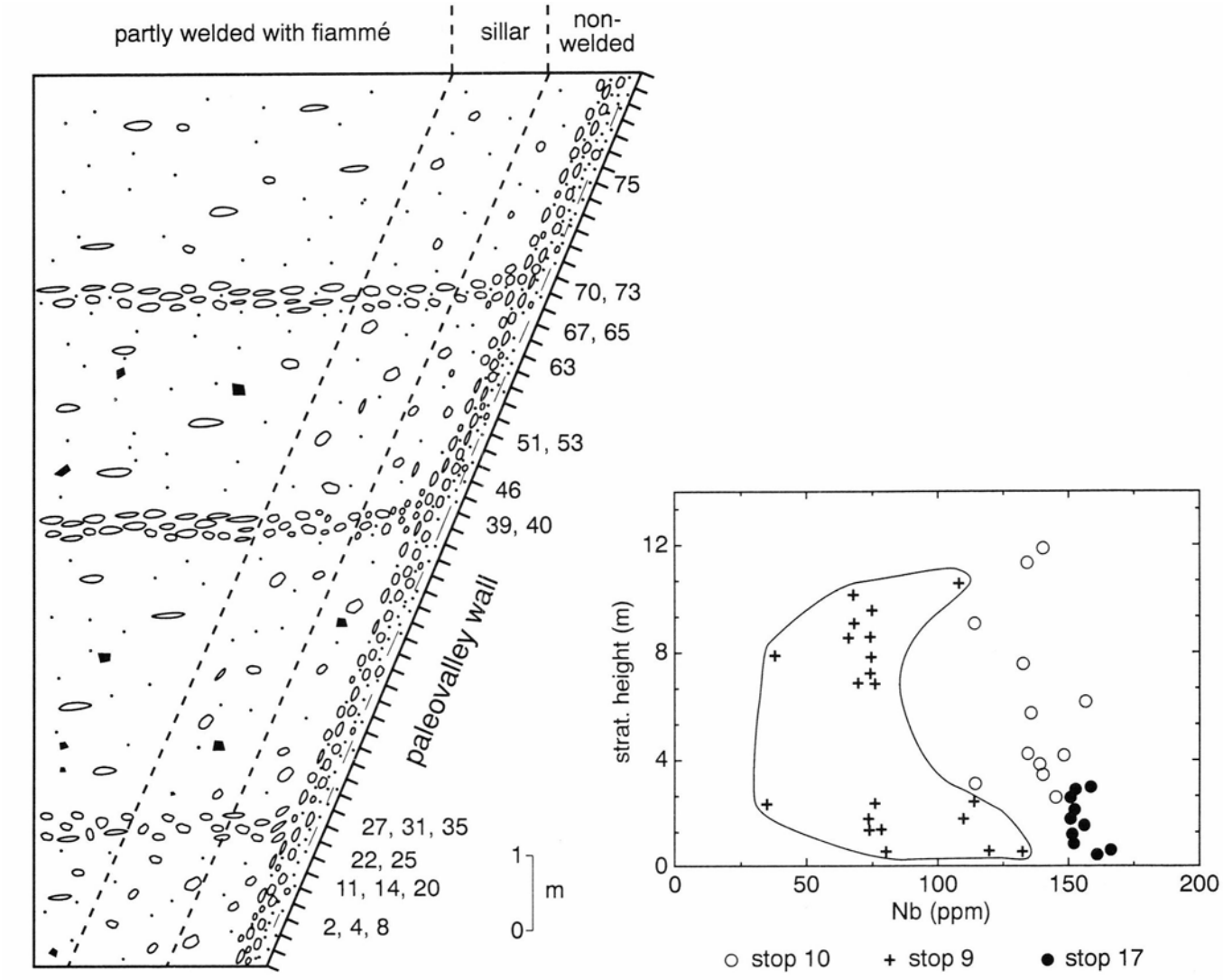

FIGURE V29—Left: Schematic diagram of contact zone between upper Bandelier Tuff (UBT) and Cochiti Formation at Stop 9 showing levels where pumice samples were collected from subhorizontal flow units for geochemical analysis (numbers at right). Right: Nb content (ppm) of whole pumice clasts plotted against stratigraphic height for two UBT locations (Stop 9, +'s; Stop 17, dots) and one LBT location (Stop 10, open circles). (after Balsley, 1988). Note the wide range of Nb contents indicative of degree of chemical evolution, especially in the lower flow units at Stop 9, (after Balsley, 1988).

in pumiceous, glassy, lithic-bearing matrix. They are evidence for syneruptive agglutination in the vent system, followed by disruption and incorporation of this material into flow units (Wolff et al., 1989).

Looking west across the small (unnamed) canyon below, a lithic-rich zone can be seen in the UBT; it is not easily accessible. The lithic-rich horizon may represent a lithic-rich zone occasionally found in the middle group of flow units in the east. It is not certain which flow unit at the roadside exposure correlates with this horizon.

In the distance to the southeast, the Parajito fault creates a bench in the Bandelier Tuff surface (downthrown to east), and the Santo Domingo Basin of the Rio Grande rift can be seen.

Summary: The deposits at this location probably record deposition during most of the ignimbrite-forming phase of the UBT eruption, from the early thin, violently emplaced veneer or surge deposits to some of the late flow units.

To reach Stop 10, proceed up FS-289 back to NM-502/4 (58.5 mi), then turn left (west) on NM-502/4. At 59.3 mi NM-502/ 4 descends into the southeasternpart of the moat of Valles caldera, called Valle Grande (see Stop 12). Follow NM-502/4 along the caldera moat; at 66.3 mi the road crosses the east fork of the Jemez River and rises onto the South Mountain rhyolite lava flow (-0.52 Ma; Table V1). Thick surficial deposits exposed along this road are El Cajete Plinian pumice and associated pyroclastic flow deposits, products of one of the latest eruptions from the caldera. Turn left off NM-502/4 at FS-10 by the row of mail boxes on the left (68.9 mi). Follow FS-10 to its intersection with FS-135, then turn right to Cat Mesa. Stop at the hairpin left-hand curve on FS-135 (73.0 mi). To reach Stop 10, walk along the small trail (just big enough to take a vehicle) that leaves FS-135 to the right (north) 25 m before the hairpin curve. Walk to the cliff edge for the view in Figure V30, or follow the small steep trail off the right side of the cliff leading down the vegetated slope until you obtain a view of the cliff face to the left. The outcrop of interest for Stop 10 occurs midway up the cliff face. Note: the outcrop can only be viewed from the steep trail.

Stop 10: Proximal lower Bandelier ignimbrite, Cat Mesa

Significance: This location on the southwest topographic wall of the Valles caldera provides an excellent overview of the southwestern part of the caldera (Fig. V30) and a complete section through the LBT ignimbrite, including proximal lithic breccias (featured in Self et al., 1986). It is one of the few places in the Jemez Mountains where one can interpret the later phases of LB ignimbrite activity, because the late-erupted facies are rarely seen exposed.

Description: The ignimbrite sequence at Cat Mesa (Fig. V31) is from the lower, thick homogeneous unit to upper welded flow units which are rarely preserved. A prominent horizon of lithic breccias occurs about two-thirds of the way up the sequence (Fig. V32). The base of the ignimbrite has no Plinian deposit, typical of caldera wall exposures. A horizon of thin flow units divides the main lower unit which is characteristic of LBT exposures in the southwest sector of the Jemez Mountains.

The lithic breccias are of several types and range in lithic content from 90 to 60 wt%. The main bed is a true lag fall or just downflow from one. This 9 m thick deposit has a lenslike form and pinches out downflow and laterally along the caldera wall. Several other pods and beds of breccia are found at this same horizon along the southwest topographic wall. Due to their coarseness these deposits must have formed close to a vent, and the proposed vent site for the Plinian deposits was too far away (about 12 km) to account for the lag breccias (Self et al., 1986). Therefore these breccias probably record the opening of vents along the ring fracture of the Valles caldera, which is about 2 km distant. Lithic clasts are 90% Paliza Canyon andesite with minor rhyolite and Paleozoic clasts and sparse basement rocks (Eichelberger and Koch, 1978). Above the breccias the LBT develops welding and evidence of late LBT flow units can be seen towards the top of the mesa. Note also the local fault offset of the LBT at Cat Mesa, down-dropped to the east.

Incipiently welded upper LBT ignimbrite flow units can also be studied close-by in small roadcuts on FS-135 just to the south, upslope from the hairpin curve.

Summary: From this exposure (and several others like it), a model related to a composite section was developed for the later parts of the LBT eruption (Fig. V33). If the lithicrich ignimbrite under the proximal breccias and the breccias themselves record the main caldera collapse phase, then the welded units above may be outflow equivalents to the intracaldera LBT. A point to consider is the origin of proximal lithic breccias and their significance to the onset of caldera collapse.

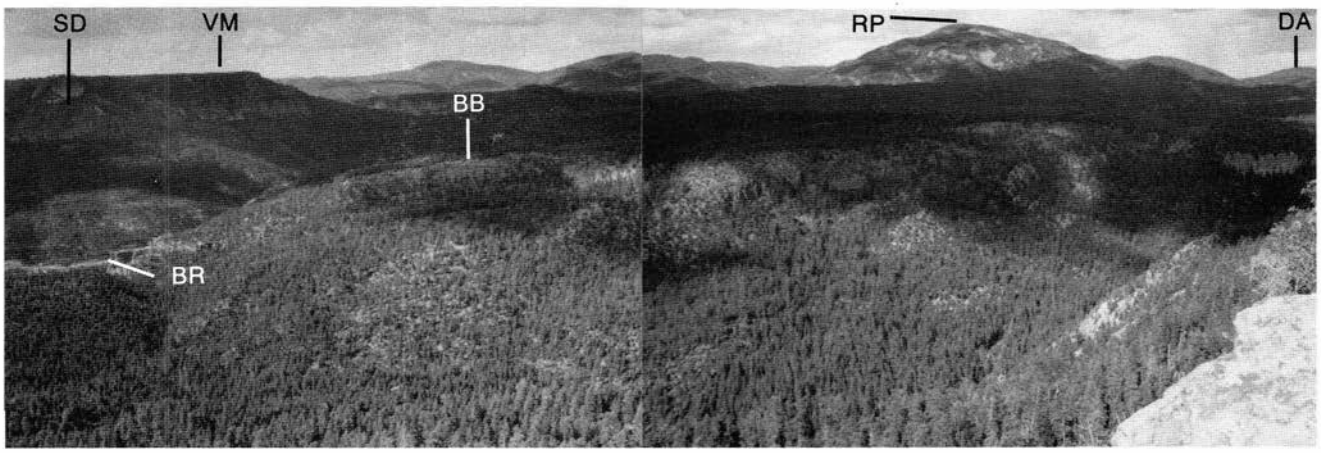

FIGURE V30—View looking north-northwest from edge of caldera rim, Stop 10, across the Valles caldera moat showing (from left to right): San Diego Canyon (SD), Virgin Mesa and southwest caldera wall (VM), Battleship Rock ignimbrite (BR), Banco Bonito vitrophyre lava flow (BB) overlying South Mountain rhyolite lava flow, Redondo Peak (RP) on resurgent block, and Cerro del Abrigo (DA), one of the Valles intracaldera lava domes.

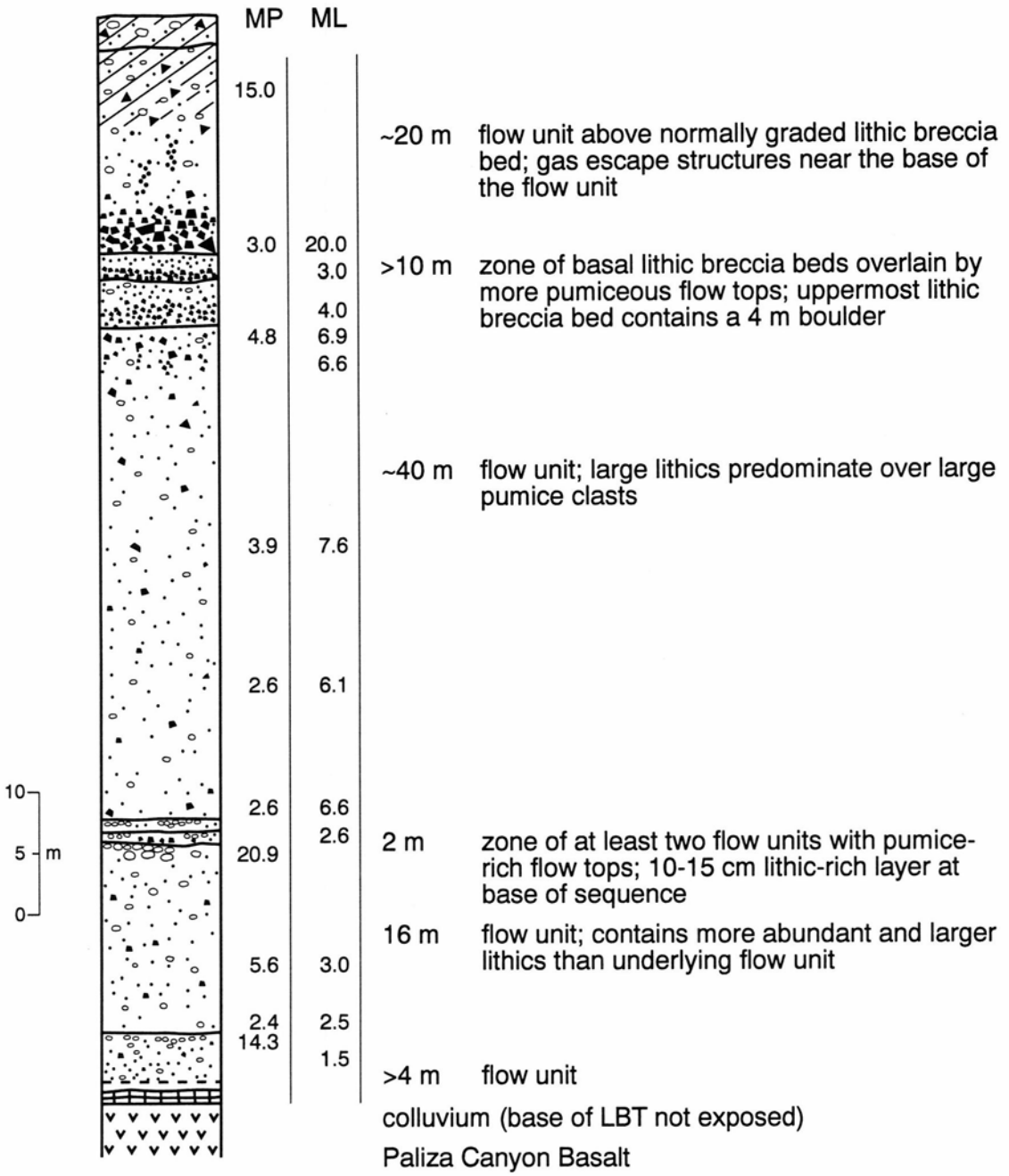

FIGURE V31—Section through the lower Bandelier Tuff (LBT) at Cat Mesa (Stop 10) showing MP and ML and flow unit boundaries, (after Kite, 1985). Note on Fig. V29 that the Nb content of whole pumice clasts samples from the lower 12 m of the lower Bandelier Tuff here show a weak up-section trend towards lower Nb content (less evolved). ML and MP = average maximum lithic and pumice clast size in centimeters, respectively. Diagonal lines indicate welded zone.

Retrace the path back up to the road and then the route on FS-135 to FS-10. If NOT proceeding to Stop 10A, turn left (route continues after Stop 10A description). To reach Stop 10A turn right on FS-10, then follow the winding road downslope for about 7 km. Stop and park where this roadcuts through obvious outcrops of grey ignimbrite on the left side of the road. The exposures of interest occur in the roadcut and in a broad valley accessed most convieniently by climbing up the roadcut and proceeding straight ahead (eastwards).

Stop 10A: Vapor phase pipes in the upper Bandelier ignimbrite

Large (up to 1 m diameter), exceptionally well-exposed subvertical pipes of hardened ignimbrite (Fig. V34) are found in the "grey zone" of the UBT, a region of thermal coloration and devitrification that is found underneath the most densely welded zones. The pipes have an annular structure with a hard outer part and a soft interior. Their origin is probably related to vapor phase alteration during cooling of the ignimbrite sheet. Climbing up the slope above the roadcut and over the crest will bring the reader into an area with 10-15 m high columns or towers of vapor-phase altered UB ignimbrite and other wall-like vapor-phase features following joints. Please take care to preserve these features, particularly the ones in the roadcut. Hammering and taking of samples will soon cause them to deteriorate.

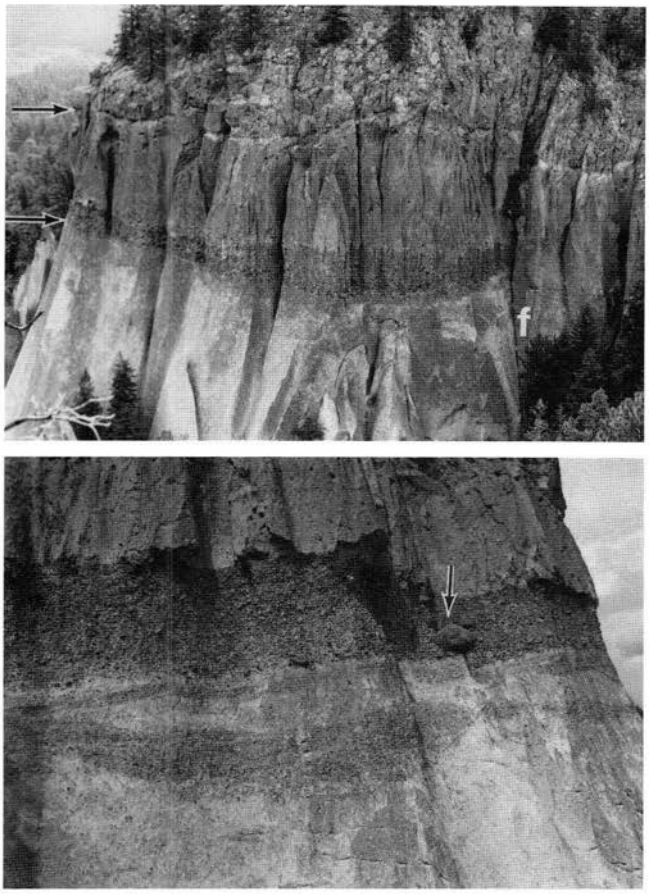

FIGURE V32—Proximal lithic breccias in the lower Bandelier Tuff (LBT) at Stop 10. Top: Proximal ignimbrite breccias of lower Bandelier ignimbrite exposed in Valles caldera wall at Cat Mesa. Prominent lithic bed (above lower arrow) is co-ignimbrite lag fall equivalent. Upper arrow marks vapor-phase alteration induced notch, above which lower Bandelier Tuff is slightly welded and vapor-phase altered. f is a fault with small downthrow on the right side. Bottom: close-up of main lithic breccia bed. Large (arrowed) boulder is > 2 m in diameter. More dispersed, lenticular lithic breccias below main bed are type 2 proximal breccias. Note lithic-rich, vertical, gas-escape pipes going from top of breccia bed into ignimbrite above.

From Stop 10A, retrace the route to the junction of FS-10 and FS-135 (rejoin route from Stop 10). Proceed north on FS-10, retracing the route to NM-502/4 (77.2 mi), then turn left. Proceed to the parking area on the right side of the road where NM-502/4 crosses the Jemez River (78.4 mi). The outcrop of Stop 11 is just uphill beyond the stream crossing.

Stop 11: Main section of El Cajete pumice deposits and Banco Bonito lava flow

Significance: The products of the two youngest eruptions from the Valles caldera are exposed here.

Description: This section in the moat of the caldera exposes South Mountain rhyolite lava (0.52 Ma; Spell and Harrison, 1993) overlain by El Cajete pumice-fall units, surge beds, and pyroclastic-flow deposits (Battleship Rock ignimbrite), in turn overlain by Banco Bonito vitrophyric lava flow (Fig. V35). The El Cajete deposit and related units have proven to be difficult to date accurately (Self et al., 1991; Spell and Harrison 1993). Until recently ages of 0.2 Ma for the Banco Bonito lava and 0.3 Ma for the Battleship Rock ignimbrite and El Cajete pumice fall (Table V1) were accepted, but recent work suggests a younger age 60 ka; Wolff and Gardner, 1995). A disconformity, probably representing more than 100 ka, occurs between the El Cajete units and two thin units associated with the lava flow. The vents for these youngest eruptive products are about 2 km north of Stop 11.

The El Cajete Plinian pumice-fall deposit is widespread in the southern Jemez Mountains and has a bulk volume of about 1.3 km^3. It was formed at the same time as small local flows and surges, seen interstratified with the Plinian units (Fig. V36). The upper flow units correlate with more extensive and voluminous pyroclastic flows that traveled southwest from the vent down San Diego Canyon, forming the Battleship Rock ignimbrite (Stop 15); further details can be obtained in Self et al. (1991). The El CajeteBanco Bonito magma batch is different compositionally from the high-silica rhyolite magmas that erupted from the Valles center up to the time of the South Mountain rhyolite. It is low-silica rhyolite, with an intermediate composition mineralogy, perhaps inherited from an andesitic source, and also contains xenocrystic sanidine (McCormick, 1989).

For Stop 12, turn around and retrace the route along NM-502/ 4 to the Valle Grande information board (88.0 mi).

Stop 12: Valles caldera overview

The southeastern moat zone of the Valles caldera is known as the Valle Grande, with the low ground underlain by caldera fill sediments and volcanics. The caldera is about 23 km in diameter from east to west and may contain more than 3000 m of fill down to the basement on the eastern side (Nielson and Hulen, 1984), see Figure V7. Figure V37 can be used to identify the features seen. In the opinion of the authors, most of the depression was formed at 1.51 Ma by the Otowi (LBT) eruption. Lava domes outline the ring fracture system of the younger (1.14 Ma) collapse event; for identification of the lava domes refer also to Figure V6. Redondo Peak (3431 m; 11,254 ft), the top of the resurgent intracaldera block, towers 800 m above the caldera floor. On the left skyline lies Rabbit Mountain, a remnant of the post-first caldera-cycle obsidian dome of Cerro Toledo age (Table V1) presumably truncated by the second-caldera-cycle collapse.

Two alternatives are possible here for the reader following this guide. Either continue southeast on NM-502/4 and return to White Rock following NM-502/4 (112 mi total for the day), or camp at one of several campgrounds in the caldera area. You may also proceed west on NM-502/4 to La Cueva or Jemez Springs, where limited motel accommodations can be found. It is not necessary to return to White Rock, because the route of Day 3 can be picked up at Stop 11, saving many miles of driving. However, mileage for Day 3 is given from White Rock. END OF DAY 2.

Day 3: Proximal facies of Bandelier ignimbrites and San Diego Canyon ignimbrites

From White Rock (0 mi) follow the route of Day 2 to Stop 11 and proceed on NM-502/4 westward to the junction with NM-126 at La Cueva (36.4 mi). La Cueva is in the moat of the Valles caldera at the point where the caldera wall is breached by the head of San Diego Canyon, which contains the only surface drainage from the caldera. Turn left on NM-502/4 and, immediately after the road crosses San Antonio Creek, turn right onto the unmarked road (36.5 mi); from this point mileage to Stop 13 is not included. Please note that although these

roads are public access, the route to Stop 13 runs across private land and access may change occasionally. Check locally for access permission to this area. Follow the dirt road, taking a left turn at the T intersection. Follow the most used road, taking only right turns that lead generally down hill, for 3.2 km or, depending on exact route, until the road comes to the base of a large cliff with tent rock erosional forms. Park when you reach a hairpin right-hand curve under prominent tent rocks. Exposures for Stop 13 occur along the road for the next 200 m and in the cliffs above. The area around the house to the left of and above the parking spot is not forestry land. Please respect the owners' wishes that it not be walked upon. The sequences of interest can be seen without crossing this privately-owned tract.

Stop 13: Caldera rim section (La Cueva) exposing four **ignimbrites**

Significance: This large section shows the UBT, LBT, and two older San Diego Canyon ignimbrites (A and B) of high-silica rhyolite composition. The latter two units are products of small eruptions of Bandelier magma that occurred before that of the LBT (about 1.78 Ma; Spell et al., 1990). This location also contains a proximal UBT Plinian deposit section. The Valles caldera wall was probably in the same approximate position as the present day topographic rim when the UBT was erupted. Spectacular erosional forms, "tent rocks," or hoodoos, are formed in the LBT.

Description: The four ignimbrites have a complex geometry in this 1 km long, curved section of caldera wall (Fig. V38). The following features can be examined:

San Diego Canyon (SDC) ignimbrites A and B: Bedded coarse proximal lithic breccias in SDC ignimbrite "B" are exposed at the southern end of the section. These demonstrate the proximity of these exposures to vents for this ignimbrite. One juvenile component of ignimbrite B is a crystal-poor (less than 3 wt%) pumice with extreme development of pipe vesicles, giving an asbestiform or woody appearance. Other, almost aphyric, pumice clasts occur in the lower part of ignimbrite B, which is a lithic-rich ignimbrite overall (Fig. V39). Ignimbrite A is also very lithic- and ash-rich; coarse pumice clasts are sparse. It is 40 m thick, and the lower part is poorly exposed. It rests on a complex, undulating surface cut into Paliza Canyon andesites. Ignimbrite A represents the earliest appearance of Bandelier-type magma from vents in the proximity of the Valles caldera. The high-silica rhyolite pumice-fall deposit seen at Stop 3A (Fig. V21) is possibly correlative with SDC ignimbrite B based on the similarity of $^{40}Ar/^{39}Ar$ ages, pumice type, and REE patterns (Spell et al., 1990; Turbeville and Self, 1988).

Lower Bandelier Tuff: The LBT is 100 m thick and has erosional remnants of upper, welded vapor-phase altered flow units. The nonwelded ignimbrite is featureless except for a horizon of large lithic clasts, representing the same level as the proximal breccias, and a lower parting marked by thin flow units. Plinian deposits are absent under the LBT at caldera-rim exposures, but units B—D can be predicted to have fallen by the isopach maps (Fig. V19). Away from the rim the Plinian deposits are exposed, thus erosion by early pyroclastic flows may account for their absence in these proximal exposures. The LBT has spectacular "tent-rock" weathering features at this location.

Upper Bandelier Tuff The UBT rests on an undulating surface eroded into the LBT. It is the upper, grey, cliff-forming unit. Here the UBT is a very condensed sequence, with only certain flow units being deposited or passing

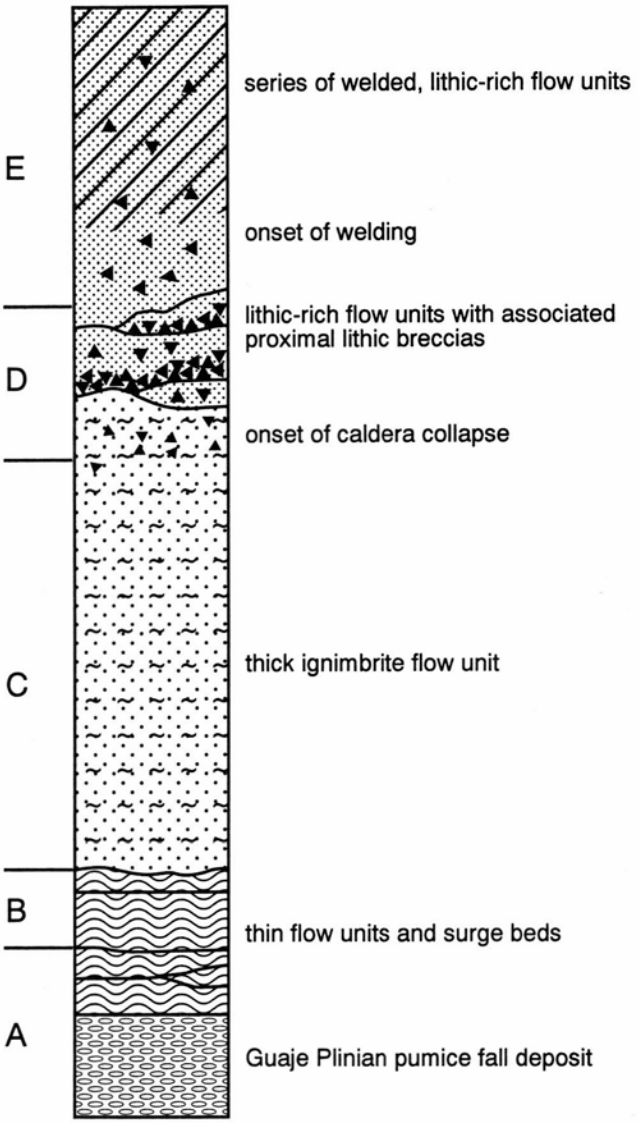

over the topographic wall. Evidence for the topographic rim of the caldera being approximately in the present position during the UBT eruption is found at another location in this southwest part of the Valles caldera, where a UB ignimbrite sequence similar to this one is banked against the base of the caldera wall. Access to this area is not currently possible.

The UBT Plinian deposit (Fig. V40) is 3.5 m thick and consists of fall units A—F (Fig. V41). The basal unit A is of restricted dispersal (see Stop 8) and consists of well-bedded "millet-seed" pumice. The prominent bedding and medium grain size possibly indicate a phreatomagmatic origin for this initial ash of the UBT. Fall unit B is the major unit, seen also on the east of the Jemez Mountains, and C is a fine-grained unit, which in places is an ash fall and in others a surge deposit. As will be seen later, the UBT units are dispersed towards the northwest from the Jemez Mountains and are the only Plinian fall deposits from the whole field to have this dispersal direction. Unfortunately, the deposits are altered at this location and are unsuitable for granulometric analysis.

Above the Plinian deposit is a very crystal-rich, fine-grained pyroclastic-flow deposit, part of the thin, basal set recognized elsewhere in the UBT. At Stop 14 this unit displays evidence of having been emplaced violently as it eroded the top of the Plinian deposits. Above this flow

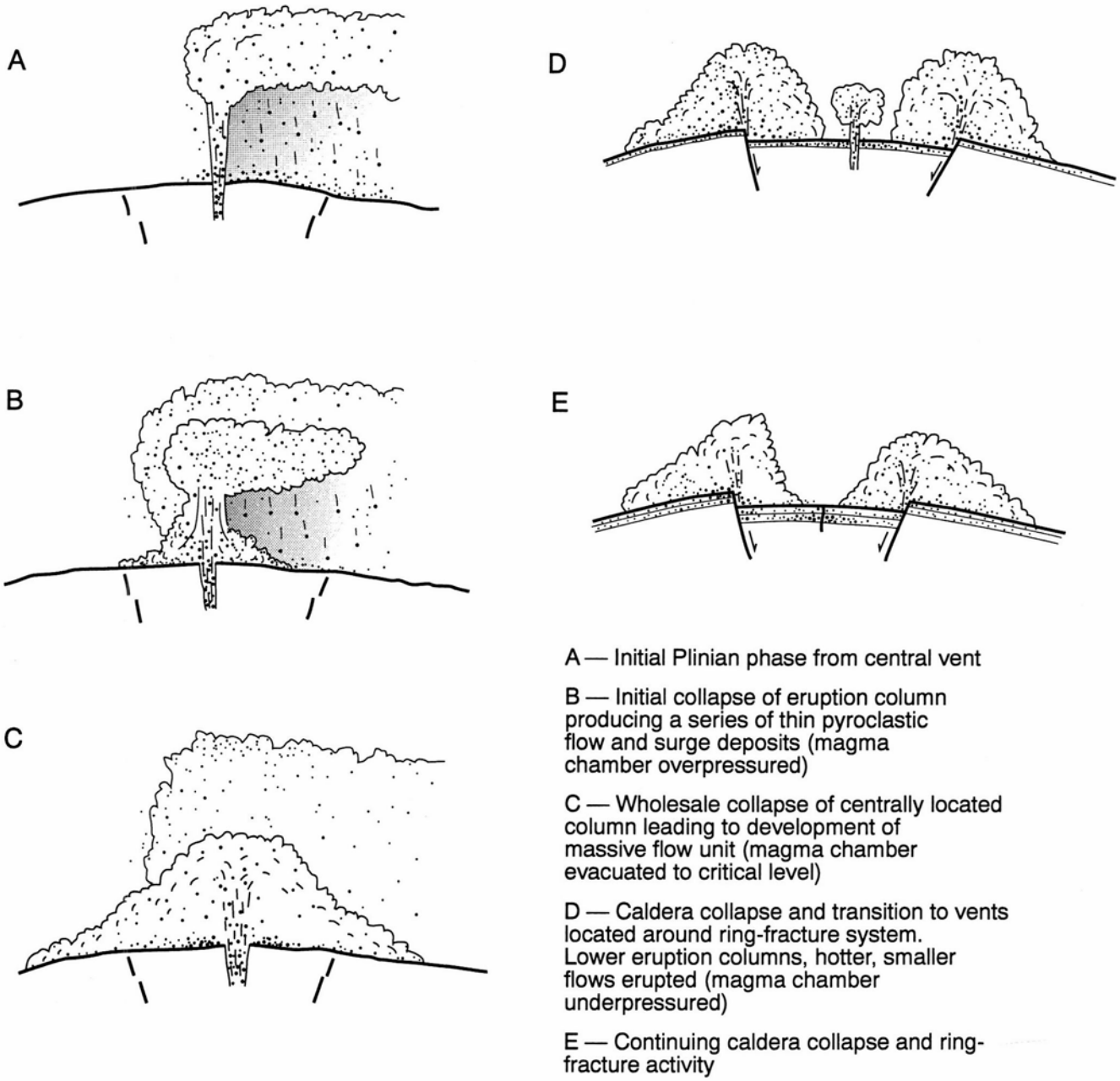

FIGURE V33—Left, composite schematic section through lower Bandelier Tuff (LBT) showing major zones. A–E refer to eruption phases interpreted from this sequence. Right, interpretation of activity during phases in the lower Bandelier Tuff eruption (after Self et al., 1986); see text.

unit, vapor-phase alteration and welding affect the UBT units, and welding increases rapidly in intensity upwards. The uppermost,welded flow unit is fine-grained, crystal-rich, and coarse-clast depleted. It may be an equivalent to the upper welded UBT units in proximal areas on the east side of the caldera (Stops 5 and 6).

Summary: The SDC ignimbrites represent eruptions of Bandelier-type magma well before eruption of the LBT. Whether these indicate a single, long-lived magma body or earlier generation of batches of similar magma is under evaluation at present. Self et al. (1986) and Nielson and Hulen (1989) suggest that these eruptions may have been associated with small early calderas now obliterated by collapse of the southwest part of the present Valles caldera. The LBT and the two SDC ignimbrites form most of the caldera wall here. The LBT is largely nonwelded and appears to have accumulated during most phases of the LBT eruption. The UBT is generally thin but welded and has a thick Plinian section at its base.

Retrace the route as far as the bridge across San Antonio Creek on NM-502/4 (36.5 mi) at La Cueva. Turn right onto NM-502/4. As this road enters the head of San Diego Canyon, grey welded Battleship Rock ignimbrite overlain by the thick, glassy Banco Bonito lava flow can be seen on the left. Downcanyon, Permian red beds (Abo Formation) crop out at the level of the canyon floor and are overlain by Paliza Canyon andesites on the west wall. At Battleship Rock (Stop 16) on the left (39.6

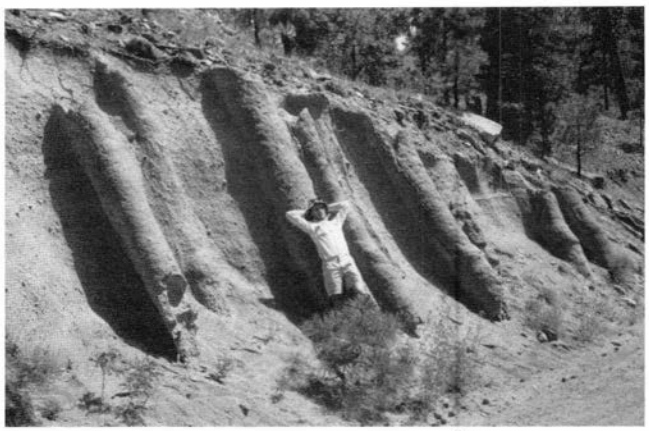

FIGURE V34—Pipes in the upper Bandelier Tuff (UBT) about 1 m thick exposed by differential erosion of vapor-phase altered ignimbrite (Stop 10A).

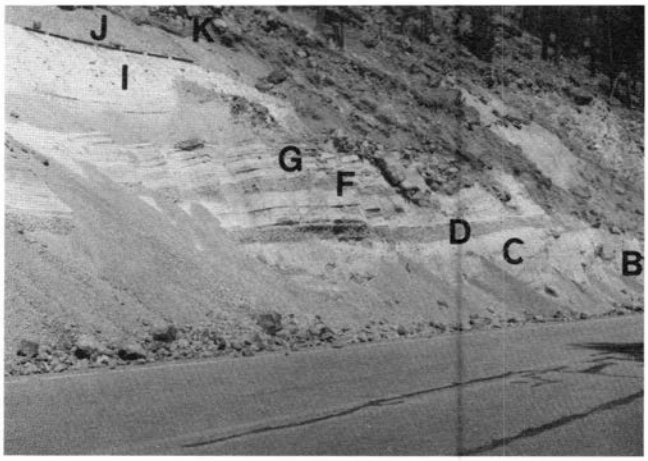

FIGURE V35—El Cajete section at Stop 11 showing unit designations. Note the disconformity (e) above unit I separating products of the El Cajete–Battleship Rock eruption from products of the Banco Bonito event.

mi), the road crosses the Valles caldera topographic rim, here cut by San Diego Canyon. As the road descends the canyon, there is a smell H_2S from fumaroles along the Jemez fault zone if conditions are favorable. The Jemez fault zone controls the presence and position of San Diego Canyon. Turn right onto an unsignposted access road to a private housing area (41.6 mi); this road is public access and leads to a small system of forestry roads. Continue on the small forestry road once past the housing area and park at the base of the steep slope where the road crosses a gulley at 43.6 mi. This stop involves a climb of about 100 m elevation to the base of the ignimbrites on the west wall of San Diego Canyon. Climb the ridge in front (west) of the parking area until you reach a plateau, then walk to the right until you are at the base of the main cliffs. The San Diego Canyon ignimbrite caps the plateau and the LBT sequence begins at the base of the main cliffs.

Stop 14: San Diego Canyon ignimbrite and lower Bandelier Tuff

Significance: These exposures demonstrate the extent of the SDC ignimbrites under the LBT and provide a view of the trivial Plinian deposit thickness at the base of the LBT and lowermost, erosive LBT flow units. The location affords some spectacular views of San Diego Canyon and the thick Bandelier Tuff outcrops in the canyon walls.

Description: The slope climbed is on Permian Abo Formation red sandstone-siltstone beds overlain by Paliza Canyon andesites (-4 Ma). Note the occurrence of travertine at several places upslope; these are hot springs deposits formed at various elevations and stranded by downcutting of San Diego Canyon. The trail emerges onto a small plateau with exposures of tent rocks in SDC ignimbrite B. These occur where fumaroles developed in the ignimbrites, and small fumarolic pipes (vapor-phase) can be seen in places. The stop shows a similar sequence to section 104 in Figure V42, although the location of section 104 is a little further down canyon. Ignimbrite B is overlain by the LBT seen in the main cliffs, here displaying a well-developed sequence of 5 to 6 basal flow units, some very fine-grained. Remnants of the upwind dispersed part of the LB Plinian deposit can be found, but it was mostly eroded away by the early pyroclastic flows.

Summary: Although probably confined to paleo-San Diego Canyon, the SDC ignimbrites were extensive and in fact persist down canyon almost to the present limits of the Bandelier ignimbrites. The LBT here shows evidence of thin, fine-grained flow units at the base of the ignimbrite sequence.

Retrace the route back to NM-502/4 (45.6 mi) and turn right for alternative Stop 15A, or left for Stop 15 (route continues after Stop 15A description). For Stop 15A, proceed down NM-502/4 for 1.1 miles (46.7 mi) to Soda Dam.

Stop 15A: Soda Dam and Jemez fault zone

The travertine dam (Fig. V43) across the gorge in Precambrian granite was built by carbonated thermal waters that discharge from a branch of the Jemez fault zone. There are 10 springs and seeps in this area, including one across the river to the north of the high travertine knob. About 30 years ago, water discharged along the top of the dam. Today Soda Dam is slowly falling apart due to severing of the source from the dam by road construction.

The waters discharge at 48°C with a chlorine concentration of 1500 mg/1. The ratios of very soluble elements, Na, Li, Cl, and B, are practically identical to those from the deep fluid within Valles caldera (Goff et al., 1981). This, and other evidence, indicates that the waters outflowing here derive from those deep within the caldera. Leakage and mixing occur to the southwest down various branches the Jemez fault zone.

Older travertine deposits are exposed high above the canyon floor to the west of Soda Dam, and include river gravels with cobbles of Bandelier Tuff. Uranium-thorium disequilibrium dates show that the Soda Dam hot-spring system has been active for the last 1 million years, and is thus almost as old as the latest caldera-forming event (Goff and Shevenell, 1987).

The Jemez fault zone is very complex in this area. The main trace trends northeast across the highway. Generally, the displacement is down to the east about 100-250 m because the Jemez fault zone is also the westernmost of the Rio Grande rift faults. At Soda Dam, a small horst of sheared Precambrian granite is uplifted and contorts the Paleozoic rocks around it.

For Stop 15, retrace your route up San Diego canyon to Battleship Rock (49.9 mi); then turn right to the Battleship Rock picnic area (50.2 mi).

Stop 15: Battleship Rock ignimbrite

Significance: This classic ignimbrite locality shows many features such as welding zonation and fiammé and

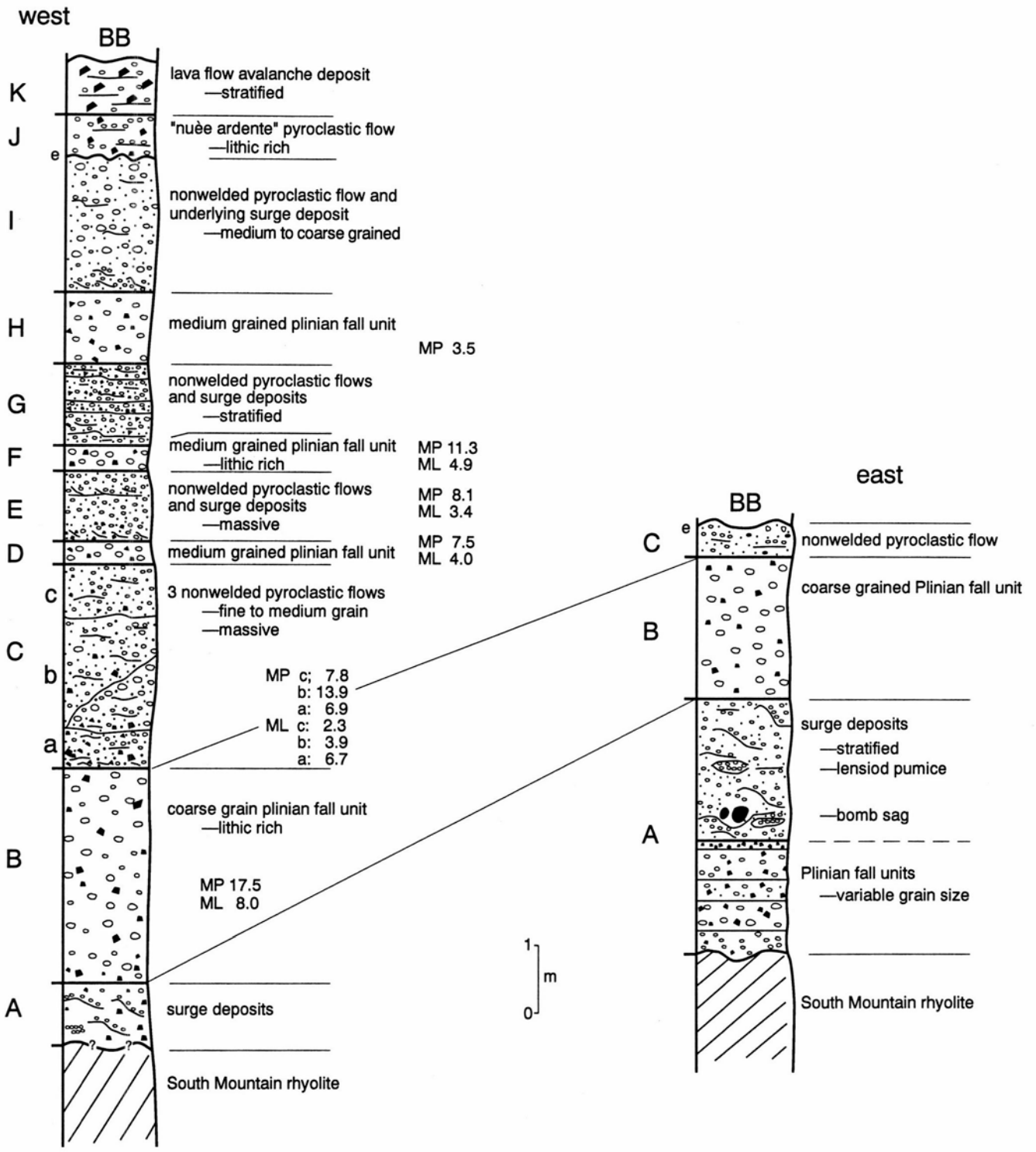

FIGURE V36—Section through the El Cajete and Banco Bonito units exposed at Stop 11, after Self et al. (1988). Note that the erosion surface between units I and J may represent the passage of about 100 ka, separating the pyroclastic products of the El Cajete eruption (> 0.3 Ma) from those of the Banco Bonito eruption (~0.2 Ma), but that recent work suggests that all these deposits are part of a long drawn-out eruptive episode about 60 ka ago (see text).

is the result of stream erosion on two sides exposing a thick localized canyon-filling sequence of flow units.

Description: Battleship Rock (BR), a spectacular outcrop of columnar-jointed, rhyolitic ignimbrite is formed of a series of postcaldera small-volume (about 1 km^3 DRE) flows that issued from a vent near El Cajete crater (Fig. V44) about 300,000 years ago (see Stop 11 for a discussion of age). The lowermost part of BR ignimbrite corre

lates with flow units in unit I of the El Cajete deposits at Stop 11. Initially, the ignimbrite may have extended a considerable distance down San Diego Canyon; it presently fills it to a maximum depth of 100 m (Self et al., 1987, 1991). Battleship Rock itself represents the exhumed welded ignimbrite-fill of a narrow gorge cut into Paleozoic Madera Limestone and Abo Formation. The limestone occurs immediately below the ignimbrite in the area

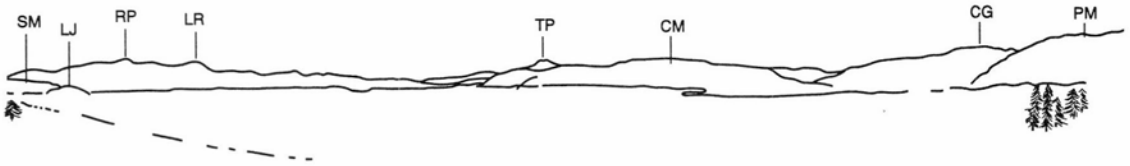

FIGURE V37—Sketch of view from Stop 12 showing Valle Grande, the southeast caldera moat, and intracaldera lava domes Cerro La Jara (LJ), South Mountain (SM) and Cerro del Medio (M). Skyline features are Redondo Peak (RP), Little Redondo (LR), and Tschicoma Peak (TP) on far northern margin of caldera, and Pajarito Mountain (PM) and Cerro Grande (CG) on eastern caldera rim.

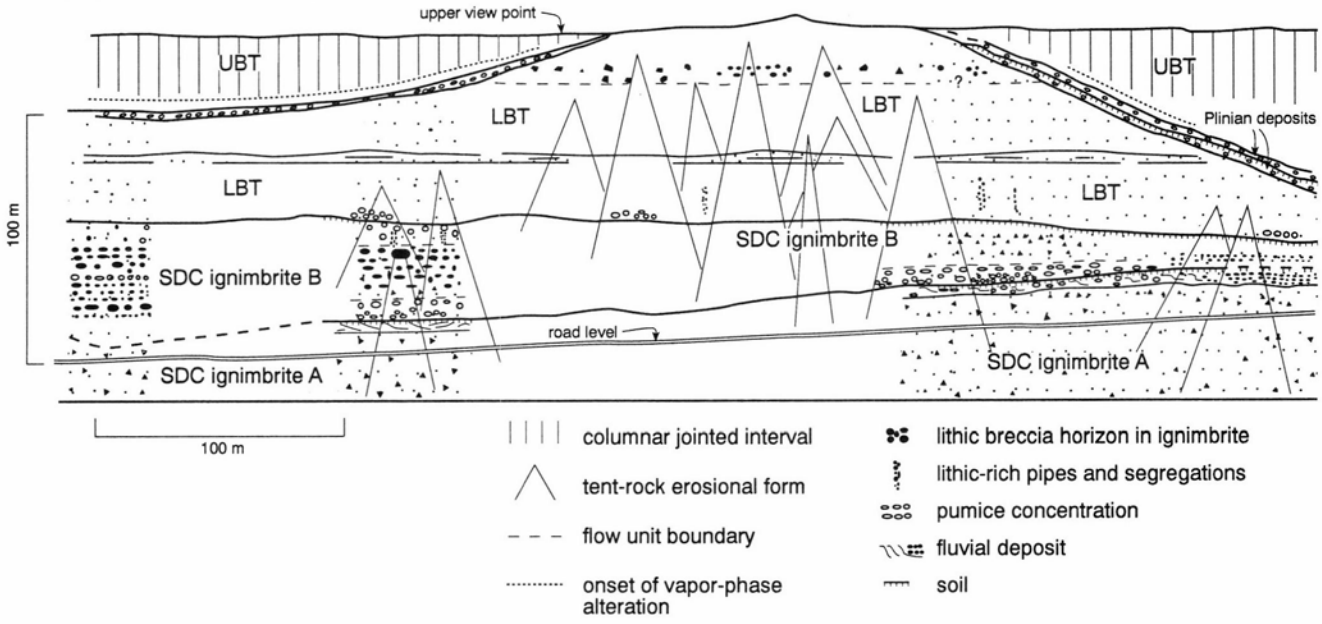

FIGURE V38—Sketch of the caldera wall near La Cueva in the area of Stop 13, showing geometry of upper Bandelier Tuff (UBT) and lower Bandelier Tuff (LBT), and San Diego Canyon (SDC) ignimbrites. Details and clast sizes are shown larger than time scale.

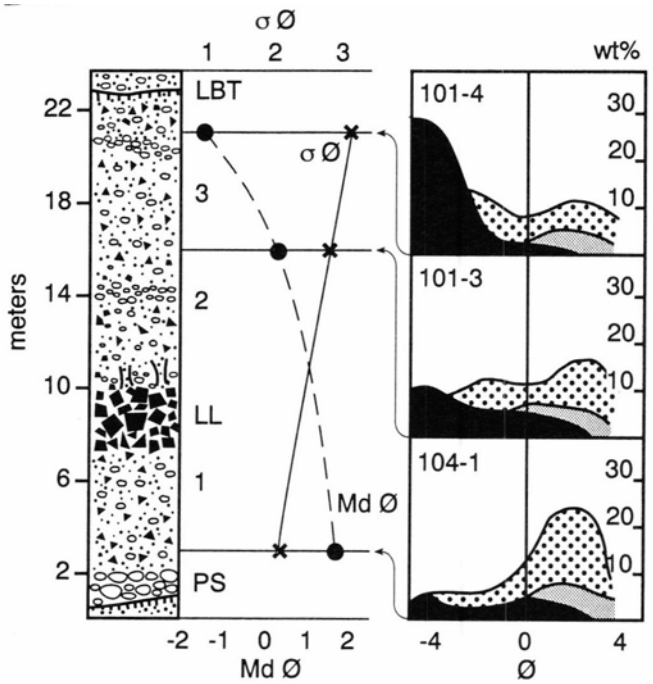

FIGURE V39—Grain size profile through 3 flow units (1–3) of San Diego Canyon ignimbrite B showing variation in median grain size and sorting of matrix fractions in the - 4ϕ to 4ϕ range; PS—coarse pumice concentration; LL—lithic breccia; LBT—base of lower Bandelier Tuff; frequency curves at right indicate relative proportions in grain size populations of lithic (shaded), crystal (black) and pumice (stippled) components, (from Turbeville and Self, 1988).

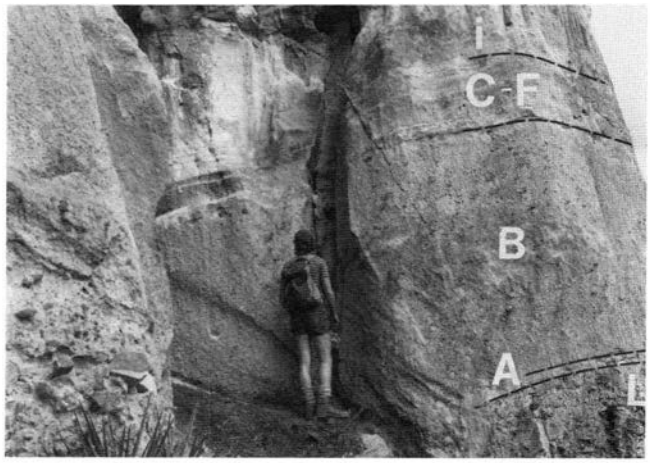

FIGURE V40—Fall units A–F of the upper Bandelier (UB) Plinian deposit on the caldera wall near La Cueva (Stop 13). L—colluvial gravels on top of lower Bandelier Tuff (LBT); i—base of UB ignimbrite.

of Battleship Rock and can be seen in the bed of the Jemez River just above the confluence with San Antonio Creek. Massive calcareous beds are separated by thin shale partings and are very fossiliferous.

The ignimbrite at Battleship Rock is about 80 m thick and contains up to six flow units that constitute a lower-cooling unit (Fig. V45). The basal 15 m consist of poorly consolidated pumiceous ignimbrite, which becomes increasingly compacted upward and grades into partly

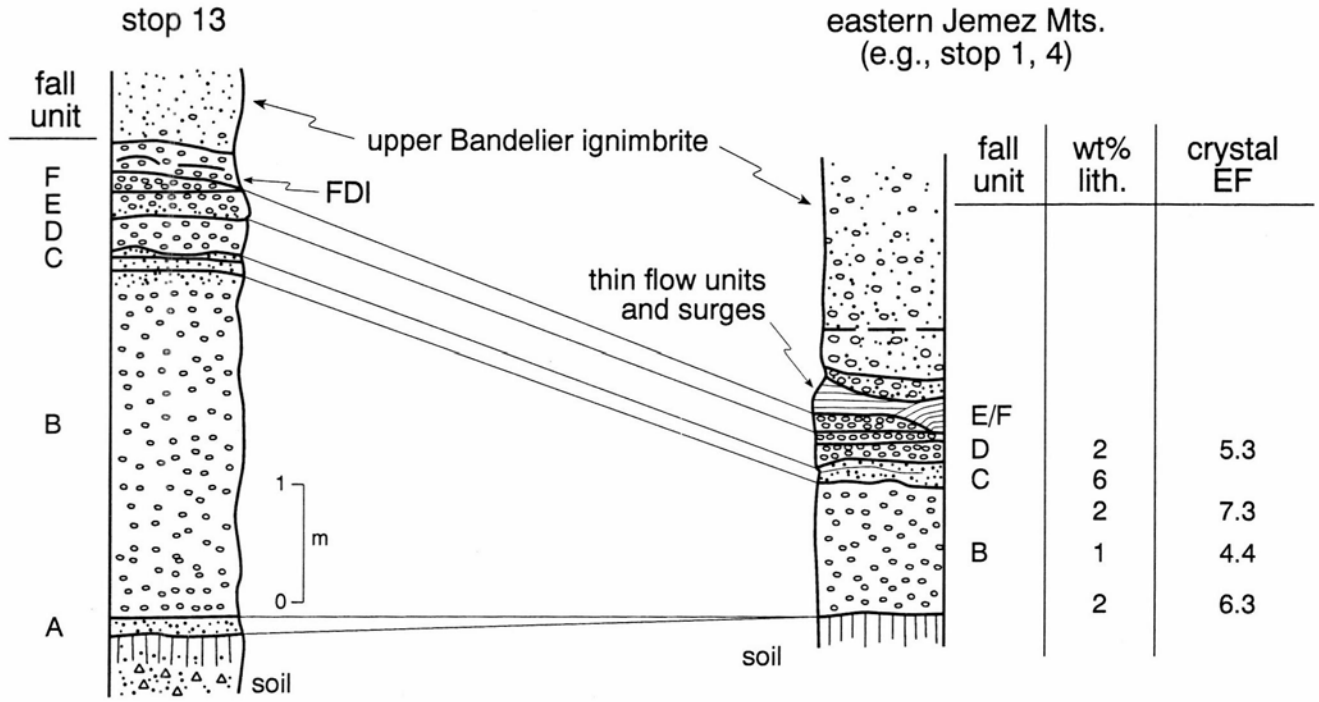

FIGURE V41—Section through upper Bandelier Plinian deposit at Stop 13 on the caldera rim, shown correlated with fall units on the east side of the Jemez Mountains. EF—crystal enrichment factor (explained at Stop 1); Lith—lithic clasts. FDI—fines depleted ignimbrite. (after Self et al., 1986).

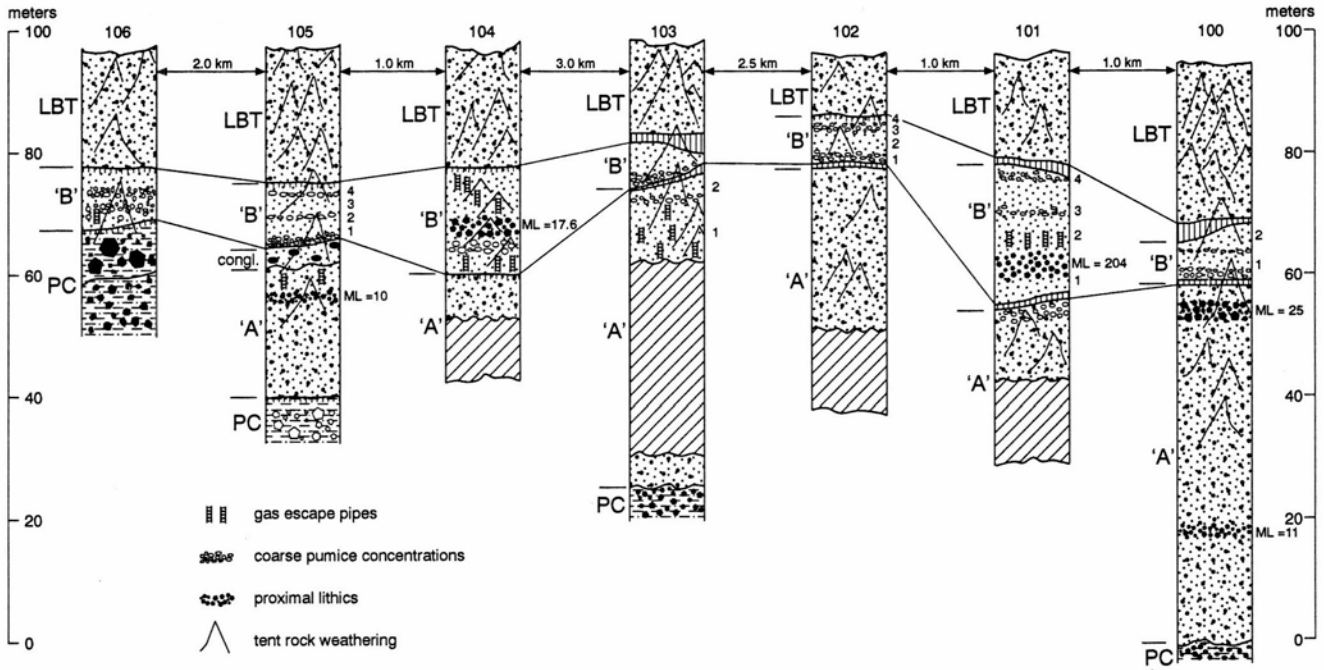

FIGURE V42—Seven sections at intervals shown along western wall of San Diego Canyon from La Cueva (Stop 14). SDC—San Diego Canyon ignimbrites A and B; PC—Paliza Canyon Formation lavas and breccias; LL—proximal lithic breccias; PS—coarse pumice concentrations; ML—maximum lithic diameter (in cm); MP—maximum pumice diameter (in cm); GEP—gas escape pipes; TR—"tent rock" weathering; numbers at right of columns—individual flow units; cross-hatched areas—covered intervals; LTB—lower Bandelier Tuff (Otowi) ignimbrite.

welded ignimbrite that has a minimum porosity of 15% at approximately 35 m above the base. Large fiammé typify this zone. Welding was accomplished by porosity-loss compaction without rheomorphism; mean strain (Rf) is 4.25 for X and Y directions (Wolff et al., 1989; Fig. V45, right). The ignimbrite becomes gradually less welded and passes into slightly vapor-phase-altered ignimbrite about 65 m above the base. The curved columnar jointing in the lower part of Battleship Rock ignimbrite is probably a consequence of fumarolic action during cooling of the hot deposits in a wet environment along the course of paleo-San Diego Canyon.

Slightly upcanyon, another cooling unit composed of at least 6 flow units is found above the lower cooling unit

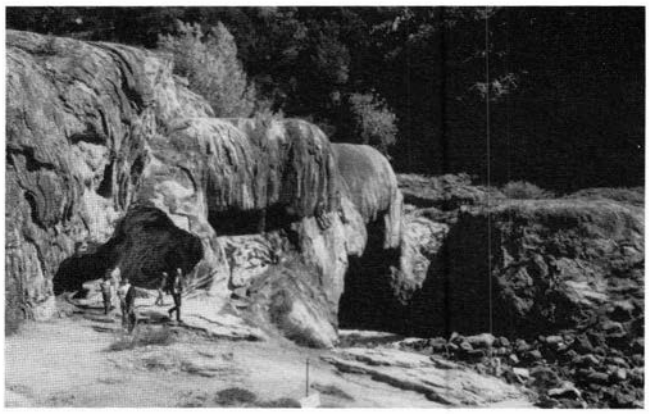

FIGURE V43—Soda Dam from the south side, with Jemez River exiting from tunnel through dam and center (lower).

(Fig. V46, section 2). They are separated by two thin partings of bedded fall deposits (not seen on this trip), most probably derived from secondary explosions occurring in the newly deposited ignimbrite. The Battleship Rock ignimbrite is thus a valley-filling compound cooling unit with a maximum thickness of 130 m to the northeast of Battleship Rock (Fig. V46, section 3), determined by Continental Scientific Drilling Project hole VC-1 (Goff et al., 1986), located 2 km upcanyon from this area.

Summary: The Battleship Rock ignimbrite provides evidence of considerable explosive activity accompanying the eruption of a new batch of low-silica rhyolite magma from the Valles caldera. It mainly followed deposition, but was to some extent coeval with the El Cajete pumice-fall deposit. A glassy lava found only in the VC-1 core was produced at the end of this eruptive event. A later, largely effusive, eruption about 0.2 Ma or 60 ka ago produced the Banco Bonito lava. These are the latest products from the Valles caldera. They are all of similar low-silica rhyolite composition and have virtually identical mineralogy (Self et al., 1988; 1991).

Retrace your route on NM-502/4 to White Rock (89.8 mi) for resumption of next day's itinerary. END OF DAY 3.

Day 4: Bandelier Tuff in the northern Jemez Mountains and intracaldera geology

This is a long day of driving with only four stops that provides many opportunities for photography of spectacular scenery. A geologic map of the area north of the

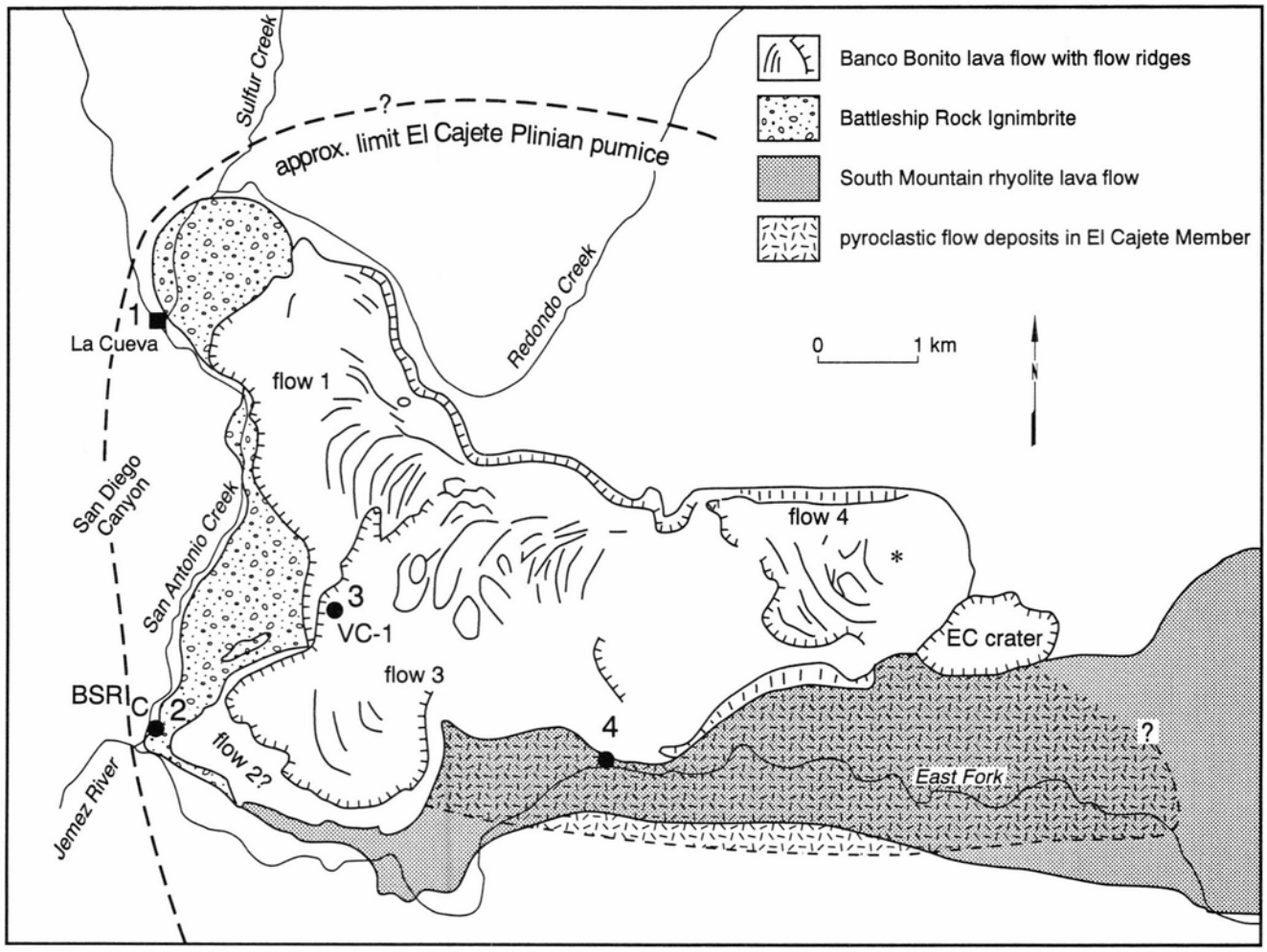

FIGURE V44—Map of Banco Bonito lava flow, Battleship Rock ignimbrite, and part of South Mountain rhyolite lava flow, with approximate dispersal limit of El Cajete pumice fall and interbedded pyroclastic flow deposits. Flow lobes of Banco Bonito lava designated as flows 1–4. Locality 4 is El Cajete type section (Stop 11). Locality 3 (VC–1) is CSDP drill hole site. Locality 2 is Battleship Rock type section (BR). Locality 1 is La Cueva. Asterisk is vent for Banco Bonito flow.

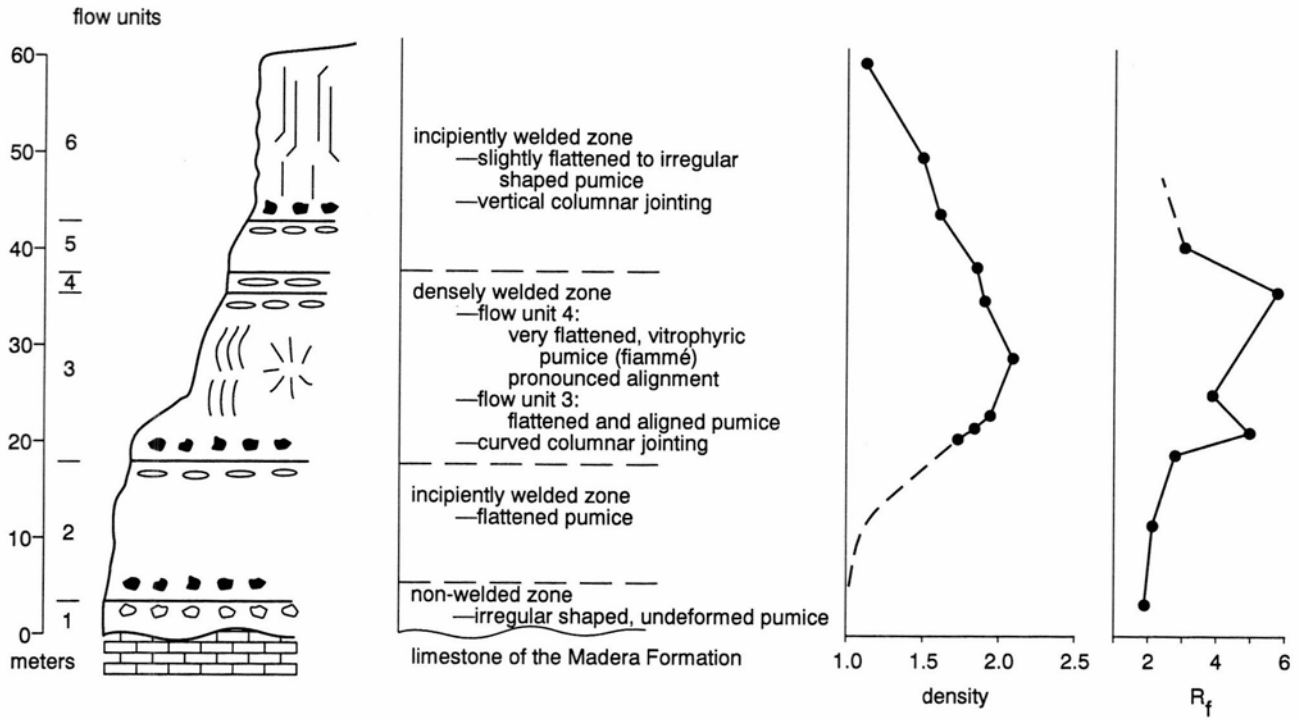

FIGURE V45—Schematic stratigraphic section of the Battleship Rock type location, including distinction between flow units and welding zones. Column at right shows flattening ratio of pumice clasts based on axial measurements made in the field.

Jemez Mountains will enhance the readers' appreciation of the non-volcanic geology in this area.

Drive north from White Rock on NM-502/4 to the Y junction and turn right (east) on NM-502/4, past Stop 1, then turn left on NM-30 (8.2 mi) towards Espanola. On the left along NM-30 is the Puye scarp, which exposes a section through the Puye fan. Older sediments include Rio Grande-rift-filling silts, sands, and gravels of the Santa Fe Group (Fig. V3). Black Mesa, on the right, is a basaltic tuff ring capped by the remnant of a solidified lava lake. Follow NM-30 to the junction with US-84/285 in Espanola (17 mi) and continue north on US-84 towards Abiquiu. At 46.3 miles turn left at the junction with NM-96. Follow NM-96 across Abiquiu Dam and at 50.4 mi turn left off NM-96 onto the unmarked dirt road to Cañones. Pass through Cañones settlement (53.4 mi), cross the first stream (Cañones Creek), then take the second right turn, then the left fork. Follow the unmarked dirt road south along the ridge to the base of the prominent Pueblo Mesa on the right (west) side of the road (55 mi). This road may be in very poor condition for the last mile; if your vehicle cannot proceed, you can walk. Climb to the top of the mesa by a well-worn walking trail up its east face. Outcrops to be examined at Stop 16 occur on the top and west sides of the mesa.

Stop 16: Pueblo Mesa, Cañones

Significance: The side walls of this mesa provide one of the few accessible, complete exposures of the Bandelier ignimbrites in the northern part of the Jemez Mountains allowing comparison with the ignimbrite elsewhere. Pueblo Mesa was formed by erosion during the 300,000 years after LBT deposition and consists of resistant Abiquiu Tuff and LBT that has an indurated zone, perhaps by vapor-phase deposition, at the present top. It was a more-or-less freestanding mesa at the time of the UBT eruption; the UBT pyroclastic flows poured around and over the mesa edge. Both ignimbrites have Plinian deposits exposed at their bases.

Description: The route up the east wall of the mesa is through the Abiquiu Tuff, volcaniclastic deposits underlying and interdigitating with the Santa Fe Group (Fig. V3). Note the presence of 1 m of UBT Plinian deposit to the right of the path. The contact between UBT and LBT runs diagonally across the mesa top and the west wall and affords an exposure of the subvertical contact (Fig. V47). Multiple UBT ignimbrite flow units with concentrations of large pumice are seen; surge deposits occur at flow unit boundaries. One boundary has fluvially-reworked pumiceous sediment under a surge layer, indicating a slight pause in deposition. The sequence of UBT units here is apparently similar to that in the area of Stop 1; the multiple flow units are in the middle group.

The LBT ignimbrite is lithic-rich and indurated but not welded. It has prominent mounds, ridges, and pipelike erosional forms on its surface, probably marking features due to vapor-phase alteration. At the southern edge of the mesa, an 8-10-cm-thick LBT Plinian unit is exposed under a thick flow unit. The flow unit has fumarolic alteration pipes near its top. Further to the south a section of the UBT exposes the UB Plinian deposit, composed of 180 cm of fall unit B.

Analyses of pumice clasts from all levels in both the LBT and UBT indicate that the ignimbrites in this sector are formed of only the more evolved high-silica rhyolite compositions. The reason for this compositional selectivity throughout both ignimbrites in this area is not yet fully understood.

Summary: Both the LBT and UBT display many of their usual characteristics in this northern outflow lobe, which is more valley-confined than with the plateau-forming sheets around the other sectors of the Jemez Mountains. Depositional zones in the UBT are broadly similar to those seen on the Pajarito Plateau in the east of the Jemez Mountains, but compositionally both the LBT and UBT have a more restricted range of pumice compositions

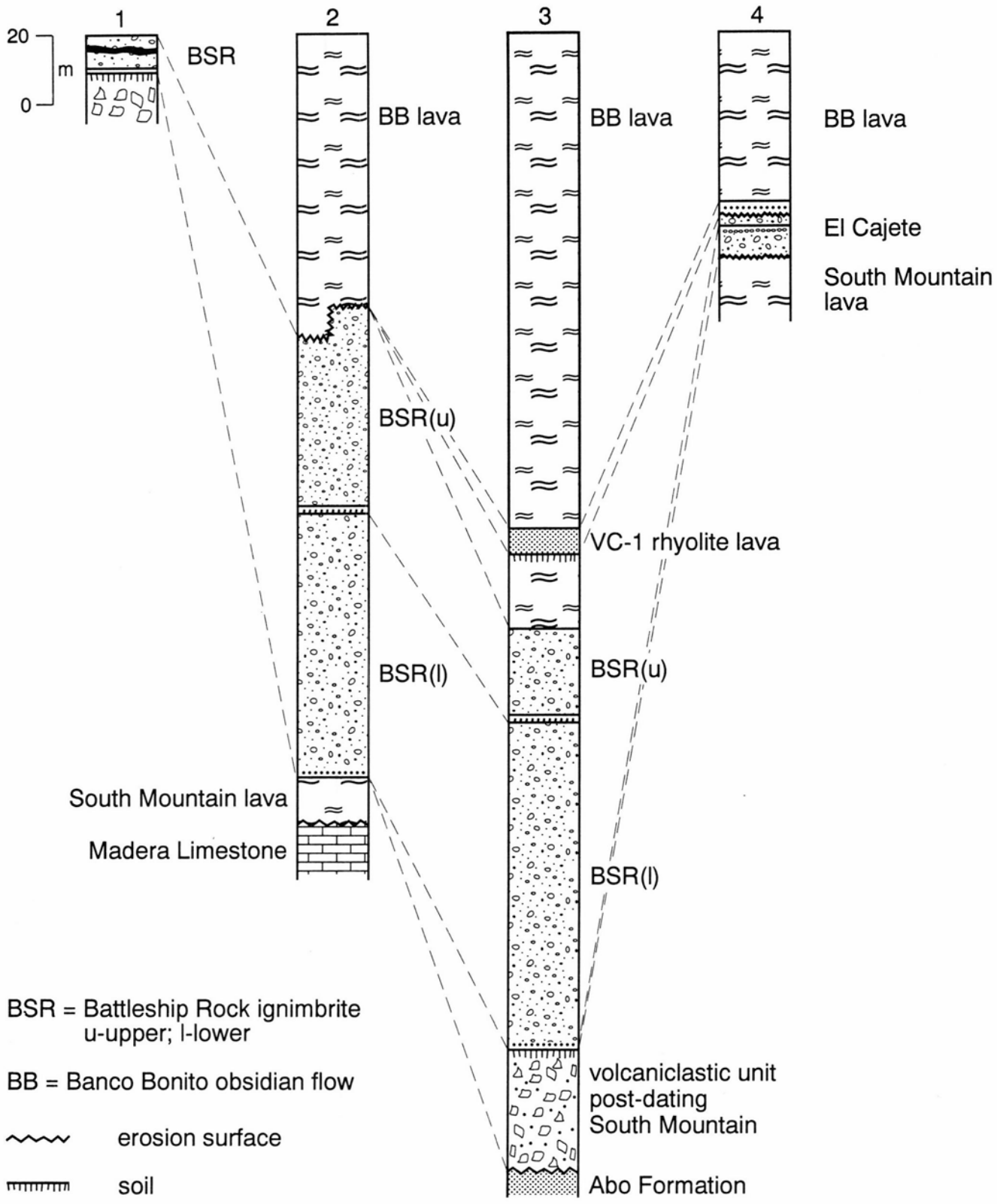

FIGURE V46—Sections and correlation of young (post 0.5 Ma) Valles caldera units including La Cueva (section 1), Battleship Rock (section 2), VC–1 drill hole (section 3), and El Cajete type section (section 4). Locations of sections are shown in Figure V44. Black layer in section l is a carbon-rich (?forest fire) deposit. (From Self et al., 1991.)

than in other parts of the ignimbrite sheet, a fact that awaits future understanding.

Retrace the route through Cañones to NM-96 and turn left. Proceed to Coyote; turn left on FS-316 just past the village (73.7 mi). On the right the road passes Loma Coyote, a small mesa capped by a distal outlier of UBT. Follow FS-316 to the sign for Jarosa (82.4 mi) where you take the left turn onto FS-103. Follow FS-103 and turn left onto FS-527 (90.2 mi); after about 1 mile FS-527 becomes FS-114 (also in this section called Pipe-

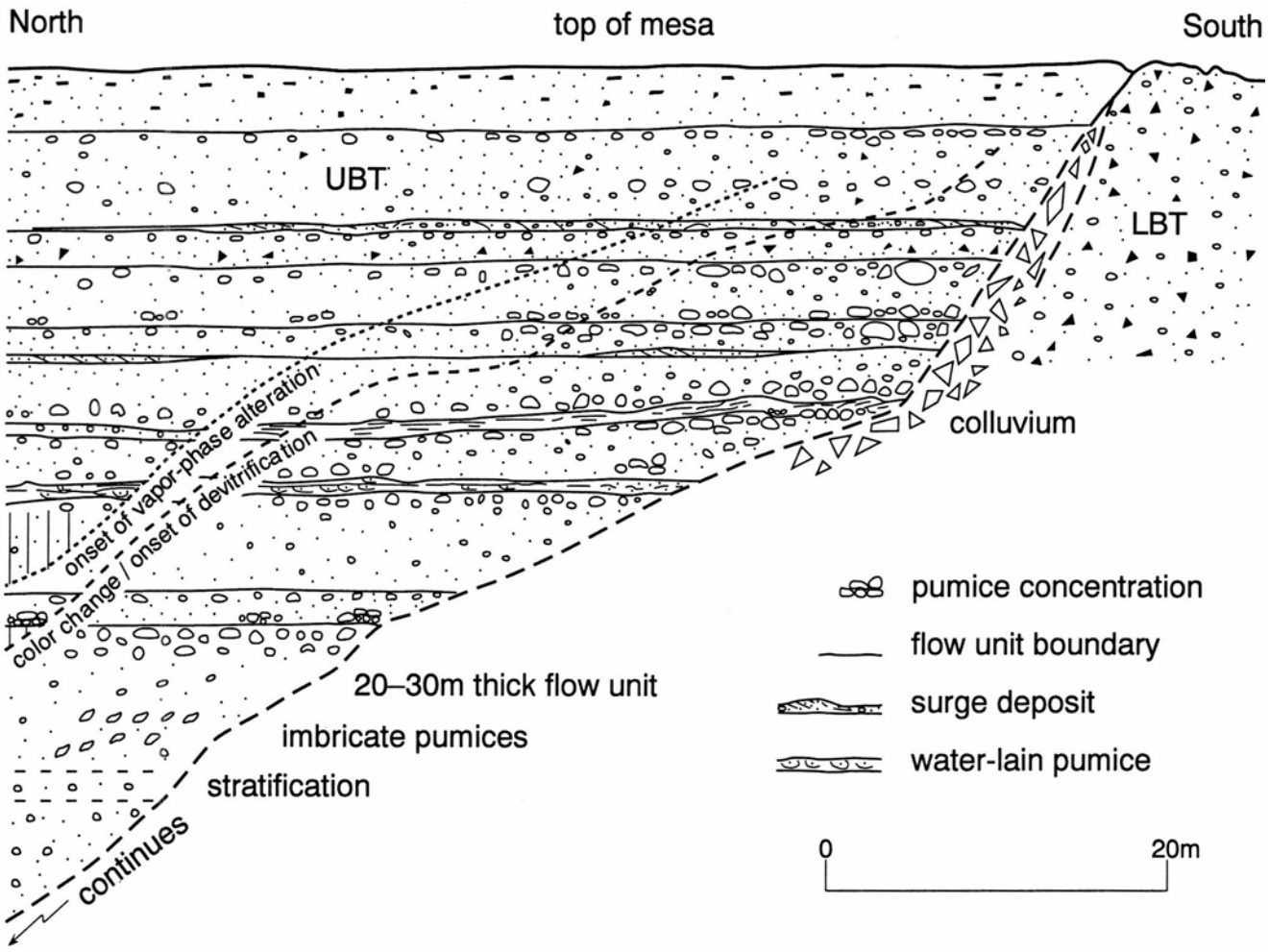

FIGURE V47—Sketch of relationships near steeply dipping contact between lower Bandelier Tuff (LBT) and upper Bandelier Tuff (UBT) at Pueblo Mesa showing geometry of flow units in UBT and pumice concentration zones.

line Road). Follow this road uphill and stop at the crest of the hill in the low cutting (92.1 mi), the outcrop for Stop 17.

Stop 17: Upper Bandelier Plinian deposit

Significance: This roadcut gives an excellent section through the Plinian deposit of the upper Bandelier Tuff at a distance of 8.5 km from the caldera rim and 20 km from the suspected vent site.

Description: This section exposes units A and B of the UB Plinian deposit and is approximately on the axis of both units. Unit A is well-bedded and has the same characteristics as at Stop 13. Unit B is little reduced in thickness from Stop 13 (Fig. V48) and shows a high degree of crystal concentration (up to six-fold). Dispersal of these two units is to the northwest, an unusual direction for Jemez Mountains Plinian deposits. All other known fall units have dispersal axes trending from NE—SSE.

The eruption that produced unit B is interpreted to have been very powerful. The large areas enclosed by maximum clast isopleths (Fig. V49) and the strong crystal concentration suggest an ultra-Plinian eruption with a model column height in excess of 45 km (using the method of Carey and Sparks, 1986). The bulk volume of fall unit B is difficult to constrain because the isopachs cannot be closed with the existing area of outcrop, but it must be greater than 26 km^3. The upper fall units, and part of unit B, were eroded by the early pyroclastic flows, which deposited fine-grained, crystal-rich flow units. The thin UBT ignimbrite here is strongly vapor phase altered 1 to 2 m above the base.

Summary: The UBT eruption began with a locally dispersed, phreatomagmatic eruption (unit A) followed by a high intensity, ultra-Plinian eruption, (unit B). The intensity of the Plinian phase may have been due to the presence of external waters in the vent region. Potential sources are a lake, aquifers, and/or a hydrothermal system within Valles caldera. Early UBT ignimbrite flow units were violently emplaced and commonly caused erosion of the upper part of the Plinian deposit. Some of the units were thin and widespread, and may have the characteristics of low aspect-ratio ignimbrite.

Continue east following FS-144, and, where the road forks, take the right branch uphill (95 mi). At 95.8 mi FS-144 begins a steep descent into Cebolla Canyon; stop at the top of the steepest section on a left-hand curve. The outcrops of interest occur in the roadcuts downslope from the curve.

It is evident from the topography and vegetation why the Bandelier ignimbrites are not well understood in the north to west sector of the Jemez Mountains. Exposures are usually limited to the welded parts of the ignimbrite valley-wall cliffs, the less-resistant tops and bottoms being rarely seen. The nonwelded basal part of the UBT is poorly and patchily exposed between Stops 17 and 18 where it rests on thick, densely welded LBT.

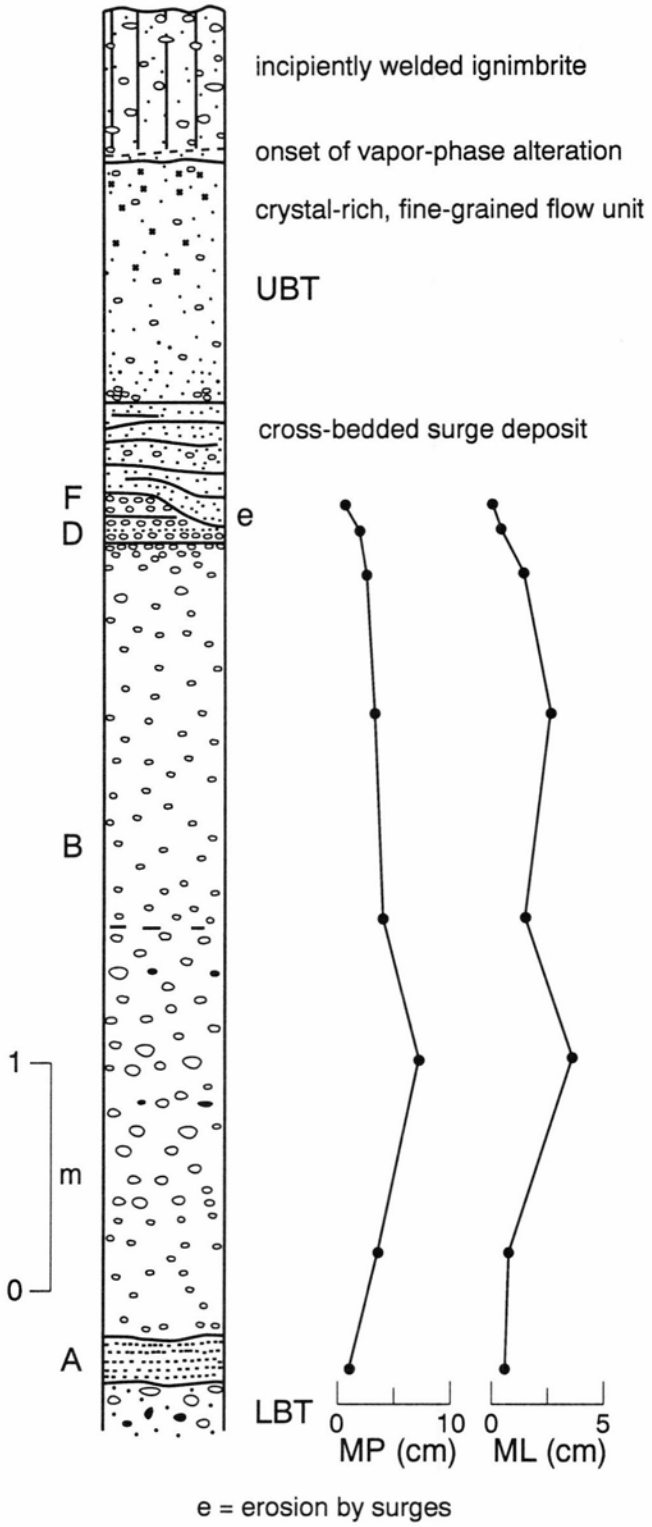

FIGURE V48—Section through the upper Bandelier (UB) Plinian deposit at Stop 17 and base of upper Bandelier ignimbrite. ML and MP = average maximum lithic and pumice clast size in centimeters, respectively.

Stop 18: Welded lower Bandelier ignimbrite, Cebolla **Canyon**

Significance: This densely welded ignimbrite facies is seen nowhere else in the LBT outflow sheet, except in the intracaldera sequence revealed by drilling (Nielson and Hulen, 1984). It was once thought by earlier workers to be a third Bandelier ignimbrite but was later proven to be part of the LBT (R. A. Bailey, personal communication, 1985).

Description: More than 90 m of grey, welded, lithic-rich LBT are exposed in the walls of Cebolla Canyon and can be traced for several kilometers down canyon. This is a homogeneous facies, and flow unit boundaries cannot be recognized. The base is not exposed, thus total thicknesses in this area must be significantly greater than 100 m. Yet ~100 m of **nonwelded** LBT is commonly seen in the southern and eastern LBT ignimbrite sheet, therefore factors other than thickness must control welding. These are most likely temperature and rapidity of deposition and environment of emplacement; the former may be related to changing composition of magma erupted and/or eruption column processes.

Summary: It is not known where in the LBT sequence this densely welded facies belongs. It may have been formed by late, hotter pyroclastic flows, and could thus be correlative with intracaldera flow units. Alternatively, the welding may be an artifact of the environment of deposition, i.e., pyroclastic flows may have ponded rapidly to a great depth in a preexisting depression, with dense welding resulting.

Follow FS-144 along and through Cebolla Canyon; turn right off Pipeline Road, still on FS-144 (96.9 mi), and follow FS-144 to its junction with NM-126 (108.8 mi). Turn left on FS-126 past the Hot Dry Rock drilling site at Fenton Hill, located just down-slope from the western topographic wall of the Valles caldera. Just below the Fenton Hill site, a photograph stop can be made for an overview of the western part of the caldera and the Redondo Peak resurgent block; there is a good view of the apical graben from a pull-out to left of the highway. Caldera resurgence occurred about 100,000 years after the UBT eruption (Smith and Bailey, 1966; Spell et al., 1990). Descend into the caldera moat via NM-126 to its junction with NM-502/4 at La Cueva (112.3 mi). Follow NM-502/4 towards Los Alamos and take FS-105 on the left, signposted Sulphur Springs (113.1 mi) proceeding to the end of the road (115.6 mi). Note that the gate is usually locked. This is private land and permission to visit this site must be obtained from the owner.

Stop 19: Sulphur Springs and intracaldera geology

Significance: This is the only chance that most people have to examine features of intracaldera geology and the resurgent center of the Valles caldera. Most information is known from drill hole logs.

Description: Sulphur Springs was once a small resort where people bathed in waters from the springs and mud pots. The hot springs occur at the intersection of the northeast-trending Sulphur Creek fault (part of the Jemez fault zone) and several local faults (Goff and Gardner, 1980). Fumaroles, hot springs, and mud pots are visible here. Temperatures approach boiling and pH may be less than 1. Geochemistry is discussed by Goff et al. (1985). Continental Scientific Drilling Project (CSDP) core hole VC-2A was drilled here to a depth of 528 m in 1986 and found a temperature of 212°C. The core hole penetrated a thick sequence of intracaldera tuffs and volcaniclastic rocks (Fig. V50).

In 1988 CSDP core hole VC-2B was drilled to a depth of 1762 m, detecting a temperature of 295°C at a site 0.5 km east-northeast of VC-2A (Fig. V50). VC-2B gives a complete intracaldera section (Hulen and Gardner, 1989). Both VC-2A and B give similar sections through the intracaldera sequence, but there are some interesting differ-

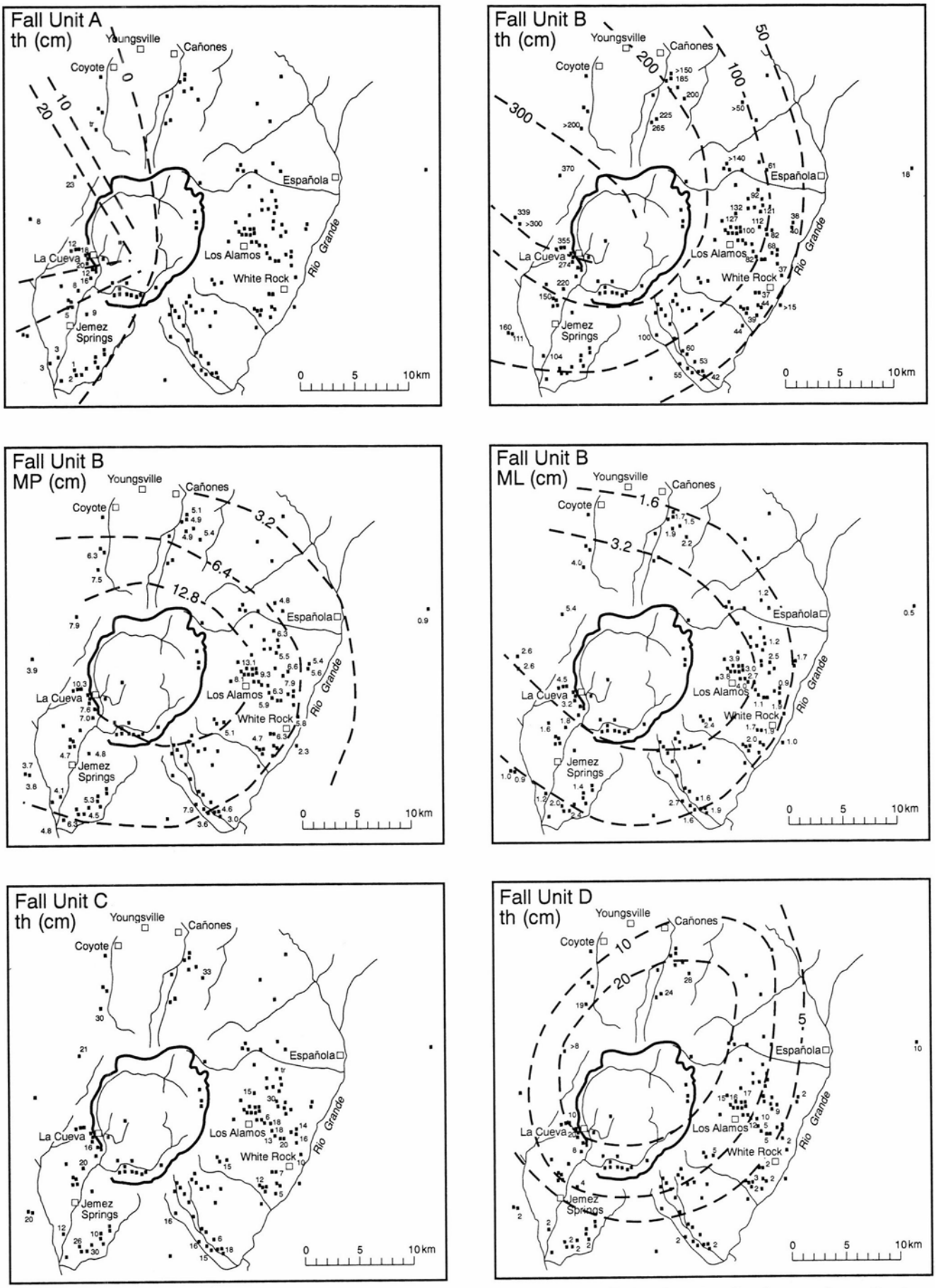

FIGURE V49—Isopachs and isopleths of selected fall units of the upper Bandelier Plinian deposit. All values are in centimeters. Heavy line is Valles caldera topographic rim.

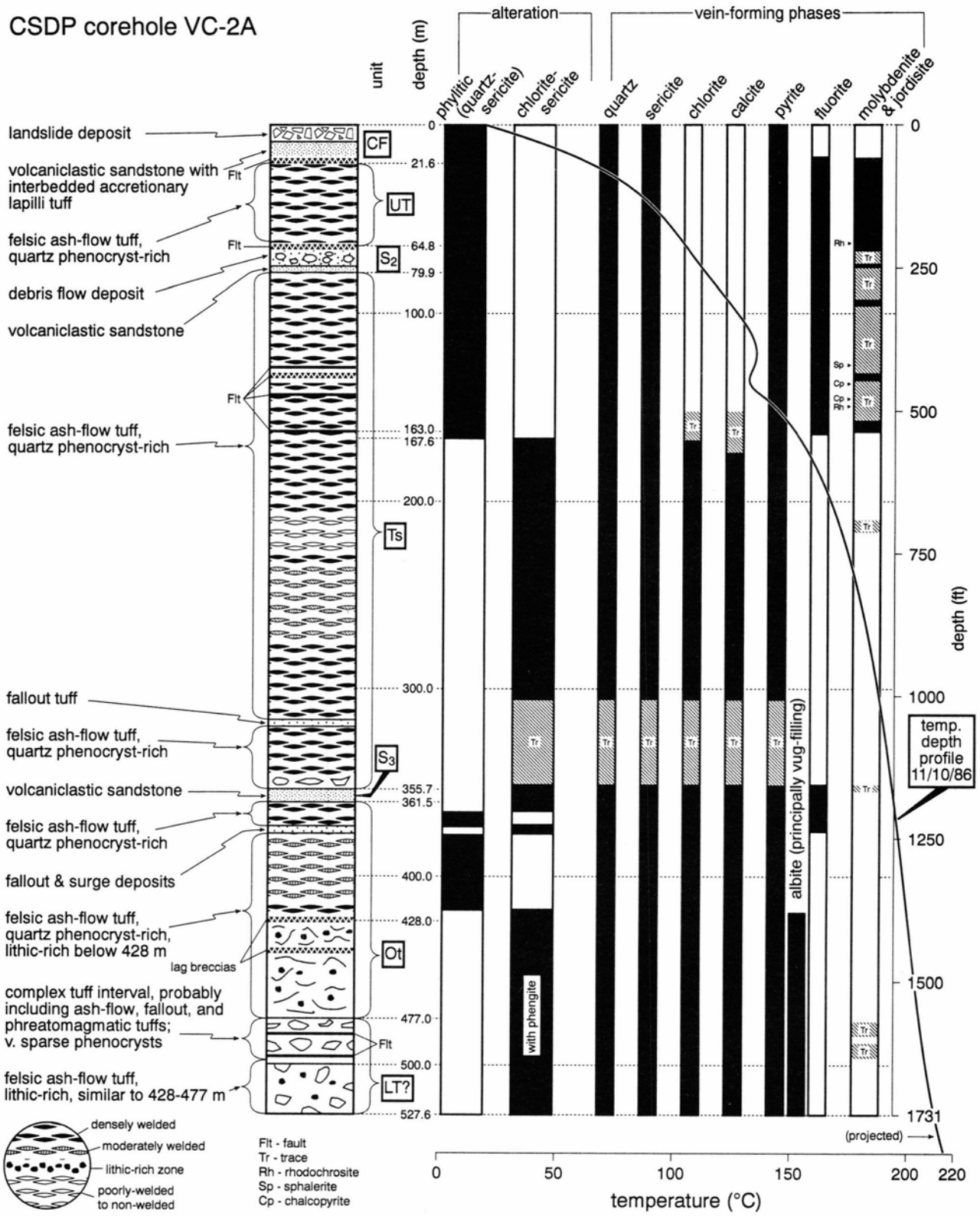

FIGURE V50—Logs of VC–2A (1986) and VC–2B (1988) core holes drilled in the Sulphur Springs area (from Hulen et al., 1988; Hulen and Gardner, 1989). CF—caldera fill; UT—Upper Tuffs; Ts—Tshirege Member (upper Bandelier Tuff); Ot—Otowi Member (lower Bandelier Tuff); LT—Lower Tuffs.

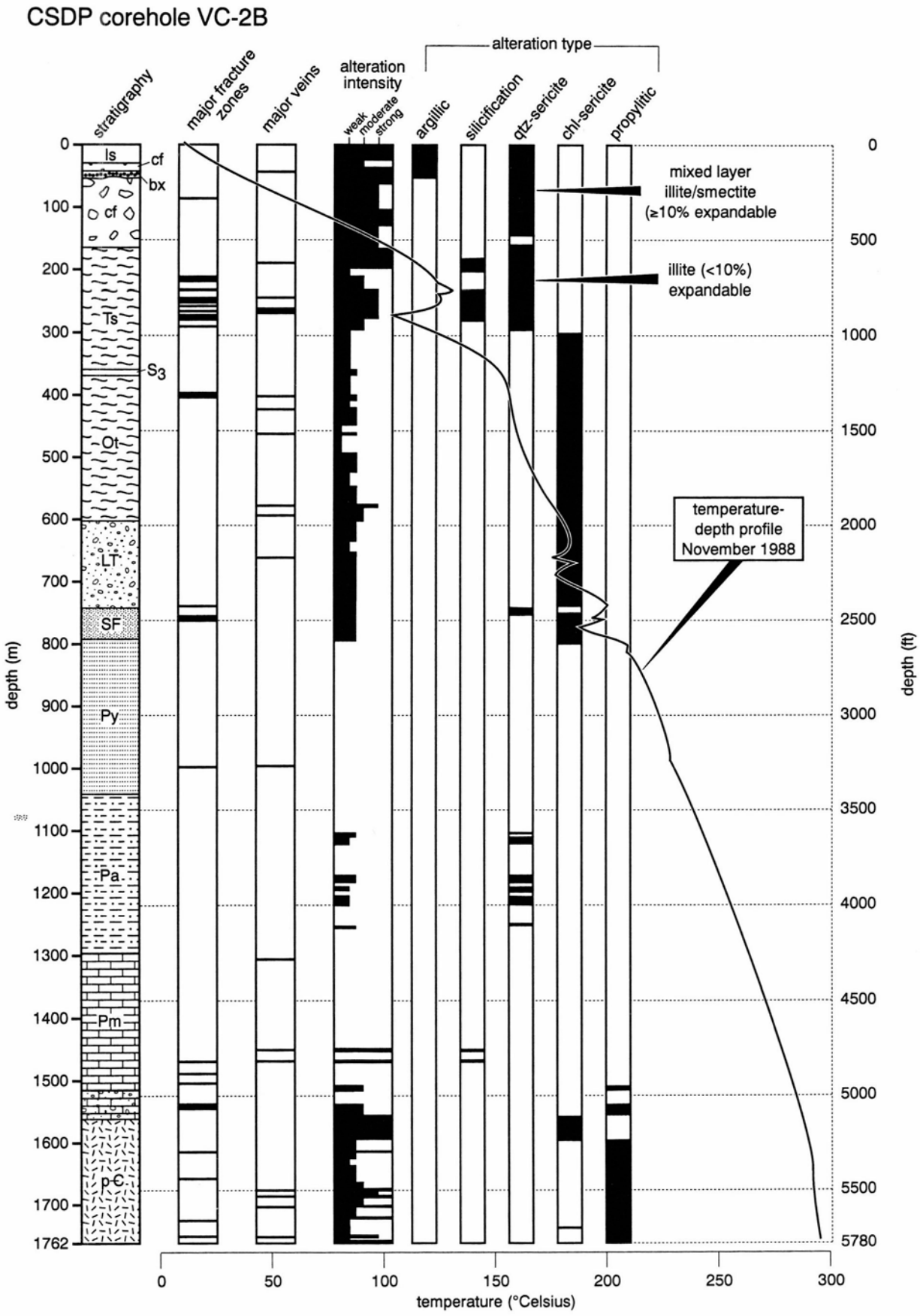
CSDP corehole VC-2B
stratigraphy
major fracture zones
major veins
alteration intensity
weak
moderate
strong
alteration type
argillic
silicification
qtz-sericite
chl-sericite
propylitic
ls
cf
bx
cf
Ts
S3
Ot
LT
SF
Py
Pa
Pm
pC
mixed layer illite/smectite (≥10% expandable
illite (<10%) expandable
temperature-depth profile November 1988
depth (m)
depth (ft)
0
100
200
300
400
500
600
700
800
900
1000
1100
1200
1300
1400
1500
1600
1700
1762
0
500
1000
1500
2000
2500
3000
3500
4000
4500
5000
5500
5780
0
50
100
150
200
250
300
temperature (°Celsius)

ences. Units in these cores correlate well with the intracaldera geology given by Nielson and Hulen (1984) from examination of cuttings from several Union Oil Company drill holes in the area to the immediate northeast of Sulphur Springs. The salient features are summarized below in stratigraphic order from oldest to youngest.

Lower tuffs: The lower most rhyolitic ignimbrites are the so called "Lower Tuffs" (Nielson and Hulen, 1984) found at depths (in VC-2B) from 599 to 742 m below the surface. These are thought to correlate with the San Diego Canyon ignimbrites, seen on Day 3, although this has not been rigorously proven (Turbeville and Self, 1988).

Lower Bandelier Tuff (Otowi Member): Up to 227 m of LBT occurs in the cores (372 to 599 m depth). It is surprisingly lithic-poor except for lithic-rich horizons at about 450 m in VC-2A (?lag breccia). The ignimbrite is generally densely welded, but the textures are overprinted by hydrothermal alteration.

Upper Bandelier Tuff (Tshirege Member): A relatively lithic-poor 275 m of homogeneous, hydrothermally altered UBT was cored in VC-2A.

Upper tuffs: At least 44 m of non- to moderately welded ignimbrite are found in many of the holes drilled in the western part of the caldera, but are missing in VC-2B. The source of the lithic-rich upper tuffs is uncertain. Nielson and Hulen (1984) and Hulen et al. (1988) recognize that they are above the UBT and are stratigraphically equivalent to the early postcaldera lava domes (circa 1.12 Ma). However, they are similar in appearance to the UBT. Interpretation depends on the nature of the S2 sandstone which separates the upper tuffs from the UBT (Hulen et al., 1991). It should be noted that in VC-2A the upper tuffs are bounded by faults, and a breccia (debris-flow deposit?) occurs above the S2 sandstone. All the ignimbrite units thicken in the subsurface from Sulphur Springs towards the east (Nielson and Hulen, 1984; Hulen et al., 1991).

Summary: Most geophysical studies across the caldera (see summaries in Goff et al., 1986; Heiken et al., 1986) indicate that caldera fill thickens to the east (Fig. V51). This is also suggested by Nielson and Hulen (1984), whc proposed that the intracaldera Bandelier tuffs thicken eastward. The intracaldera structure and geology are becoming moderately well known in the western-central parts. The geology of the eastern part is poorly understood due to a lack of good exposures and to a dearth of information east of the area of interest to geothermal exploration. The center of the resurgent block is not a simple up-domed structure but a horst (block uplift) along the trend of the Jemez fault zone, which crosses the resurgent center trending southwest-east-northeast (Fig. V2).

Sulphur Springs is located just east of the suspected ring fracture zones of the caldera on the western edge of Redondo resurgent block. The geology of the units is much affected by alteration. Units in the area of the springs are young landslide deposits, phreatic or phreatomagmatic tuffs (including accretionary lapilli) due to explosive activity in the thermal area, and post-caldera lake beds some of which dip westwards along with the underlying intracaldera ignimbrite, although this is difficult to appreciate from the hot-spring area. An early post-caldera Redondo Creek rhyolite lava flow, the Redondo Creek unit, is exposed along FS-105 just before the gate to Sulphur Springs.

Return along FS-105 to NM-502/4, where you turn left and proceed to White Rock following the route of previous days (144 mi).

END OF DAY 4.

Day 5: Bandelier outflow sheet and basalts of Cerros del Rio volcanic field

This day's route is considerably shorter than the previous one's and visits several locations exposing mainly UBT in the White Rock—Frijoles Canyon area, both in the Bandelier National Monument and along NM-501 and NM-502/4. Basaltic lavas and pyroclastic deposits of the Cerros del Rio field are also seen. This field is one of three basaltic centers peripheral to the Jemez Mountains that

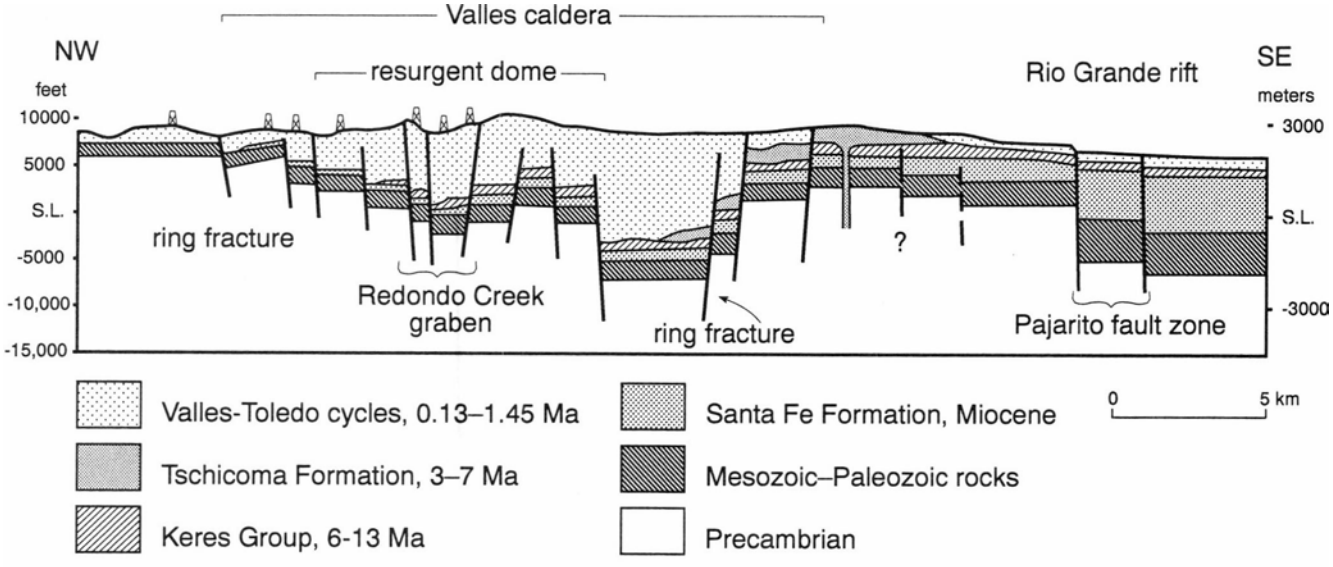

FIGURE V51—Schematic cross section northwest-southeast across the Valles caldera based on deep drill holes of Union Oil Co (see Hulen and Nielson, 1984) and the gravity interpretation of Segar (1974). Drill hole control (sites shown schematically by rigs) to the Precambrian basement is excellent from the west caldera flank to the center of the resurgent dome and agrees well with the gravity data, (from Goff, 1983).

were active immediately before and during the period of the Bandelier eruptions (2 Ma to present; Dunker et al., 1991). The trip stops, plus time allowed for enjoying the non-geologic attributes of the Bandelier National Monument, add up to a full day's field trip.

Leave White Rock driving west on NM-502/4 to the end of a sweeping right hand curve (5.9 mi). Pull off to left and turn through gate on unsignposted dirt road that runs parallel to NM-502/4 for 100 m and then turns abruptly left. Follow this rough dirt road (four-wheel drive advised but not essential) for 4 mi (not included in guide mileage) across the UBT surface. After the road runs under power lines, turn right at the fork and proceed until the road ends. Park and walk about 100 m along the path to the cliff edge at the right; the path continues steeply down to the Rio Grande in White Rock Canyon, but do not descend. The outcrop for Stop 20 occurs for about 50 m along the cliff face, where access is by ledges eroded into the UBT.

Stop 20: Topographic control of upper Bandelier ignimbrite and ash cloud surges, Ancho Canyon—White Rock Canyon junction

Significance: The UBT thickens in this area from a few meters to 200 m over a distance of less than a kilometer in response to the paleotopography. Characteristics of lateral flow unit margins are seen. The upper flow units have strong clast-size grading. Fisher (1979) interpreted surge deposits between the ignimbrite flow units as ash-cloud deposits in the original study of this phenomenon.

Description: Fall unit B of the UBT Plinian deposit is found at the base of the exposure, underlying basaltic lavas of the Cerros del Rio field. Flow units of the ignimbrite pinch out against the basaltic topographic "high", and have marginal concentrations of very coarse pumice (up to 1 m). Above a level equivalent to the top of the lower main flow unit (Stop 1), pumice- and crystal-rich cross-stratified surge beds occur between flow units. Fisher (1979) mapped extensive surge deposits at this horizon in the UBT over the Pajarito Plateau and ascribed to them an ash-cloud surge origin, the first recognition of such deposits.

The "sandy parting", in the original terminology of Smith and Bailey (1966), between the first and second UBT flow units has been interpreted as an ash-cloud deposit formed by elutriation from the underlying pyroclastic flow (Fisher 1970). This is based upon field observations that the sandy deposit does not begin to develop until about 15 km from the caldera rim and then steadily becomes thicker and more continuous away from the source (Fig. V52). The sandy lenses first appear in outcrop as very thin (millimeter thick) lenses of short lateral extent (less than 25 cm). As the lenses become thicker and longer, there is development of laminated bedding, dune structures, and low-angle cross beds. Maximum thickness is about 30-35 cm and several dune crests occur in a continuous pinch-and-swell layer (Fig. V53, top). In several places more than one ash cloud layer occurs at the top of the unit. Indications that the ash cloud originated at the top of the underlying flow rather than at the base of the next overlying flow are: (1) small-diameter, crystal-rich gas pipes extend from the underlying ignimbrite into the laminated ash cloud deposits; (2) the main surface horizon locally interfingers and is texturally gradational with the underlying flow unit; and (3) subsidiary surge lenses occur beneath the main surge horizon in several places. The subsidiary surge lenses are laterally

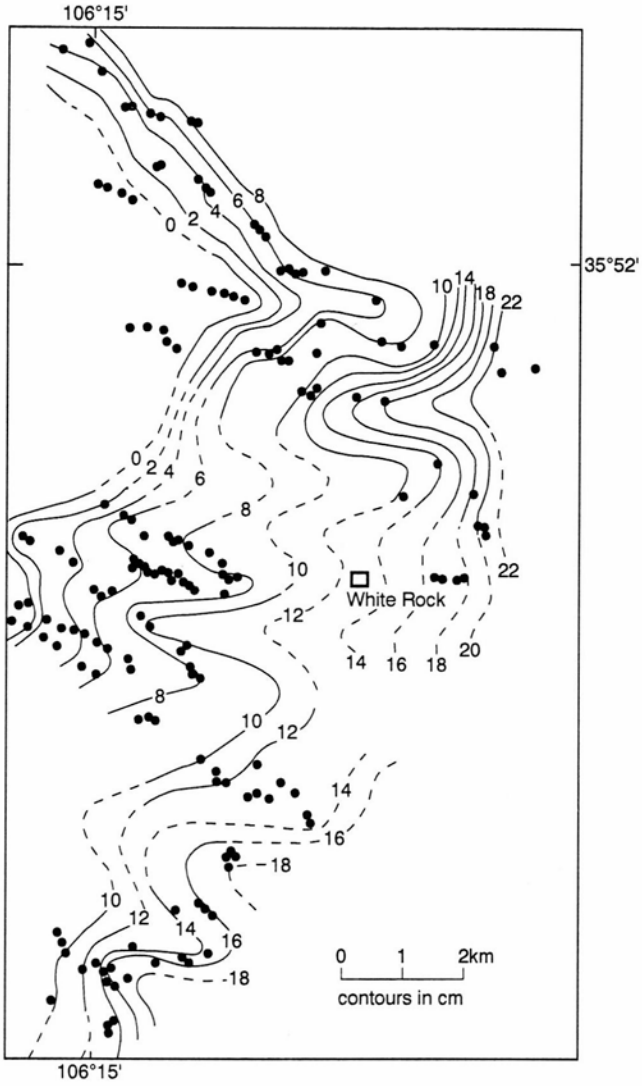

FIGURE V52—Averaged maximum thickness of ash cloud lenses at top of upper Bandelier Tuff flow unit 1 in the Pajarito Plateau area. The map was made by moving averages because maximum thickness changes are irregular and sampling was random. Dots are section localities, (from Fisher, 1979).

discontinuous and occur entirely within massive deposits of flow-unit 1 or else lie above thin pumice swarms or flows within its upper part. Figure V53 (bottom) shows schematically the development of an ash-cloud surge above a pyroclastic flow.

Retrace the route to NM-502/4, then turn left and drive 0.3 mi (6.2 mi) until the road begins to descend into Ancho Canyon. Park along the side of the road and walk downhill about 100 m into the canyon. The outcrop for Stop 21 occurs in the roadcut in upper Bandelier tuff on the right.

Stop 21: Upper Bandelier Tuff inter-flow unit surges and possible secondary explosion deposits, Ancho Canyon wall

This is a fairly small-scale detail of the upper part of the UBT exposed where **the** road begins its descent to Ancho Canyon. A very localized unit of bedded, crystal-rich tuff occurs between incipiently welded and vapor-phase altered ignimbrite flow units. This unit appears to drape a V-shaped depression in the top of the underly-

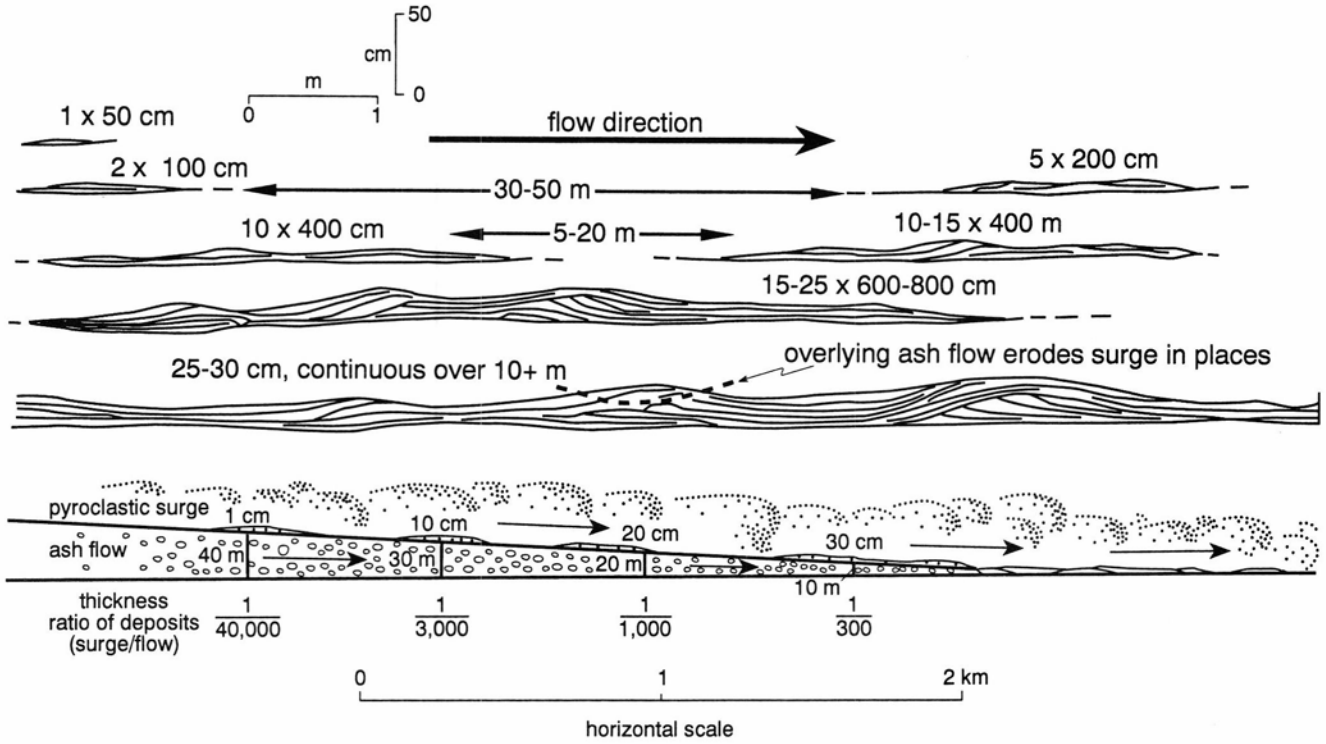

FIGURE V53—Top, illustration of actual dimensions of ash cloud lenses, distance between them, and relationship among thickness, length and internal structures across the width of the isopach field (R. V. Fisher, unpublished illustration). Bottom, schematic illustration of lateral thickness changes of the pyroclastic flow and the ash cloud surge developing above it, (from Fisher, 1979).

ing flow unit which is filled by material from the flow unit above (Fig. V54). The bedded material could be the result of fumarolic activity and/or secondary explosions in a newly deposited flow unit. In either case, it indicates slight pauses between flow unit emplacement events in the upper Bandelier (Tshirege) eruption, sufficient to permit minor explosive activity.

Return to vehicle and continue downhill into Ancho Canyon on NM-502/4. Pull off the road at 6.9 mi., where the exposure for Stop 22 is in a roadcut on the right (north) side.

Stop 22: Lower Bandelier Tuff and upper Bandelier Tuff with basal pumice-rich flow units, Ancho Canyon

A rare exposure is in this part of the Pajarito Plateau. The cream-colored LBT occurs beneath the UBT, separated by an erosion surface. Pumice-rich lower flow units occur in the UBT, with a thin, fine-grained ground-surge deposit between Plinian-fall deposit and ignimbrite. Note also the subhorizontal to dipping layers in the UBT in the outcrop and throughout this part of Ancho Canyon, thought to be fossil water table horizons cemented by clinoptilolite (R. A. Bailey, personal communication, 1985).

Proceed on NM-502/4 to the entrance to Bandelier National Monument (8.2 mi). Mileage in the monument is not added to the log. Turn left and drive into Frijoles Canyon, where you should proceed to the parking area at the Visitor Center. Geologists following the field guide should consult with the National Monument Rangers about locations they wish to visit. A short geological field guide for the canyon by G. Heiken and J. Eichelberger is available at the Visitor Center shop. The free leaflet on walks and features in the canyon may also be picked up at the Visitor Center.

Stop 23: Frijoles Canyon

NOTE: PLEASE, NO GEOLOGICAL HAMMERS OR SAMPLING IN THE NATIONAL MONUMENT AREA.

Upcanyon from the Visitor Center, the whole thickness of UBT and the very upper part of the LBT are exposed along the canyon walls. The floor of Frijoles Canyon near the Visitor Center is approximately the UBT/LBT contact, and LBT is exposed about 1 mile upcanyon. UBT in upper Frijoles Canyon is more than 100 m thick, has three cooling units, and has Plinian fall units B and **D** at the base. These can be seen in the west wall of a small arroyo (gully) just downcanyon from the first Indian dwelling

FIGURE V54—Bedded secondary deposits in upper part of flow unit around a possible explosion crater (enclosed by dashed lines) to left of small person, between flow units of upper part of upper Bandelier Tuff, Stop 21. Arrow indicates flow unit boundary with thin pyroclastic surge; L—fumarolic pipe with lithic concentration in ignimbrite filling explosion crater.

sites on the path to the Long House (see the Bandelier National Monument leaflet available at the Visitor Center). Further along this path, in the area of the Indian dwellings, pipelike structures of possible fumarolic origin can be seen weathering out of the UBT. The geological sites can be interspersed with investigation of Indian dwelling places and artifacts. Frijoles Canyon contained a major Indian community until about 1100 A.D. when climate change probably drove the inhabitants to lower elevations.

Walk downcanyon from the Visitor Center following the path to Frijoles (Upper) Falls. After the third foot bridge crossing the stream, leave the main path and head upslope into the area of tent rocks which occur at the base of the cliff to the right (east) of the area where the UBT suddenly increases in thickness (see Fig. V55).

Stop 24: Frijoles Canyon—topographic controls on upper Bandelier Tuff thickness and entrainment of surface lithic clasts

Significance: The UBT ignimbrite thickens dramatically over a short distance as it fills an old canyon (Fig. V55). The base of the ignimbrite has many surface-derived basaltic lithic clasts that match the underlying lithologies of Cerro del Rio tholeiitic basalt lavas, scoria cones, and tephra deposits showing that ignimbrite deposition overwhelmed this part of the Cerros del Rio volcanic field.

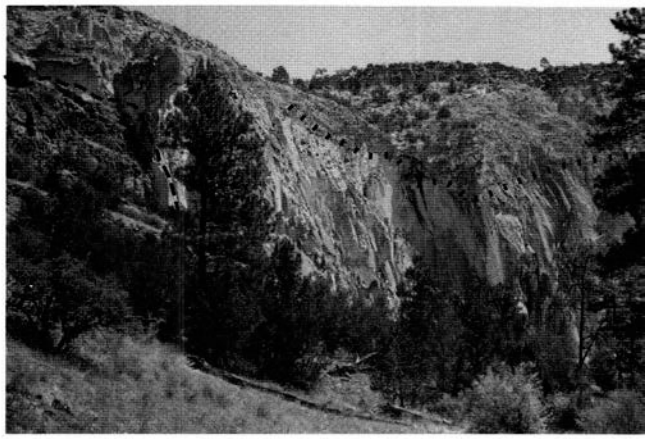

FIGURE V55—View of northeast face of Frijoles Canyon wall above Stop 24, showing upper Bandelier Tuff (UBT) thickening over paleocanyon wall (dashed line) with Cerros del Rio basalts (CB) under ignimbrite. On right > 100 m of upper Bandelier Tuff show tent rocks in nonwelded facies at base, dipping boundary of onset of strong vapor phase alteration (dotted line), and incipiently welded and vapor phase altered upper thin flow unit facies at top (upper cliffs).

Description: Thick nonwelded UBT ignimbrite rests on basaltic rocks including base surge deposits, a scoria cone, and fountain-fed lava flows from the Cerros del Rio field. Small remnants of the UB Plinian deposit can be found amongst the underlying scoria. These tholeiitic volcanics are from extremely local sources, as evidenced by the scoria cone and clastogenic lava flows exposed at this location. Continuation of the walk down Frijoles Canyon brings one to thick tholeiitic lavas and bedded phreatomagmatic tuffs of the Cerros del Rio group. The base surge deposits and phreatomagmatic tuffs are the result of basalt magma being erupted into the Rio Grande channel or into lakes derived by blockage of the river by Cerros del Rio lava flows. Further details of this area can be found in the other field guide in this bulletin (Heiken et al., this volume).

Return to the Visitor Center and leave Bandelier National Monument, turning right at NM-502/4 and retracing your route toward White Rock. At 14.4 mi, just before the residential area of Pajarito Acres (White Rock), stop at the last outcrop on the left side on a left-hand curve in the road. The roadcut and the small mesa of ignimbrite above form the outcrop for Stop 25.

Stop 25: Thin Bandelier ignimbrite on basalt of western part of Cerros del Rio volcanic field

Significance: Here the UBT is composed of only three flow units and is 12 to 15 m thick compared with the many 10s-100s of meters seen previously today. The ignimbrite in this area thins against a basaltic topographic high upon which White Rock is built. The rubbly top of a basalt lava flow overlain by a calichified soil is exposed under the ignimbrite and Plinian deposit. The erosive effects of the lowermost UB pyroclastic flows can be seen by the thinning of the underlying Plinian deposit (unit B) onto the paleo-high, as well as surge partings between thin flow units further up-section. The Plinian deposit would have mantled the topography evenly before the arrival of the erosive pyroclastic flows.

END OF DAY 5 AND OF THE FIELD GUIDE TO BANDELIER TUFF AND VALLES CALDERA

References

Aldrich, M. J., 1986, Tectonics of the Jemez lineament in the Jemez Mountains and the Rio Grande rift: Journal of Geophysical Research, v. 91, no. B2, pp. 1753-1762.

Aldrich, M. J., Jr., and Laughlin, A. W., 1984, A model for the tectonic development of the southeastern Colorado Plateau boundary: Journal of Geophysical Research, v. 89, no. B12, pp. 10,207-10,218.

Ankeny, L. A., Braile, L. W., and Olsen, K. H., 1986, Upper crustal structure beneath the Jemez Mountains volcanic field, New Mexico, determined by three-dimensional simultaneous inversion of seismic refraction and earthquake data: Journal of Geophysical Research, v. 91, no. B6, pp. 6188-6198.

Bachman, G. 0., and Mehnert, H. H., 1978, New K-Ar dates and the late Pliocene to Holocene geomorphic history of the central Rio Grande region, New Mexico: Geological Society of America, Bulletin 89, pp. 283-294.

Bailey, R. A., Smith, R. L., and Ross, C. S., 1969, Stratigraphic nomenclature of volcanic rocks in the Jemez Mountains, New Mexico: U.S. Geological Survey, Bulletin 1274-P, 19 pp.

Balsley, S. D., 1988, The petrology and geochemistry of the Tshirege Member of the Bandelier Tuff, Jemez Mountains volcanic field, New Mexico, USA: Unpublished MS thesis, University of Texas (Arlington), 159 pp.

Balsley, S. D., Wolff, J. A., Kuentz, D. C. Kyle, P. R., and Gardner, J. N., 1987, The inter-relationship of the upper and lower Bandelier Tuff-evidence from incompatible trace elements: American Geophysical Union, EOS, Transactions, v. 68, no. 44, p. 1512.

Carey, S., and Sparks, R. S. J.,1986, Quantitative models of fallout and dispersal of tephra from volcanic eruption columns: Bulletin Volcanologique, v. 48, no. 2, pp. 109-125.

Crowe, B. M., Linn, G. W., Heiken, G., and Bevier, M. L., 1978, Stratigraphy of the Bandelier Tuff in the Pajarito Plateau: Los Alamos National Laboratory, Informal Rept LA-7225-MS, 56 pp.

Doell, R. R., Dalrymple, G. B., Smith, R. L., and Bailey, R. A., 1968, Paleomagnetism, potassium-argon ages, and geology of rhyolites and associated rocks of the Valles caldera, New Mexico *in* Coats, R. R., Hay, R. L., and Anderson, C. A., (eds), Studies in volcanology-a memoir in honor of Howell Williams: Geological Society of America, Memoir 116, pp. 211-248.

Dunbar, N. W., and Hervig, R. L., 1992, Volatile and trace element composition of melt inclusions from the lower Bandelier Tuff-implications for magma chamber processes and eruptive style: Journal of Geophysical Research, v. 97, no. B11, pp. 15,151-15,170.

Dunker, K. E., Wolff, J. A., Harmon, R. S., Leat, P. T., Dickin, A. P., and Thompson, R. N., 1991, Diverse mantle and crustal components in lavas of the NW Cerros del Rio volcanic field, Rio Grande rift, New Mexico: Contributions to Mineralogy and Petrology, v. 108, no. 3, pp. 331-345.

Eichelberger, J. C., and Koch, F. G., 1979, Lithic fragments in the Bandelier Tuff, Jemez Mountains, New Mexico: Journal of Volcanology and Geothermal Research, v. 5, no. 1-2, pp. 115- 134.

Fisher, R. V., 1979, Models for pyroclastic surges and pyroclastic flows: Journal of Volcanology and Geothermal Research, v. 6, no. 3-4, pp. 305-318.

Gardner, J. N., and Goff, F., 1984, Potassium-argon dates from the Jemez volcanic field-implications for tectonic activity in the north-central Rio Grande rift: New Mexico Geological Society, Guidebook 35, pp. 75-81.

Gardner, J. N., Goff, F., Garcia, S., and Hagan, R. C., 1986, Strati-graphic relations and lithologic variations in the Jemez volcanic field, New Mexico: Journal of Geophysical Research, v. 91, no. B2, pp. 1763-1778.

Goff, F., 1983, Subsurface structure of Valles caldera-a resurgent cauldron in northern New Mexico: Geological Society of America, Abstracts with Program, v. 15, no. 5, p. 381.

Goff, F., and Gardner, J. N., 1980, Geologic map of the Sulphur Springs area, Valles caldera geothermal system, New Mexico: Los Alamos Scientific Laboratory, Map LA-8634-MAP, two sheets, scale 1:5000.

Goff, F., Gardner, J. N., Baldridge, W. S., Hulen, J. B., Nielsen, D. L., Vaniman, D., Heiken, G., Dungan, M. A., and Broxton, D., 1989, Excursion 17B-volcanic and hydrothermal evolution of Pleistocene Valles caldera and Jemez volcanic field, *in* Chapin, C. E., and Zidek, J. (eds); Field excursions to volcanic terranes in the western United States, Volume I: Southern Rocky Mountain region: New Mexico Bureau of Mines and Mineral Resources, Memoir 46, pp. 381-431.

Goff, F., Gardner, J. N., Vidale, R., and Charles, R., 1985, Geochemistry and isotopes of fluids from Sulphur Springs, Valles caldera, New Mexico: Journal of Volcanology and Geothermal Research, v. 23, no. 3-4, pp. 273-289.

Goff, F., Grigsby, C., Trujillo, P., Counce, D., and Kron, A., 1981, Geology, water geochemistry, and geothermal potential of the Jemez Springs area, Cañon de San Diego, New Mexico: Journal of Volcanology and Geothermal Research, v. 10, no. 1-3, pp. 227-244.

Goff, F., Heiken, G., Tamanyu, S., Gardner, J., Self, S., Drake, R., and Shafiqullah, M., 1984, Location of Toledo caldera and formation of the Toledo embayment, Jemez Mountains, New Mexico: American Geophysical Union, EOS, Transactions, v. 65, no. 45, p. 1145.

Goff, F., Rowley, J., Gardner, J. N., Hawkins, W., Goff, S., Charles, R., Wachs, D., Maassen, L., and Heiken, G., 1986, Initial results from VC-1: first Continental Scientific Drilling Program core hole in Valles caldera, New Mexico: Journal of Geophysical Research, v. 91, no. B2, pp. 1742-1752.

Goff, F., and Shevenell, L.,1987, Travertine deposits of Soda Dam, New Mexico, and their implications for the age and evolution of the Valles caldera hydrothermal system: Geological Society of America, Bulletin 99, pp. 292-302.

Heiken, G., Goff, F., Stix, J., Tamanyu, S., Shafiqullah, M., Garcia, S., and Hagan, R., 1986, Intracaldera volcanic activity, Toledo caldera and embayment, Jemez Mountains, New Mexico: Journal of Geophysical Research, v.91, no. B2, pp. 1799-1815.

Hildreth, W., 1979, The Bishop Tuff-evidence for the origin of compositional zonation in silicic magma chambers: Geological Society of America, Special Paper 180, pp. 43-85.

Hulen, J., Gardner, J. N., Neilson, D., and Goff, F., 1988, Stratigraphy, structure, hydrothermal alteration, and ore mineralization encountered in CSPD core hole VC-2A, Sulphur Springs, Valles caldera, New Mexico-a detailed overview: University of Utah Research Institute, Earth Science Laboratory, Report ESL-88001-TR, 44 pp.

Hulen, J. B., and Gardner, J. N., 1989, Field geologic log for Continental Scientific Drilling Program core hole VC-2B, Valles caldera, New Mexico: University of Utah Research Institute, Earth Science Laboratory, Report ESL-89025-TR, 92 pp.

Hulen, J. B., Neilson, D. L., and Little, T. M., 1991, Evolution of the western Valles caldera complex, New Mexico-evidence from intracaldera sandstones, breccias, and surge deposits: Journal of Geophysical Research, 96, no. B5, pp. 8127-8142.

Izett, G. A., 1981, Volcanic ash beds-recorders of upper Cenozoic silicic volcanism in the western United States: Journal of Geophysical Research, v. 86, no. B11, pp. 10,200-10,223.

Izett, G. A., and Obradovich, J. D., 1994, $^{40}Ar/^{39}Ar$ age constraints for the Jaramillo normal subchron and the MatuyamaBrunches geomaghnetic boiundary: Journal of Geophysical Research, v. 99, pp. 2925-2934.

Izett, G. A., Obradovich, J. D., Naeser, C. W., and Cebula, G. T., 1981, Potassium-argon and fission-track zircon ages of Cerro Toledo rhyolite tephra in the Jemez Mountains, New Mexico: U.S. Geologic Survey, Professional Paper 1199-D, pp. 37-43.

Izett, G. A., Wilcox, R. E., and Borchardt, G. A., 1972, Correlation of a volcanic ash bed in Pleistocene deposits near Mount Blanco, Texas, with the Guaje Pumice Bed of the Jemez Mountains, New Mexico: Quaternary Research, v. 2, no. 4, pp. 554578.

Kite, W. M., 1985, Caldera-forming sequences and facies variations in the Bandelier Tuff, central New Mexico: Unpublished MS thesis, Arizona State University (Tempe), 374 pp.

Kite, W. M., and Self, S., 1985, Caldera-forming eruption pat-

terns in the Jemez Mountains, *in* Heiken, G. (ed.) Proceedings of the Workshop on Recent Research in the Valles caldera, Los Alamos, NM, USA: Los Alamos National Laboratory, Rept. LA-1-339-C, pp. 29-30.

Kuentz, C. D., 1986, The Otowi Member of the Bandelier Tuff-a study of the petrology, petrography, and geochemistry of an explosive silicic eruption, Jemez Mountains, New Mexico: Unpublished MS thesis, University of Texas (Arlington), 165 PP.

Loeffler, B. M., Vaniman, D. T., Baldridge, W. S., and Shafiqullah, M., 1988, Neogene rhyolites of the northern Jemez volcanic field, New Mexico: Journal Geophysical Research, v. 93, no. B6, pp. 6157-6168.

McCormick, T. M., 1989. Partial homogenization of cryptoperthites in an ignimbrite cooling unit: Contributions to Mineralogy and Petrology, v. 101, no. 1, pp. 104-111.

McPherson, J. G., Flannery, J. R., and Self, S.,1989, Discussion-soft-sediment deformation (fluid escape) features in a coarse-grained pyroclastic-surge deposit, north-central New Mexico: Sedimentology, v. 36, no. 5, p. 943-947.

McPherson, J. G., Waresback, D. B., and Flannery, J. R., 1984, Volcanogenic fan building, Puye Formation, Jemez Mountains, New Mexico [abs.], American Geophysical Union, EOS, Transactions, v. 65, no. 45, p. 1134.

Neilsen, D. L., and Hulen, J. B., 1984, Internal geology and evolution of the Redondo dome, Valles caldera, New Mexico: Journal of Geophysical Research, v. 89, no. B10, pp. 8695-8711.

Neilson, D. L., and Hulen, J. B., 1989, New evidence for a concealed, pre-Bandelier age caldera in the western Valles caldera complex, New Mexico, IAVCEI Santa Fe meeting on Continental Magmatism (abstracts): New Mexico Bureau of Mines and Mineral Resources, Bulletin 131, p. 202.

Nocita, B. W., 1988, Soft-sediment deformation (fluid-escape) features in a coarse-grained pyroclastic-surge deposit, north-central New Mexico: Sedimentology, v. 35, no. 2, pp. 275-285.

Potter, D. B., and Oberthal, C. M., 1983, Vent sites and flow directions of the Otowi ash flows (lower Bandelier Tuff), New Mexico: Geological Society of America, Bulletin 98, pp. 6676.

Pyle, D. M., 1989, The thickness, volume and grain size of tephra deposits: Bulletin Volcanologique, v. 51, no. 1, pp. 1-15.

Ross, C. S., and Smith, R. L., 1961, Ash-flow tuffs-their origin, geologic relations, and identifications: U.S. Geological Survey, Professional Paper 366,81 pp.

Segar, R. L., 1974, Quantitative gravity interpretation, Valles caldera area, Sandoval and Rio Arriba counties, New Mexico: University of Utah Research Institute, Earth Science Laboratory, Open File Report NM/BACA-27,12 pp.

Self, S., Gardner, J. N., and Goff, F., 1987, A field guide to the Jemez Mountains volcanic field, New Mexico, *in* G. H. Davis and E. M. VandenDolder (eds.), Geologic diversity of Arizona and its margins-excursions to choice areas: Arizona Bureau of Geology and Mining Technology, Special Paper 5, pp. 95-112.

Self, S., Goff, F., Gardner, J. N., Wright, J. V., and Kite, W. M., 1986, Explosive rhyolite volcanism in the Jemez Mountains-vent locations, caldera development and relation to regional structure: Journal of Geophysical Research, v. 91, no. B2, pp. 1779-1798.

Self, S., Kircher, D. E., and Wolff, J. A., 1988, The El Cajete Series, Valles caldera, New Mexico: Journal of Geophysical Research, v. 93, no. B6, pp. 6113-6128.

Self, S., Wolff, J. A., Sykes, M. L., and Skuba, C.E., 1991, Isotopic and trace element characteristics of rhyolites from the Valles caldera, New Mexico: Final Tech. Rept. for U.S. D.O.E. grant DE-GEO5-87ER13795, 113 pp.

Skuba, C. E., Wolff, J. A., and Balsley, S. D., 1989, Trace element evidence for the origin of the Bandelier Tuff and associated rhyolites of the Valles caldera, Jemez Mountains, New Mexico: Geological Society of America, Abstract Programs 21, p. 41.

Smith, R. L., and Bailey, R. A., 1966, The Bandelier Tuff-a study of ash-flow eruption cycles from zoned magma chambers: Bulletin of Volcanology, v. 29, no. 1, pp. 83-104.

Smith, R. L., and Bailey, R. A., 1968, Resurgent cauldrons *in* Coats, R. R., Hay, R. L., and Anderson, C. A. (eds.) Studies in volcanology-a memoir in honor of Howell Williams: Geological Society of America, Memoir 116, pp. 613-662.

Smith, R. L., Bailey, R. A., and Ross, C. S.,1961, Structural evolution of the Valles caldera, New Mexico, and its bearing on the emplacement of ring dikes: U.S. Geological Survey, Professional Paper 424-D, pp. D145-D149.

Smith, R. L., Bailey, R. A., and Ross, C. S., 1970, Geologic map of the Jemez Mountains, New Mexico: U.S. Geological Survey, Miscellaneous Geological Investigations Map 1-571, scale 1:125,000.

Spell, T. L., 1987, Geochemistry of Valles Grande Member ring fracture rhyolites, Valles caldera, New Mexico: Unpublished MS thesis, New Mexico Institute of Mining and Technology, Socorro, New Mexico, 212 pp.

Spell, T. L., and Harrison, T. M., 1993, $^{40}Ar/^{39}Ar$ geochronology of post-Valles caldera rhyolites, Jemez volcanic field, New Mexico: Journal of Geophysical Research, v. 98, no. B5, pp. 8031-8051.

Spell, T. L., and Kyle, P. R., 1989, Petrogenesis of Valle Grande Member rhyolites, Valles caldera, New Mexico-implications for evolution of the Jemez Mountains magmatic systems: Journal of Geophysical Research, v. 94, pp. 10,379-10,396.

Spell, T. L., Harrison, T. M., and Wolff, J. A., 1990, $^{40}Ar/^{39}Ar$ dating of the Bandelier Tuff and San Diego Canyon ignimbrites, Jemez Mountains, New Mexico-temporal constraints on magmatic evolution: Journal of Volcanology and Geothermal Research, v. 43, no. 1-2, pp. 175-193.

Spell, T. L., McDougall, I., and Doulgeris, A. P., in preparation, $^{40}Ar/^{39}Ar$ geochronology of the transition between two caldera-forming eruptions: the Cerro Toledo Rhyolite, Jemez volcanic field, New Mexico: submitted to Geological Society of America Bulletin.

Stix, J., Goff, F., Gorton, M. P., Heiken, G., and Garcia, S. R., 1988, Restoration of compositional zonation in the Bandelier silicic magma chamber between two caldera-forming eruptions-geochemistry and origin of the Cerro Toledo Rhyolite, Jemez Mountains, New Mexico: Journal of Geophysical Research, v. 93, no. B6, pp. 6129-6147.

Turbeville, B. N., and Self, S., 1988, San Diego Canyon ignimbrites-pre-Bandelier tuff explosive rhyolitic volcanism in the Jemez Mountains, New Mexico: Journal of Geophysical Research, v. 93, no. B6, pp. 6148-6156.

Turbeville, B. N., Waresback, D. B., and Self, S., 1989, Lava-dome growth and explosive volcanism in the Jemez Mountains, New Mexico-evidence from the Plio-Pleistocene Puye alluvial fan: Journal of Volcanology and Geothermal Research, v. 36, no. 4, pp. 267-291.

Walker, G. P. L., 1981, Plinian eruptions and their products: Bulletin Volcanologique, v. 44, no. 4, pp. 223-240.

Walker, G. P. L., 1972, Crystal concentration in ignimbrites: Contributions to Mineralogy and Petrology, v. 36, no. 1, pp. 135- 146.

Waresback, D. B., and Turbeville, B. N., 1990, Evolution of a PlioPleistocene volcanogenic-alluvial fan-the Puye Formation, Jemez Mountains, New Mexico: Geological Society of America, Bulletin 102, no. 3, pp. 298-314.

Wilson, C. J. N., 1985, The Taupo eruption, New Zealand-II. The Taupo ignimbrite: Philosophical Transactions of the Royal Society of London, Series A, no. 314, pp. 229-256.

Wilt, M., and Vonder Haar, S.,1986, A geologic and geophysical appraisal of the Baca Geothermal field, Valles caldera, New Mexico: Journal of Volcanology and Geothermal Research, v. 27, no. 3-4, pp. 349-370.

Wolff, J. A., Elwood, B. B., and Sachs, S. D., 1989, Anisotropy of magnetic susceptibility in welded tuffs-application to a welded-tuff dyke in the Tertiary Trans-Pecos Texas volcanic province, USA: Bulletin Volcanologique, v. 51, no. 4, pp. 299310.

Wolff, J. A., and Gardner, J. N., 1995, Is the Valles caldera entering a new cycle of activity?: Geology, V. 23, pp. 411-414.

Part II: Field guide to the maar volcanoes of White Rock Canyon

Acknowledgments

This study was supported by the University of California Institute of Geophysics and Planetary Physics, Los Alamos Branch. Information on the hydrology of the region came from hydrologist and geologist Bill Purtymun, Los Alamos National Laboratory, who also helped us with access to the lower reaches of White Rock Canyon.

Grant Heiken and Kenneth Wohletz
Los Alamos, New Mexico 87545

Richard V.Fisher
Santa Barbara, California 93106

David P. Dethier
Williamstown, Massachusetts 01267

Introduction

Rift volcanism is often characterized by the complex interplay between volcanic and geomorphic processes. By their very nature, rifts are the loci for basaltic volcanism and often host the continental depressions that serve also as groundwater basins, major rivers, and lakes. Eruption processes are controlled by the depths at which rising magma intercepts either ground or surface water; in some instances, modern or ancient aquifers can be mapped by identifying the degree of phreatomagmatic activity that characterizes cones or tuff rings within a rift-bound volcanic field.

The Cerros del Rio volcanic field, located in the Espanola Basin, immediately west of Santa Fe (Fig. W1), contains typical examples of the products of rift processes that have occurred within the Rio Grande rift over the last 3 m.y. The best exposures of sedimentary and volcanic rocks of the rift and of proximal pyroclastic rocks from the adjacent Jemez volcanic field are along White Rock Canyon. This canyon of the Rio Grande, with a maximum depth of 300 m, begins at Otowi, along the road between Santa Fe and Los Alamos, and ends at Cochiti Pueblo (Fig. W2); much of the lower half of the canyon has been partly flooded by Cochiti Reservoir, a flood control and irrigation dam constructed upstream from the pueblo.

There are no roads and only difficult trails along White Rock Canyon; for this reason it is easiest to use a boat to gain access to the locations described in this guide. The following descriptions along the canyon are keyed to prominent geographic features in a manner similar to a traditional geological field guide.

Geologic setting and history of the Rio Grande rift

The Rio Grande rift is a chain of grabens over 1000 km long, which trend south from Leadville, Colorado, to the U.S.—Mexico border near Presidio Texas (Baldridge et al., 1984). The northern rift, from central Colorados to central New Mexico is well-defined, but breaks into a broad zone of grabens and horsts south of Socorro, New Mexico, where the actual rift is better defined by geophysical characteristics than by geomorphic features. Based upon petrologic, gravity, heat flow, and magnetotelluric surveys, the crust under the rift thins to as little as 30 km, in contrast with crustal thicknesses of 40 to 45 km east and west of the rift (summarized in Baldridge et al., 1984).

Extension, leading to rift formation, began between 32 and 26 m.y. ago, along a N—S-trending zone of weakness that had developed during late Paleozoic time (Chapin, 1979). Within the central segment, from Alamosa, Colorado, to Socorro, New Mexico, the rift consists of a NNE-trending line of en echelon basins.

The Cerros del Rio volcanic field, the subject of this field trip, is located in one of these en echelon basins, the Espanola Basin (Fig. W3); this basin is 40 km by 65 km, separated from adjacent basins by basement ridges (Manley, 1979). The predominantly coarse-grained clastic sedimentary rocks (partly consolidated arkosic sandstones, siltstones, and conglomerates) of the basin are overlain by or intertongued with volcanic and volcaniclastic rocks of the Jemez Mountains to the west, basaltic lava flows of the Taos Plateau to the north, and the Cerros del Rio volcanic field along its southern margin. Many of these sedimentary rocks represent alluvial fan deposits from the Precambrian and Paleozoic highlands to the east, north, and west (underlying the volcanic rocks of the Jemez Mountains) (Cavazza, 1986).

Most of these clastic sedimentary rocks are included in the Santa Fe Group, which ranges in age from —21 Ma to 1.0 Ma (Hawley, 1978; Manley, 1979). Interbedded with these Santa Fe Group rocks are fallout tuffs, which serve well as marker beds and can be observed in outcrops along the road from Santa Fe to Espanola. These tuffs have ages of 9-14 Ma (fission track ages) and are probably from the Jemez volcanic field. Total thickness of these sedimentary rocks is between 1.5 and 2.5 km, depending upon the model used to interpret the gravity data or by extending slopes measured on the older rocks exposed at the basin margins (Manley, 1979). Detailed stratigraphic and paleontologic studies are covered in a monograph by Galusha and Blick (1971); later basin studies have built upon this work.

How old is the Rio Grande and how long has it been in its present location along the central rift? Originating in central Colorado, this river presently connects the rift basins until the rift is no longer visible in west Texas (where the river forms the border between the U.S. and Mexico it is known as the Rio Bravo del Norte). Fluvial gravels that include lithologies derived from outside the basin to the north, unconformably overlie sedimentary rocks dated at between 5.6 m.y. and 2.9 m.y. (Manley, 1979). The Rio Grande was established as a throughgoing river during early Pliocene time (Machette, 1978; Waresback, 1986).

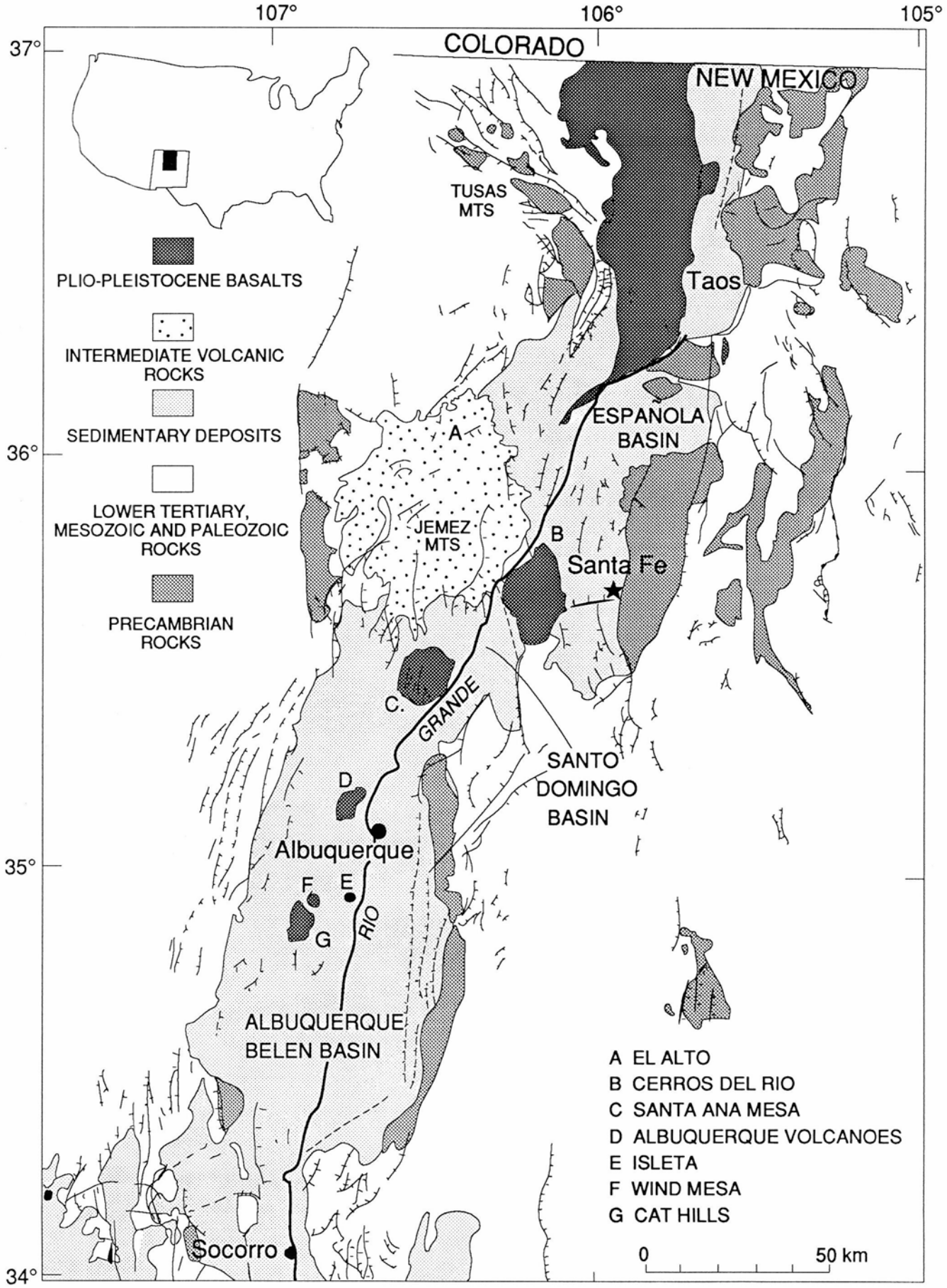

FIGURE W1—Generalized geologic map of the central Rio Grande rift (from Baldridge, 1979). Letters A to G indicate major Plio–Pleistocene volcanic fields. White Rock Canyon begins at the letter "B", on the north side of the Cerros del Rio volcanic field (see Fig. W6).

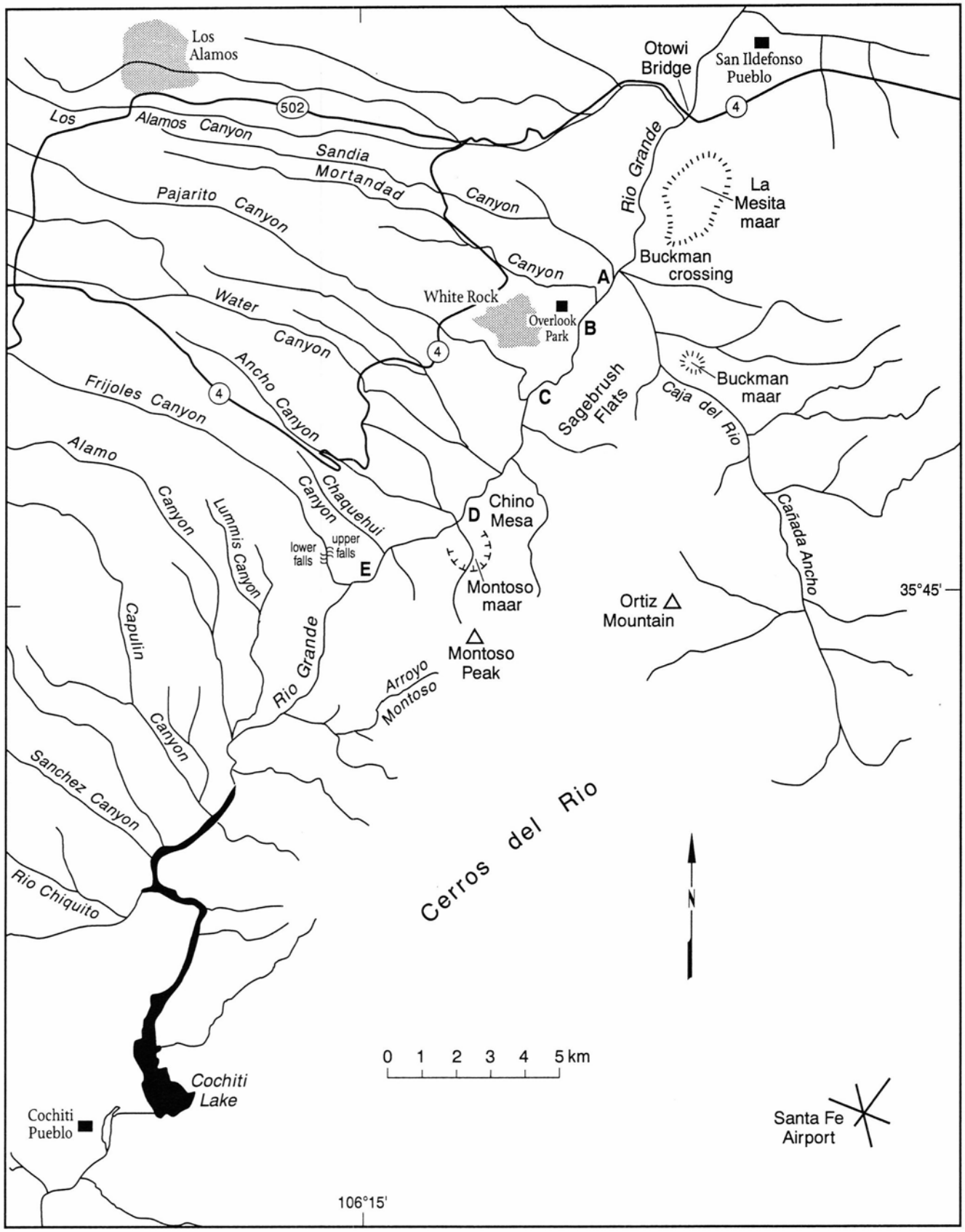

FIGURE W2—Map of White Rock Canyon, from Otowi Bridge, where NM–502 crosses the Rio Grande, to Cochiti Lake. Sites discussed in the text are keyed to geographic names on the map.

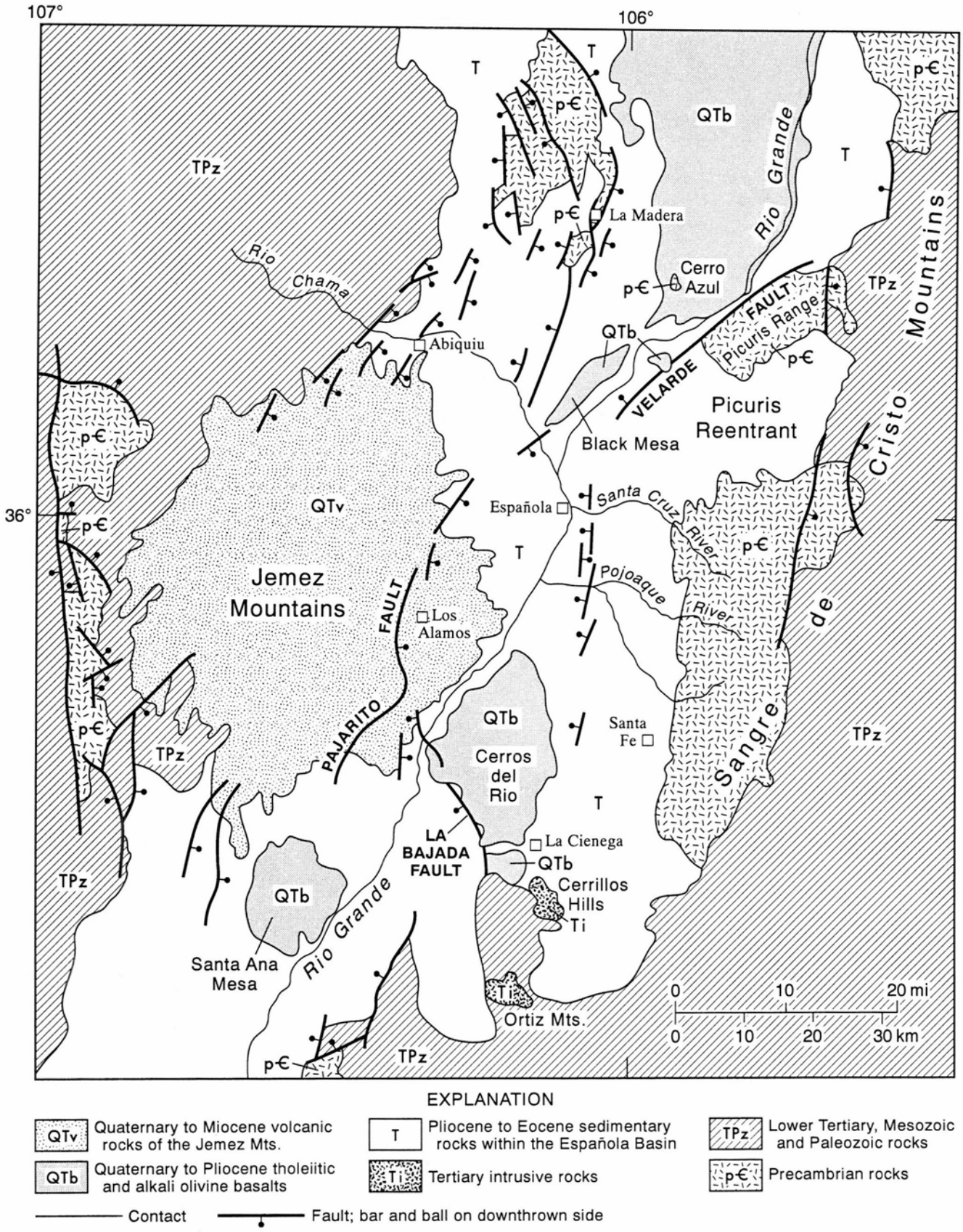

FIGURE W3—Geologic map of the Española Basin, from Manley (1979). White Rock Canyon is located within the northwestern portion of the Cerros del Rio volcanic field, north of the La Bajada fault (see Fig. W6).

At approximately 36° N, near the cities of Los Alamos and Espanola, New Mexico, the rift is crossed by a major crustal structure, the Jemez lineament. This lineament is defined by a SW—NE-trending line of volcanic fields, from the Springerville field in east-central Arizona to the Raton field of NE New Mexico and western Oklahoma (see Baldridge et al., 1989). The Jemez volcanic field, which has formed over the last 14 m.y., is located at the intersection of the Jemez lineament with the Rio Grande rift (Smith et al., 1970; Gardner et al., 1986).

Volcanism over the zone of extension and mantle diapirism represented by the Rio Grande rift shows considerable variation, from olivine tholeiites of the Albuquerque volcanoes (visible when looking west from the Albuquerque airport) to basanites and alkali olivine basalts of the Cerros del Rio volcanic field (Baldridge, 1979; Aubele, 1978; Dunker, 1988). The largest volume of basalt within the rift is in the Taos Plateau volcanic field, which consists of low-alkali tholeiitic rocks and interbedded intermediate and silicic lavas and tuffs (Dungan et al., 1984). Most of the basaltic volcanism visible within the rift has occurred over the last 5 m.y., although volcanism occurring along N—S faults on the rift margin within the Jemez volcanic field dates back to 14 Ma (Table **W1).**

White Rock Canyon

A diverse sequence of Miocene through Holocene rocks, in which are recorded volcanism, sedimentation, and erosion along the Rio Grande rift in the Espanola Basin, is exposed in White Rock Canyon. Sedimentary rocks of the lower and middle Santa Fe Group, overlying volcano-genic alluvial fan deposits (the Puye Formation), and Pliocene alluvium (upper Santa Fe Group), record alternating aggradation and canyon cutting centered near the present-day White Rock Canyon during late Tertiary time. This broad coalescent fan deposit (Santa Fe Group) extended beneath the eastern edge of what is now the Jemez Mountains. The thick basin fill accumulated to a local elevation of over 1860 m (6100 ft); this slowly aggrading base level existed from at least mid-Miocene to Pliocene time.

By mid-Pliocene time (-3 Ma), southwest-trending arroyos (from the east) and east- to southeast-trending canyons (from the Jemez Mountains) were deeply eroded to the level of the paleo-Rio Grande. Many of these paleocanyons are preserved under lavas and pyroclastic rocks of the Cerros del Rio volcanoes and by the two members of the Bandelier Tuff, erupted at 1.4 Ma and 1.0 Ma. Stratigraphic relationships may be seen by hiking up side canyons from White Rock Canyon.

The present location of the Rio Grande did not change much during activity of the Cerros del Rio volcanic field (-3 Ma). Although many of these lava flows are buried by the Bandelier Tuff, there are outcrops in canyons and on high ridges, around which the Bandelier Tuff flowed; basaltic lavas are intersected by water wells up to 10 km west of the Rio Grande (Dransfield and Gardner, 1985). In all of these cases, it appears that lavas erupted on the west side of the canyon flowed east and those on the east flowed west. The Cerros del Rio volcanic field covers over 800 km^2.

White Rock Canyon was repeatedly dammed by lava flows of the Cerros del Rio volcanic field. Lacustrine sedimentary rocks have been mapped in and north of White Rock Canyon; along the highway to Los Alamos there is a lava delta, where lavas from a vent on the west side of the valley flowed into a lake with a water surface of at least 1860 m (6100 ft). Similar lava deltas are visible in many canyons between Los Alamos Canyon and the village of White Rock.

Along the northwestern margin of White Rock Canyon is a 200 km^2 volcanogenic alluvial fan (the Plio-Pleistocene Puye Formation), which consists of volcanogenic sedimentary rocks and interbedded tuffs derived from the dacitic and rhyolitic domes of the Tschicoma Formation of the Jemez volcanic field (Turbeville et al., 1989, Fig. W4). The intertonguing Totavi Formation (Totavi Lentil of Griggs, 1964) includes the earliest dated deposits of the ancestral Rio Grande in northern New Mexico (4-4.5 Ma; Waresback, 1986). The river does not appear to have changed course considerably since before mid-Pleistocene time, when the growing Puye alluvial fan may have pushed the river several km east of its present position (Waresback, 1986). Deposition of this alluvial fan was con-

TABLE W1–Geochronology of volcanic events along the Río Grande, Cerros del Río. F.T. = fission track date.

Event	Age (Ma)	Method	Reference
Santa Fe Group sedimentary rocks	~21–1.0	K/Ar; F.T.	Hawley, 1978; Manley, 1979
Basaltic and andesitic volcanism, Cerros del Rio volcanic field	3.0–0.96	K/Ar; inferred from stratigraphy	Dethier (in press); Manley, 1976
Puye Formation alluvial fan, with a source area in the Jemez Mountains (contains interbedded tuffs from the Tshicoma volcanoes)	~5–2	K/Ar; inferred from stratigraphy	Turbeville, et al., 1989
Bandelier Tuff Upper (Tschirege) Member	1.12	K/Ar	Doell et al., 1968
Bandelier Tuff Lower (Otowi) Member	1.45	K/Ar	Doell et al., 1968
Damming of White Rock Canyon by slump blocks	>0.15	inferred from stratigraphy	Dethier (in press)
El Cajete Pumice (from Valles intracaldera rhyolite domes and craters)	0.13	K/Ar	Self et al., 1988

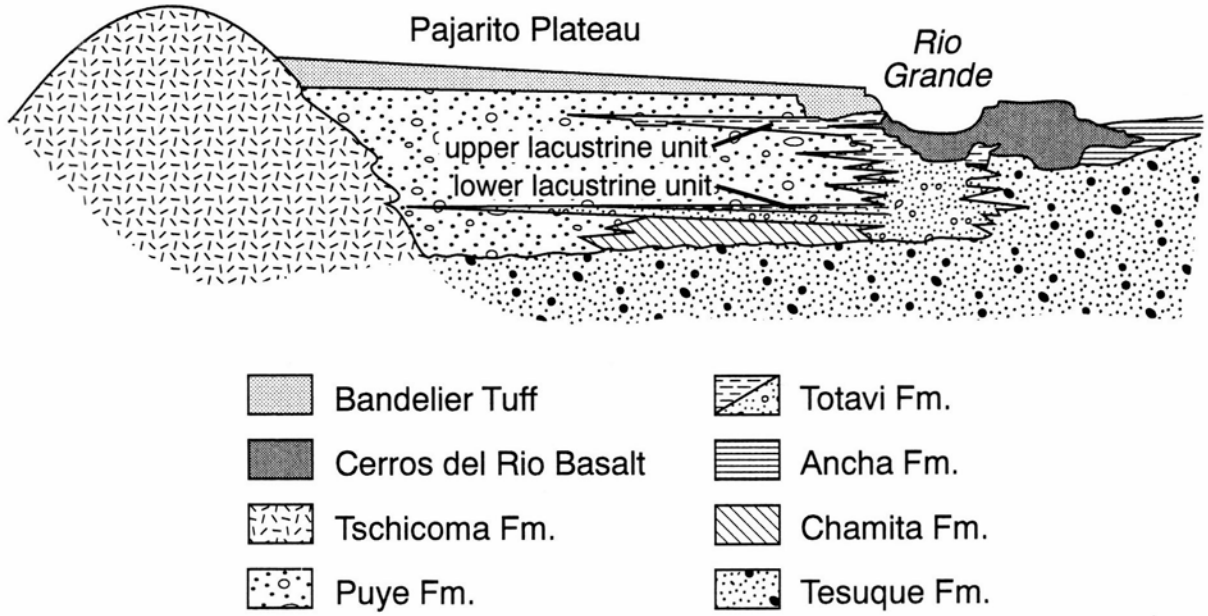

FIGURE W4—Schematic cross section of the Pajarito Plateau of the eastern Jemez Mountains volcanic field, the canyon of the Rio Grande, and Cerros del Rio, showing the relationships between the Puye alluvial fan (derived from the intermediate volcanic rocks of the Tschicoma Formation), sedimentary rocks of the Santa Fe Group (including ancestral river deposits—Totavi Formation, as well as Tesuque, Chamita, and Ancha Formations), and the basaltic rocks of the Cerros del Rio (from Turbeville et al., 1989).

temporaneous with basaltic volcanism, as basaltic ash layers were interbedded with the volcanogenic clastic rocks.

The upper portions of White Rock Canyon are flanked by slump blocks (toreva blocks), which appear to have been stable since at least mid-Pleistocene time (Bandelier Tuff is part of some of the slide blocks, but the blocks are overlain by 150 ka El Cajete pumice that has not been dislocated). Most of these slump blocks consist of basaltic lava flows that overlie rift sedimentary rocks.

Before about 2 Ma, the Rio Grande appears to have flowed at an elevation of less than 1834 m (6020 ft). Field relations demonstrate that the upper part of White Rock Canyon was at least 76 m (250 ft) deep at that time. Before eruption of the lower member of the Bandelier Tuff (1.45 Ma), side canyons west of the Rio Grande (south of Water Canyon) had been incised into basalt flows to a depth of at least 150 m (500 ft). White Rock Canyon was probably cut into landslide debris to an elevation of 1768 m (5800 ft).

Since eruption of the upper member of the Bandelier Tuff, White Rock Canyon has been deepened by about 122 m (400 ft). Elsewhere in the Espanola Basin, rapid incision of the river occurred during mid-Pleistocene time, probably in response to climatic change and to complex regional geomorphic factors, such as (1) integration with a through-flowing "Lower Rio Grande" system, and (2) upstream enlargement of the headwater areas to include the San Luis Valley region of Colorado. Soil development in the canyon supports the climatic hypothesis, but stream terrace remnants are small. The highest fluvial terrace preserved in this area is about 46 m above the Rio Grande and is older than 150 ka.

Hydrology of White Rock Canyon and Effects on Eruption Processes

The Santa Fe Group clastic sedimentary rocks underlying the Cerros del Rio volcanic field are generally considered to be a single hydrologic unit and part of the Tesuque aquifer system (Hearne, 1980; Coons and Kelly, 1984). Yields of 2725 m^3/ day (500 gpm) have been reported from this aquifer. General flow is from recharge areas at the base of the Sangre de Cristo Mountains toward the west and the Rio Grande. Thickness of the Santa Fe Group and the aquifer is not known.

Under the Cerros del Rio volcanic field, the water table slopes from an elevation of 1798 to 1768 m (5900 to 5800 ft) along the eroded margins of the field down to 1676 to 1615 m (5500 to 5300 ft), where the aquifer reaches the surface at the Rio Grande (Borton, 1963). During the last 2 Ma, the level of this aquifer was possibly 150-175 m (492-575 ft) higher, depending upon the depth of erosion since then. Aquifer levels were between 90 and 275 m (300 and 900 ft) below the base of lava flows and cones that make up most of the field.

Vents of the Cerros del Rio located closest to the Rio Grande are maar volcanoes (Fig. W5). During the period from -2.5 to -1.5 Ma these were erupted at a time when the level of the Rio Grande (and the aquifer) was at an elevation of 1768 m (5800 feet). Bases of the northernmost maar volcanoes, located along northern White Rock Canyon, are at an elevation of about 1768 m (5800 ft); maars farther down White Rock Canyon are 30-60 m lower, but so was the river. Other vents, located at elevations over 100m higher than those of the tuff rings (also farther from the ancestral river), are all composed of cinder cones, spatter cones, and associated lava flows.

All of the eruptions within the Cerros del Rio volcanic

field, occurring where the aquifer was shallow (nearly at the surface), were phreatomagmatic (hydrovolcanic). Vents reaching surfaces 100 m or more above the water table formed cinder or spatter cones with little or no evidence of magma/water interaction. An excellent example of this effect can be seen by walking up Frijoles Canyon (a side canyon trending NNW from the Rio Grande). Basaltic volcanoes are exposed along this and adjacent canyons. Maar volcanoes are visible from elevations of -4675 m (5500 ft) to 1706 m (5600 ft). From elevations of -1800 m (5900 ft) and up, there are cinder cones. The elevation effect is also visible in the larger maars, where the craters are filled with scoria and lavas.

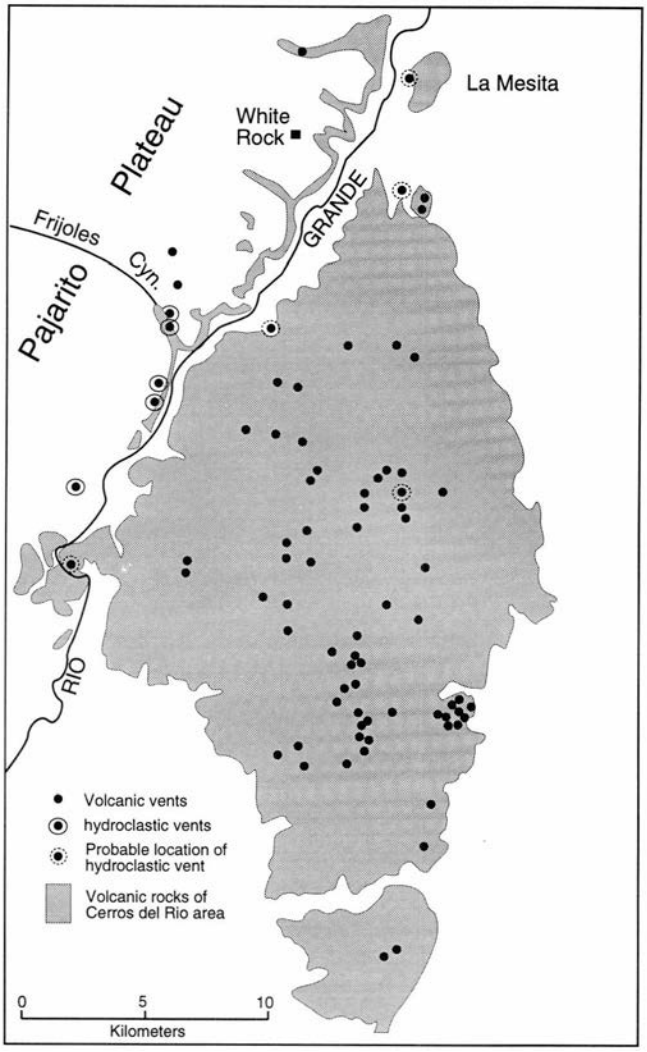

FIGURE W5—Sketch geologic map of the Cerros del Rio volcanic field, showing the location of known vents, including hydroclastic vents (tuff rings) (modified from Kelley, 1978).

Guide to White Rock Canyon

Reaching the head of White Rock Canyon (Fig. W6)

All of White Rock Canyon is accessible by foot, although much of it requires rigorous hiking and a little scrambling. The head of the Canyon, at the intersection of NM-502 and the Rio Grande (Otowi Bridge), is on land belonging to San Ildefonso Pueblo; you most obtain permission from the Pueblo before entering the canyon at this point. The most effective way of seeing the canyon is by boat, entering either from Otowi Bridge (permit required) or from Buckman Crossing (no permit required), which can be reached from Santa Fe. If you float, plan on at least one very long day, or perhaps two days, camping in the canyon.

Entering from the North

The easiest way of reaching this canyon is to drive north of Santa Fe along US-84/285 until you reach NM-502, turning west toward Los Alamos (15 mi from the intersection of Alamo Drive and St. Francis Drive at the northern end of Santa Fe). Most of the sedimentary units along this drive are arkosic sandstone, siltstone, and conglomerate of the Tesuque Formation of the Santa Fe Group. Type sections of this formation are exposed in arroyos below the Santa Fe Opera.

Travel west along NM-502 to Otowi Bridge on the Rio Grande (7 mi). If you enter the river and canyon here, you must acquire a permit from the offices of San Ildefonso Pueblo (fee required). Even if you do not enter the canyon here, there is a great view from the highway of La Mesita maar, discussed below.

Entering from the East

Travel north of Santa Fe (1.3 mi past the traffic light at St. Francis Drive and Alamo Drive) to the La Tierra Road (left off of US-84/285). Take this paved road due west for about 5 miles until it becomes a gravel road (be careful during the summer, for flash floods can inundate this road). This road becomes Buckman Road, which ends at Buckman Crossing on the Rio Grande.

The road continues WNW, following the old Chili Line railroad grade, through Santa Fe Group sedimentary rocks until it reaches the base of an escarpment formed by lavas of the Cerros del Rio volcanic field, which overlie the sedimentary rocks. At this point, the road turns north and continues along Canada Ancho, at the base of the escarpment, for 6 mi until it reaches the Rio Grande at Buckman Crossing. This is an excellent place to begin your trip down White Rock Canyon. It is also the loca-

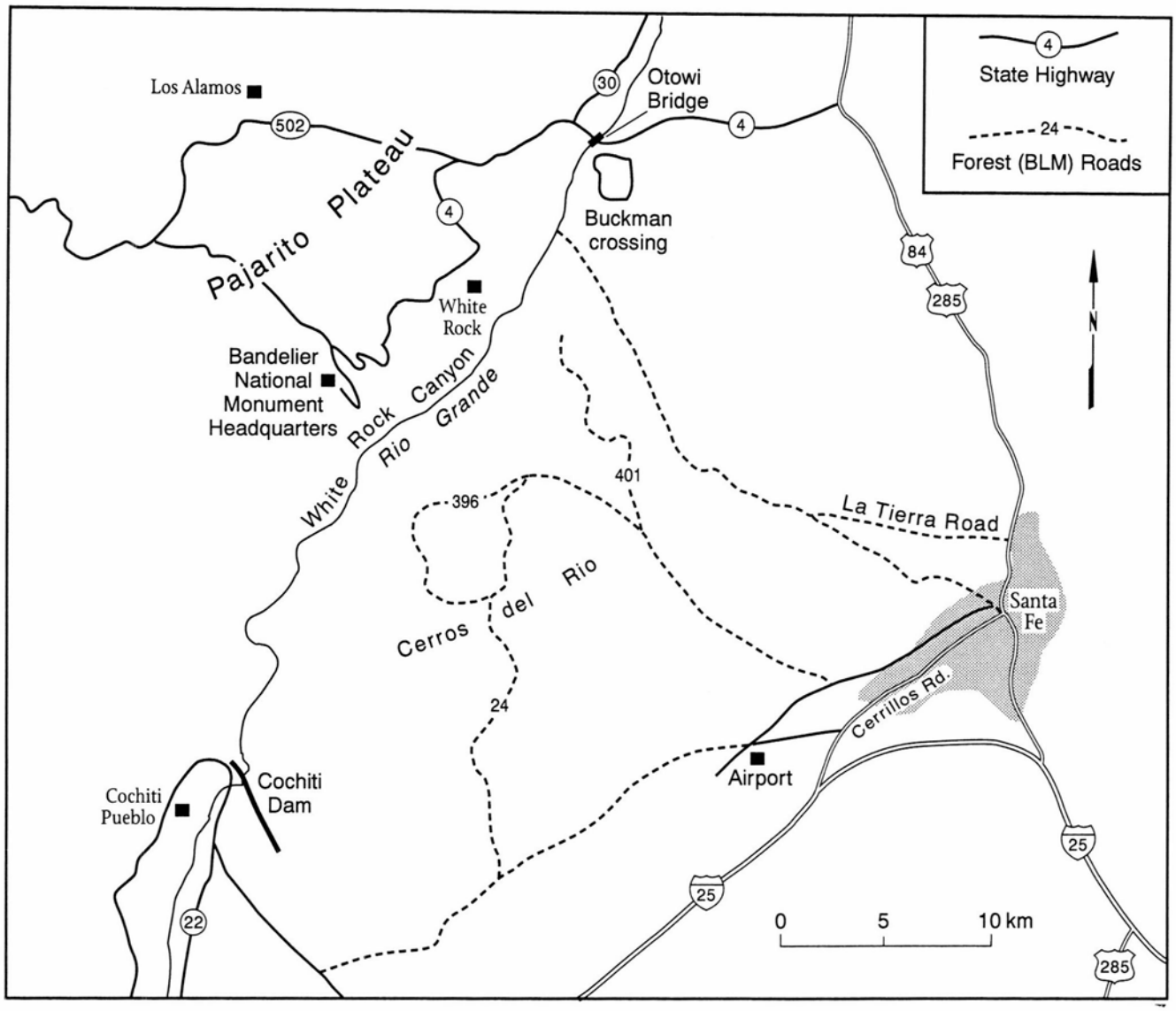

FIGURE W6—Access to White Rock Canyon: (1) via NM–502 to Otowi Bridge, (2) gravel and dirt roads from Santa Fe across the Cerros del Rio and to Buckman Crossing, (3) from Cochiti Dam, and (4) trails from White Rock village and Bandelier National Monument.

tion of two of the best exposed maar volcanoes along the canyon; La Mesita to the north of Buckman Crossing and the maar of Caja del Rio, south of the Crossing.

Entering from the West

White Rock Canyon can be reached by foot from the western side of the Rio Grande in several places from NM-4:

White Rock: Trails lead from the village of White Rock. Ask for their location at businesses within the village or at the new White Rock Information Center along NM-4.

Between White Rock and Bandelier National Monument: Trails are east of NM-4, between the village of White Rock and Bandelier National Monument. The most accessible of these trails is the one to Ancho Rapids. Trailheads are visible on the left (east) side of the highway (going toward Bandelier) as dirt roads with gates.

Bandelier National Monument: There are many trails in the Bandelier National Monument Wilderness Area. The easiest trail to the Rio Grande is that along Frijoles Canyon, below the Monument Headquarters (the Falls Trail), which will take you through several maar volcanoes in cross section. The geology along the Falls Trail is described later in this guide, in reverse, starting at the river. Other trails, including the one to Capulin Canyon, will require a very long day or camping overnight.

La Mesita maar

Introduction

La Mesita maar is the northernmost of the 70 volcanoes of the Cerros del Rio volcanic field. It is one of the best exposed maars in the volcanic field and is visible from NM-502 at Otowi Bridge. The southern end of this volcano can be reached from Buckman Crossing on the Rio Grande; to visit the northern half requires permission from San Ildefonso Pueblo. The purpose here is to describe the role of water in the development of La Mesita maar, as determined from detailed examination of the bedded deposits.

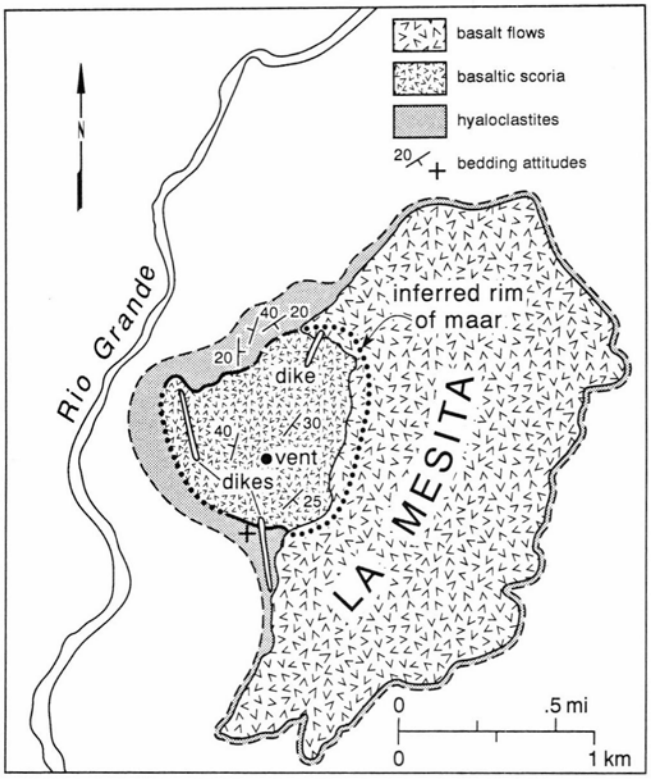

FIGURE W7—Geologic sketch map of La Mesita maar. The northern end of this maar is easily seen from the Otowi Bridge on NM–502.

S tratigraphy

La Mesita maar (Fig. W7) originally had a wide crater, but it is now filled with basaltic ash, scoria, and agglutinate from Strombolian eruptions. The maar rim beds that lie beneath the Strombolian fallout tephra make up the rim of the original maar volcano. They are about 100 m thick and are composed of fragments derived from hydroclastic eruption processes, as will be shown in a later section. The stratigraphic sequence, from maar rim beds to crater-filling scoria, is now exposed in cliffs for about 3 km along the course of the Rio Grande.

Paired coarse-fine bed sets. The rim beds of La Mesita maar are composed of a repetitive sequence of bedding sets consisting of coarse layers overlain by fine layers, with contacts being sharp to broadly transitional on a centimeter scale. The thickness ratio of coarse- to fine-grained layers varies greatly but averages about 1:1. The coarse-grained layers contain fragments that range from coarse ash to medium lapilli (-3-10 mm). The coarse-grained layers grade from those lacking fine particles (< ash size) with an open-work texture to those with a fine-grained matrix.

The coarse-grained layers with clast-supported texture are considered to be depleted in fine particles, which occurred by processes of elutriation within ascending eruption columns or pyroclastic surges. The more poorly sorted coarse-grained layers are believed to have also formed by one or the other of the two processes but with sorting processes not reaching completion. The fine-grained layers within single paired sets may have been derived by separation from the coarser debris. However, many of the fine layers contain coarser clasts and appear not to have undergone any sorting process.

Some of the rim beds contain bedding-plane sags, wavy units, and crossbedded units. Most of the layers, however, are plane beds commonly with inverse grading.

Within many of the coarse- or fine-grained beds there are laminations of coarser- or finer-grained ash but without sharp bedding planes (Figs. W8, W9). For example, in some of the coarse-grained beds there is a faint layering that is manifested only by light dusting of fine ash along a horizontal plane. Lines in some of the finer-grained beds are of slightly coarser ash grains, of one to several grain widths, that are imbedded in the silt-sized material. The ash in these laminations may increase or decrease up or down in the layer to produce small-scale graded bedding. The laminations within the section at La Mesita commonly show very subtle low-angle cross-bedding and lenticularity.

Each coarse-fine bedding set in the La Mesita maar rim beds is considered to be the result of an eruptive pulse, with tephra being deposited by fallout or by flowage processes. The initial assessment of whether beds are emplaced by flowage or by fallout processes is based upon certain bedding criteria. If internal laminations show subtle cross-bedding, the bedding set is interpreted to have been emplaced by flowage. Coarse-grained layers that lack bedding-plane sags at their bases and show inverse grading are also interpreted to have been emplaced by flowage processes. Another criterion of flowage emplacement is the sharply defined basal unconformity where the upper beds have eroded underlying beds, resulting in crosscut-

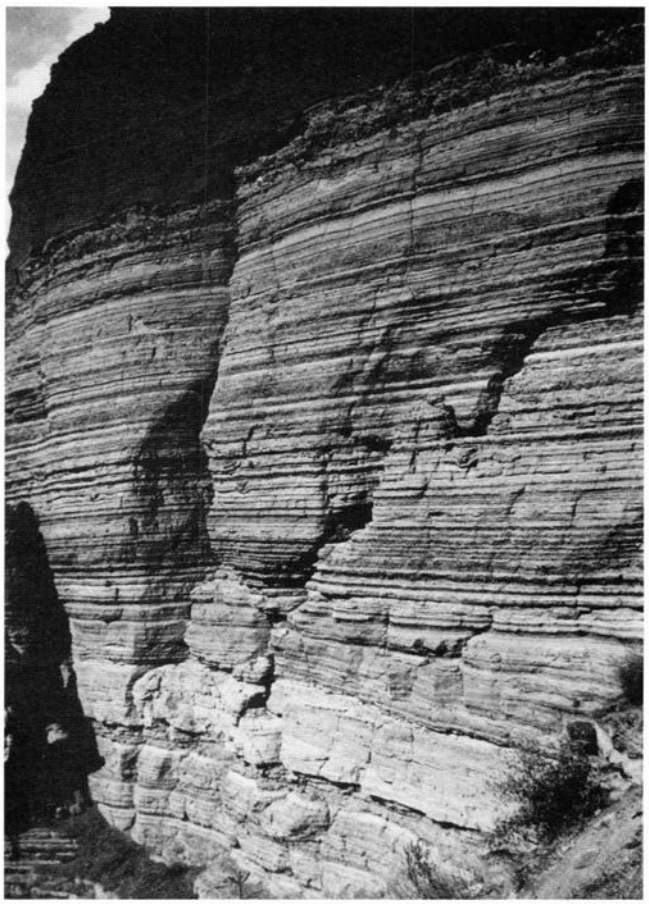

FIGURE W8—Bedding sets within the La Mesita maar deposits.

FIGURE W9—Close-up of bedding sets within La Mesita maar deposits. Bedding sets are a few cm thick. The scale is 2 cm wide.

ting relationships. Erosion by surges is also indicated by the mixing of two layers at their contact or the presence of material from the underlying layer in the overlying layer.

Evidence for deposition by fallout includes: (1) fragments at the base of a layer that distort the underlying layers (impact); (2) layers and laminations that drape smoothly over minor roughness elements of the underlying layer; (3) internal laminations that are parallel and are not associated with lenticular layers or other angular elements; and (4) relatively good sorting.

The explanation for why bedding pairs begin with a coarse-grained layer and end with a fine-grained layer depends upon whether the bed is believed to be of flow or fallout origin. Fallout beds with inverse grading can be interpreted in terms of eruptive energy: eruptions with progressively larger kinetic energy, expelling larger clasts as the eruption progresses (Wohletz and Sheridan, 1983). Normal grading can form during energetic eruptions, with the finest material elutriated from the eruption column, falling after the eruption phase.

Beds emplaced by flowage also show a progression from coarse to fine-grained tephra, but for a different reason. Coarse-grained basal units may form from the head of a passing surge, which is followed by the finer-grained and more poorly sorted body of the surge (Fisher et al., 1984, 1986). Because most of the beds have been assessed as emplaced by flowage at La Mesita maar, the following discussion assumes flow emplacement unless otherwise stated.

Description of the Eruption Sequence

The stratigraphic sequence at La Mesita maar is about 100 m thick, but complete sections could not be measured in any single locality. The upper portions of the sequence are well-preserved on the uphill side of a dike, whereas the lowermost part of the sequence is exposed in a large, dissected slide block, 400 m east of an elevation of 5487 ft along the Rio Grande (4 km downstream from the Otowi Bridge).

There are subtle color differences within the tuff beds, which reflect changes in clast compositions. Pink hues characterize beds containing abundant sand- and silt-sized material from the underlying Tesuque Formation. Yellowish hues are derived from palagonitized vesicular basaltic pumice fragments. Bluish-gray (medium gray) hues are typical of deposits containing abundant angular or subangular accessory to juvenile pyroclasts of hydroclastic (phreatomagmatic) origin. Dark gray and black deposits are mostly quartz xenocryst-bearing tachylitic scoria of Strombolian origin.

Beginning at the base, the first half meter of section is dominantly pink to medium gray, changing to yellowish gray over the next 3-4 m, and pink and gray for the next 20-30 m of interbedded fine-grained and coarse-grained layers. This sequence contains abundant lithic clasts (sand grains) derived from the underlying sandstones; these are progressively diluted upward with abundant juvenile hydroclastic particles. The uppermost sequence is mostly pink and contains a much higher percentage of accidental lithic clasts.

Petrology and granulometry of the sequence. Eleven samples of La Mesita tephra were sieved and characterized by scanning electron microscopy (SEM). In general samples are finer-grained in the middle of the eruption sequence and coarser-grained near the base and top; the strongest hydroclastic fragmentation occurred midway through the eruption. Figure W10 distinguishes scoria from hydroclastic tephra on a sorting-median diameter plot, which also shows relative fields of fallout and pyroclastic surge bed forms. Histograms of size frequency show a distinct polymodality for most samples, a feature typical of many tephra samples in general.

Clast shapes, as revealed by SEM, show several general trends: (1) lithic clasts of the Tesuque Formation are subangular to subrounded quartz and feldspar grains and ag-

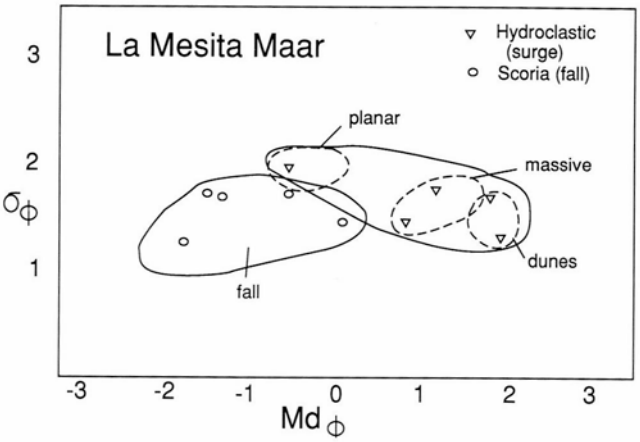

FIGURE W10—Sorting (σϕ) vs. median diameter (Mdϕ) plot for hydroclastic (phreatomagmatic) surge deposits and scoria fall deposits of the La Mesita maar.

gregates of mudstone; (2) juvenile clasts larger than 0.5 mm are dominantly scoriaceous while smaller grains consist of angular blocks and plates; (3) variable degree of palagonitization has produced hydration cracks and rinds that separate from glassy clasts; (4) some samples contain numerous spherical clasts with median sizes of about 2.5 4) (0.175 mm)—some of these appear to be alteration products, while most appear to be juvenile; (5) aggregation of fine ash is common; and (6) the scoria show fused surfaces, whereas hydroclastic shards have very irregular surfaces with abundant coatings of alteration products. The presence of spherical ash suggests some relatively fluid magma fragmented by hydrodynamic instabilities. However, the hydroclastic ash is dominantly angular, having been derived from brittle breakage of pre-vesiculated magma.

Conclusions regarding the origin of La Mesita maar

The hydroclastic tephra of the rim beds has abundant fine-grained clasts typical of hydroclastic eruptions. Experiments with water and thermite melt to simulate water-magma interactions indicate that explosive efficiency is strongly controlled by water-melt mass ratios and by confining pressure. Explosive efficiency is a percentage of mechanical to thermal energy, which is at its maximum when water-melt ratios are between 0.3 and 1.0 (Wohletz and Sheridan, 1983). The efficiency of fragmentation increases with explosive energy and the degree of water superheating.

One important measure of explosive energy and water-melt ratios is the amount of fine-grained ash in pyroclastic deposits ("fine-grained" is < 62.5 pm). The increased melt surface area caused by efficient fragmentation promotes highly efficient heat exchange between water and melt. More glass is produced because the particles are rapidly chilled.

Figure W11 (from Wohletz and McQueen, 1984) shows one of the models that can be used to interpret our data from La Mesita maar. As is shown for the model, rising magma encounters near-surface ground water; water is vaporized and magma and basement rocks are fractured and fragmented. Fragments from this level of magma–water interaction are composed of chilled juvenile pyroclasts and lithic clasts.

Figure W12 shows the variables that can be used to relate the deposits to the model shown in Figure W11. The volume of fine-grained glassy pyroclasts in the deposits is a measure of the amount of water in the system. The amount of lithic clasts (from rocks underlying the volcano) reflect the size, permeability, and volume of water within the aquifer that comes into contact with magma in the vent. Volcanic lithic clasts (crystalline) are a measure of the magma/water ratio in the system. Using these three parameters, we can define four fields, based upon clast components in hydroclastic deposits (Fig. W13).

Preliminary estimates suggest that in the lower part of the La Mesita maar, the fields move from C to D (high magma input and low to high volumes of water. Higher in the deposits, the fields alternate between A and B, which suggests enlargement of the vent area (increasing basement lithic clasts) and less magma input relative to the volume of available water.

In the lower half of the La Mesita deposits the layers occur as bedding sets, each consisting of a coarse-grained base and fine-grained top. We consider each bedding set to represent a single explosion of the eruption (see Fisher and Schmincke, 1984, p. 348); explosions progress from

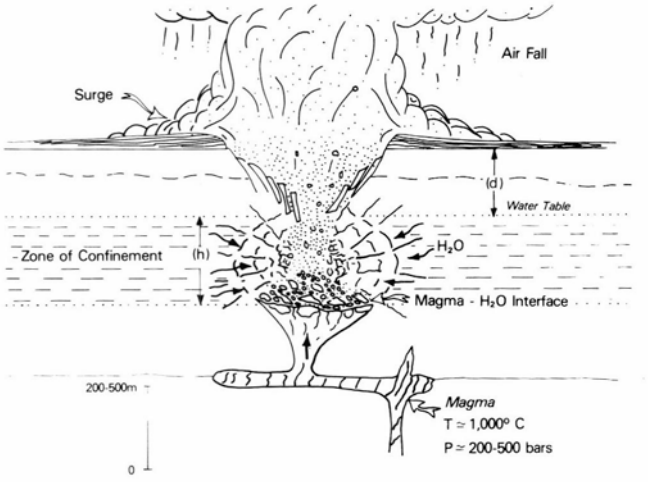

FIGURE W11—Model of hydroclastic (phreatomagmatic) eruption (from Wohletz and McQueen, 1984); explosive magma-water interactions are occurring within a shallow aquifer.

Rate and/or Volume

Rate and/or Volume: Water	Magma: Low	Magma: High
Low	(A) VL low; BL higher; G low	(C) VL abund.; BL low; G low
High	(B) VL lower; BL higher; G abund.	(D) VL abund.; BL low; G abund.

VL = Volcanic lithics
BL = Basement lithics
G = Glass

FIGURE W12—Variables that can be used to relate maar deposits to the model shown in Fig. W11.

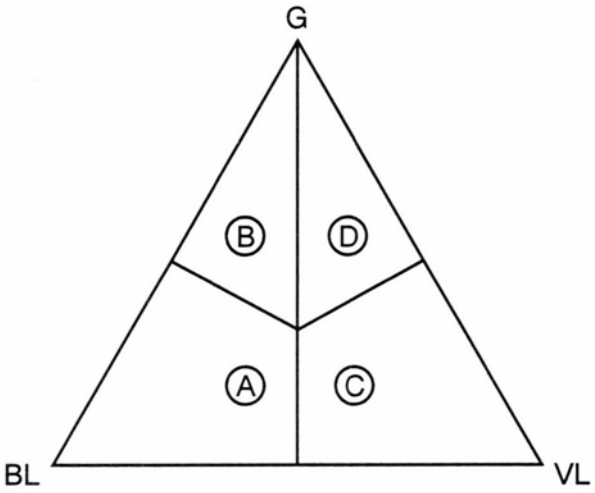

FIGURE W13—Four fields for hydroclasticdeposits, based upon component clasts; see Fig. W12 for explanation.

low to high efficiency where some water entered the vent, triggering the eruption and fracturing rocks adjacent to the vent. Subsequently, more water moves into the area of rising magma. We visualize a rapid, progressive buildup of released energy, higher eruption columns with associated surges, and greater production of fine-grained ash.

Near the top of the maar deposits lithic clasts from basement rock exceed those derived from the vent, but there is still alternation between coarse- and fine-grained (and glassy) hydroclastic tephra. Thus, these bedding sets are still characteristic of the same transport and depositional style, but enlargement of the vent results in a greater proportion of basement lithic clasts. With continued eruptive activity and construction of a volcanic tuff ring or cone, the hydrovolcanic activity ceases, followed by magmatic, Strombolian eruptions. One hypothesis explaining these changes is that fractures are closed by chilled magma along dike margins as the vent is enlarged, closing off inflow of ground water.

Another hypothesis is that vesicle growth gives higher surface area within rising magma, which promotes efficient interaction with external water. Hydrovolcanism is absent where pyroclastic sections are greater than 100 m thick. Vesicle growth in many basaltic magmas typically occur at depths of > 100 m (Heiken, 1971). It is possible that the conduit pressure increased as the tuff ring grew to the point at which vesiculation was inadequate to promote interaction with ground water at depths < 100 m, and the eruption ended with Strombolian activity and filling of the crater with a lava lake.

Buckman maar

An oval, 1 x 1.2 km, 150—m-high mesa, located along the Caja del Rio, 2.2 km SE of Buckman Crossing, Buckman maar (unofficial name) is an eroded maar topped with deposits of scoria and bombs and a basaltic lava flow. The summit is most easily approached from the east, along a trail from Buckman Road.

The general stratigraphic sequence consists of massive, block-bearing hyalotuff, overlain by well-bedded orangish-brown hyalotuff (mostly plane beds). Interbedded with the well-bedded tuffs are blocks of pink, fine-grained sandstone, up to 30 m long. Dikes cut the tuff sequence and were feeders for the lava lake and flows overlying the maar. A lava flow capping the mesa south of this maar has an age of 2.3 ± 0.1 Ma.

Beginning of float trip

(distances are measured from Buckman Crossing)

From Buckman Crossing to the mouth of Water Canyon (west), 0-8 km, the widest section of White Rock Canyon (2 km to 2.4 km wide) is characterized by large slump blocks on both sides of the river. Capping the slumps next to the river (E side at km 0.1) are slack-water deposits, 35 m thick, that record damming of the river sometime before 60 ka.

Mortandad **Canyon**

(location A, west side, 1 km south of the Crossing)

Mortandad Canyon is little modified by slumping and contains a well-exposed section of rocks typical of White Rock Canyon (Fig. W14). This section includes 76 m of sandstones and conglomerates, which are intertongued

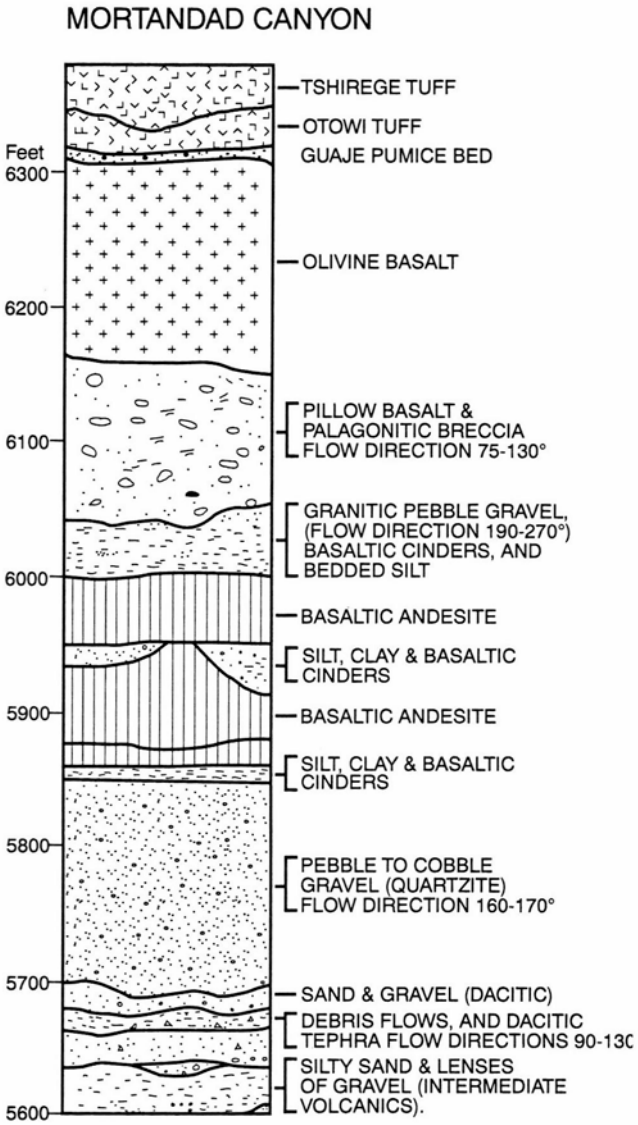

FIGURE W14—Stratigraphic section, Mortandad Canyon (A, west side of the river; elevations are in feet).

Santa Fe Group sedimentary rocks (metamorphic and plutonic provenance) and Puye Formation (volcanic provenance), and ancestral Rio Grande deposits (Totavi Formation of Waresback, 1986).

140 m of lavas of the Cerros del Rio overlie this with some interbedded river gravels. The lower third consists of basaltic andesite flows and some scoria, the middle third is a lava delta, consisting of interbedded palagonitized hyaloclastites and pillow lavas (the foreset beds of the lava delta indicate flow from west to east); these appear to have flowed into one of the lakes formed by damming of the Rio Grande by lava flows or slumps. The upper third of the basalt section is a massive olivine basalt flow with well-developed columnar jointing near the flow top, which has a K—Ar age of 2.3 ± 0.1 Ma.

The section is overlain by members of the Bandelier Tuff, including the Guaje pumice fall and distal Otowi (lower) Member (1.4 Ma) and Tshirege (upper) Member (1.0 Ma). Paleovalleys and paleocanyons cut into the Cerros del Rio basalts, west of the Rio Grande, are partly filled with Bandelier Tuff; most of the canyons seen today are resurrected paleocanyons.

North end of Sagebrush Flats

(location B, immediatly south of the Crossing, east side of the river)

The ridge immediately south of Buckman Crossing is modified by slumping, but a section of about 140 m can be pieced together. It consists mostly of intertongued sandstones and conglomerates of both the Santa Fe Group and Puye Formation. This is the only location in the canyon where the Puye Formation crops out east of the Rio Grande. Olivine basalt flows are exposed in the middle and top of the section (Fig. W15).

Southwest Sagebrush Flats

(location C, 6 km south of the Crossing, east side of the river)

Thirty meters of interbedded sandstones, cinders, and phreatomagmatic tuffs are exposed below the base of a paleocanyon that is partly filled with 100 m of the Tshirege (upper) Member ignimbrite of the Bandelier Tuff (Fig. W16). This is one of only three or four places in the canyon where Bandelier Tuff ignimbrites are preserved on the canyon's east side.

Chino Mesa and Montoso maar

(location D, 7.9 km south of the Crossing, east side of the river)

Most of the 210 m of section exposed here consists of interbedded phreatomagmatic tuffs, thin basalt flows, and an andesite flow (Fig. W17). The andesite of Montoso Peak is exposed along the Canyon for nearly 10 km, and may have been a major unit responsible for one of the episodes of damming the Rio Grande.

The Montoso maar is located in a side canyon (east side of river), 2.3 km due north of Montoso Peak. Aubele (1978, 1979) interprets this as the dissected throat of a collapsed maar. The amphitheater-shaped, inward dipping tuff beds of these phreatomagmatic deposits overlie well-exposed talus deposits and show no evidence of collapse. It is possible that this maar was erupted in a paleocanyon, coating the walls of the canyon with sticky surge and fall deposits, which extended beyond the edge of this paleocanyon and out onto the lava plateau. On the plateau, these deposits are overlain by later lava flows. The canyon-filling tuff deposits were later cut by dikes feeding younger lava flows.

Chino Mesa, Montoso Peak, and the Montoso maar may also be reached via U.S. Forest Service and powerline roads across the central Cerros del Rio. These roads should be tackled only with vehicles having high clearance and passengers with tough kidneys (see IAVECI field trip guide excursion 8A, Day 6, Stop 2, Baldridge, 1989).

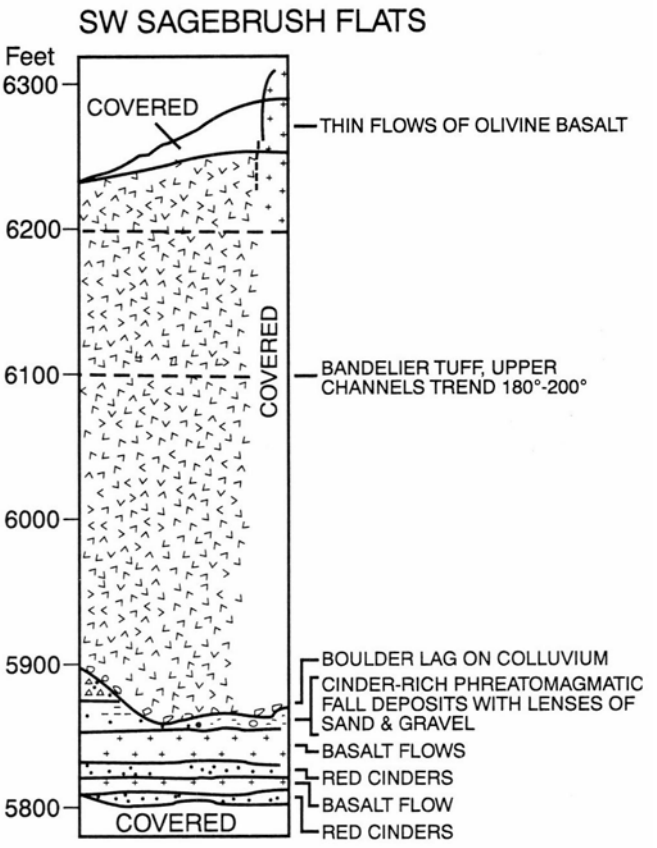

FIGURE W16—Stratigraphic section, southwest end of Sagebrush Flats (C, east side of the river; elevations are in feet).

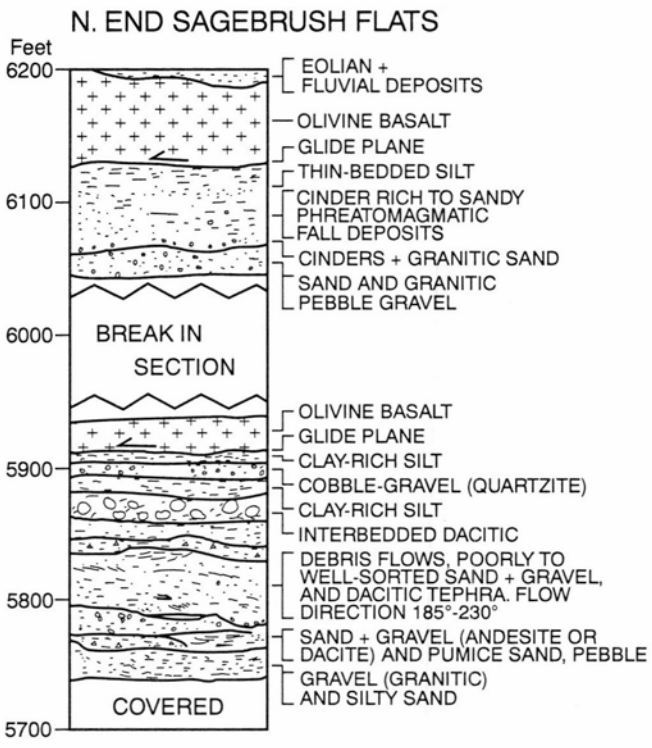

FIGURE W15—Stratigraphic section, north end of Sagebrush Flats (B, east side of the river; elevations are in feet).

Chaquehui and **Frijoles Canyons**

(location E, 12.7 km south of Buckman Crossing, west side of the river)

While floating down the river between these two canyons, notice the interplay between the ancestral Rio Grande and volcanic activity, exemplified by deposits that are well-exposed in the western canyon walls. There are several maar volcanoes, each 2-3 km in diameter (reconstruction); their distal surge deposits are visible, interbedded with thin tholeiitic basalt flows, many of which are overflow from crater lava lakes within the maar craters (Fig. W18). These maars and lavas were cut by drainages from the Jemez volcanic field, which in turn were filled by the thick andesitic lavas from the Cerros del Rio field, cut again by streams in resurrected canyons, partly buried

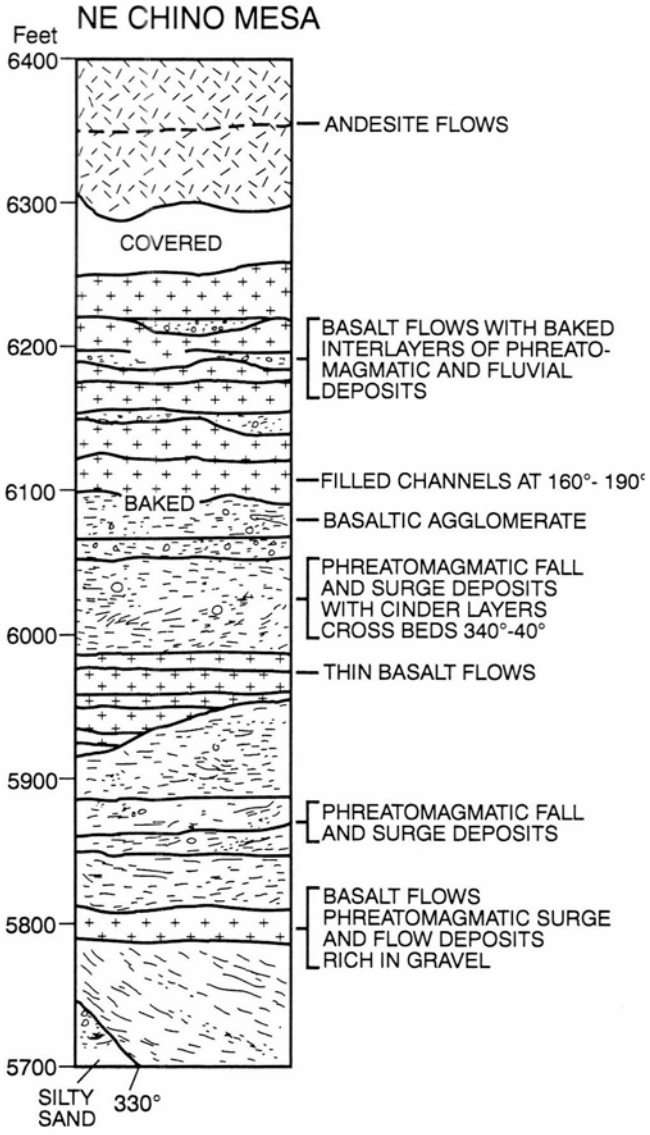

FIGURE W17—Stratigraphic section, northeast Chino Mesa (D, east side of the river; elevations are in feet). This section is representative of the stratigraphy of the Cerros del Rio.

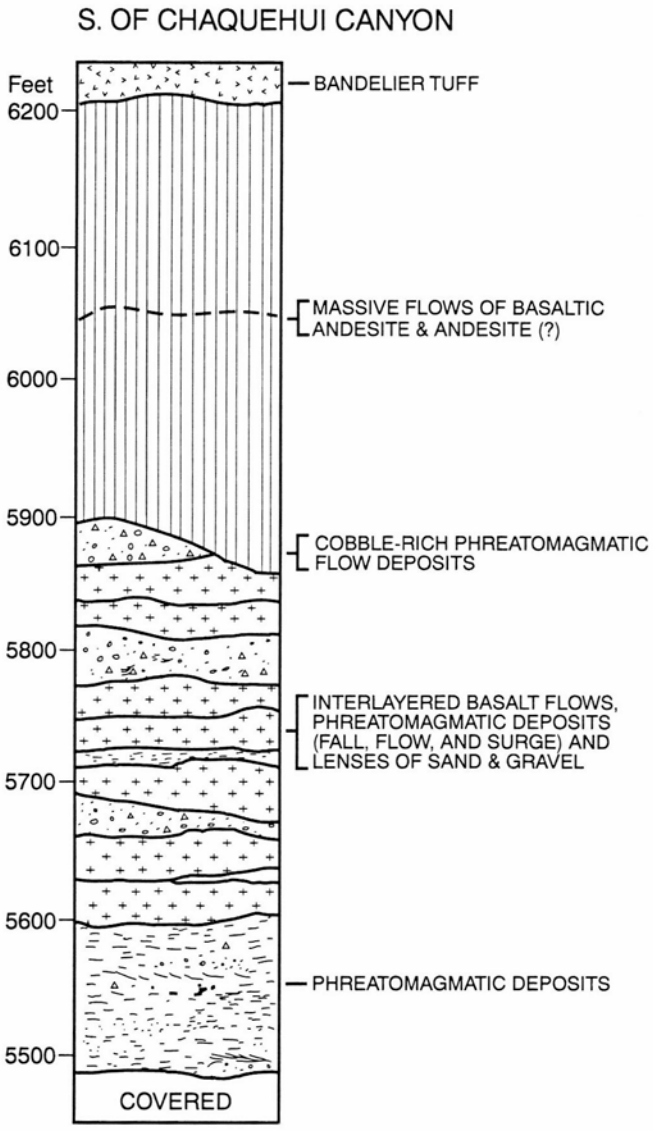

FIGURE W18—Stratigraphic section, immediately south of Chaquehui Canyon (E, west side of the river; elevations are in feet).

by canyon-filling ignimbrites of the Bandelier Tuff, then cut again by streams to form the canyons visible today.

Sidetrip up Frijoles Canyon to Bandelier National Monument Headquarters.

This well-used trail is within a national monument; **do not collect samples!** A walk of 1.5 km up (north) Frijoles Canyon to Upper Frijoles Falls will take you through a well-exposed section of these maar volcanoes. The uppermost of these maars can be walked from its distal margins at the Rio Grande to its throat at the upper falls, where the crater is filled with scoria deposits and crater lake lavas (Figs. W19, W20). This maar is about 3 km in diameter and 30 m thick at the crater rim. It is overlain by thick andesite flows that are probably from a vent located east of the river.

North of Upper Frijoles Falls (and upsection from the river), there is a cinder cone exposed to the east of Frijoles Canyon, above the flats above upper falls. This line of vents includes another large cinder cone, located along NM-4, 2.3 km north of Upper Frijoles Falls. As was mentioned earlier, those vents near river level (and the water table) formed phreatomagmatic tuff rings, whereas those about 100 m above the river were erupted as cinder cones. Another interpretation is that the cinder cones were erupted later, after deeper incision of the river canyon and lowering of the water table.

Above Upper Frijoles Falls, the canyon broadens, and you can see a well-exposed paleocanyon along the northeastern canyon wall, which is filled with upper member Bandelier Tuff ignimbrite. Frijoles Canyon was also filled with Bandelier Tuff, but much of the paleo-Frijoles Canyon has been resurrected, leaving only patches of tuff clinging to paleocanyon walls. As you continue up the canyon, the basaltic lavas of this paleocanyon are exposed along the trail.

As the trail begins to climb again, toward the Bandelier Headquarters, it passes through nonwelded ignimbrite of the upper member of the Bandelier Tuff. There are no Plinian pumice fall deposits at this location because the upper member pumice deposit is located northwest of the Valles caldera.

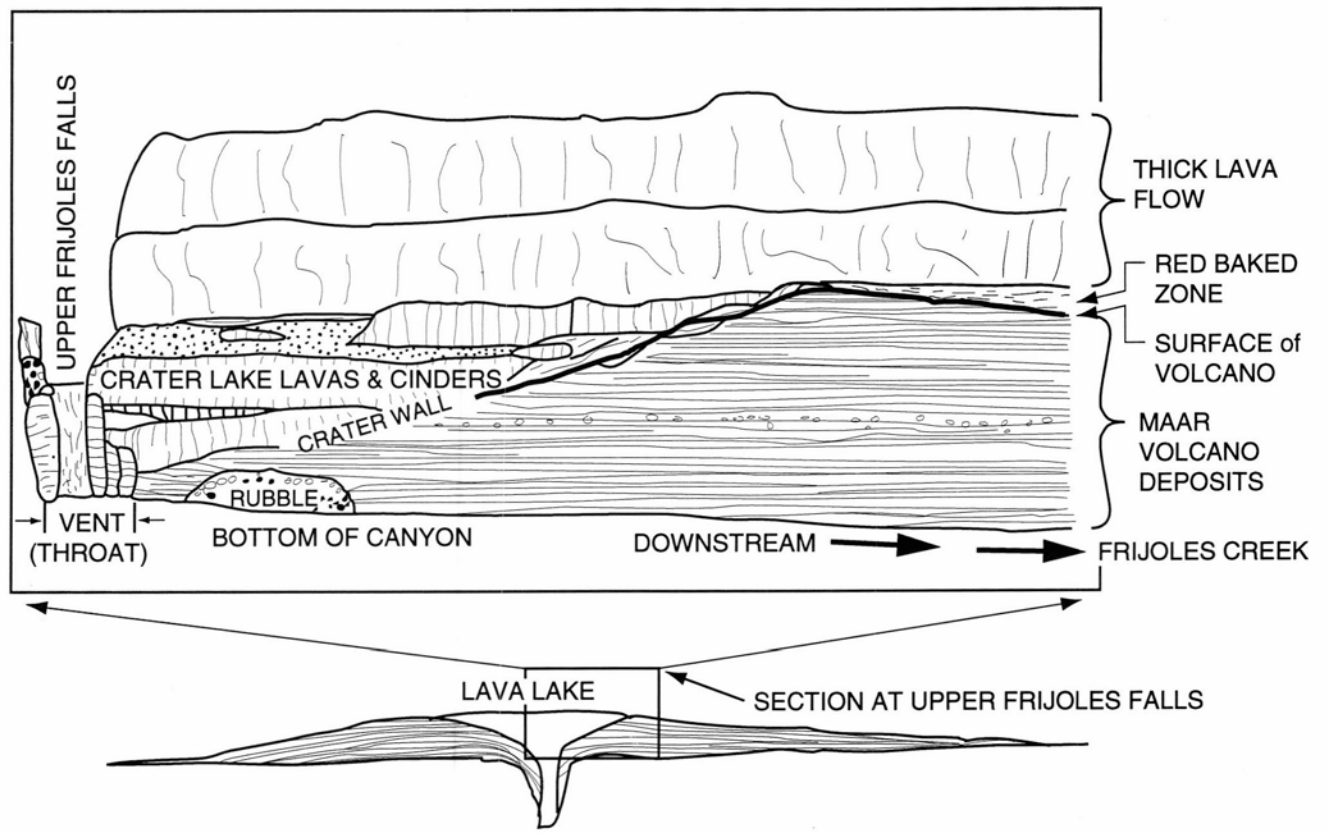

FIGURE W19—Exposures and reconstruction of the maar volcano at Upper Frijoles Falls, Frijoles Canyon (west side of the river).

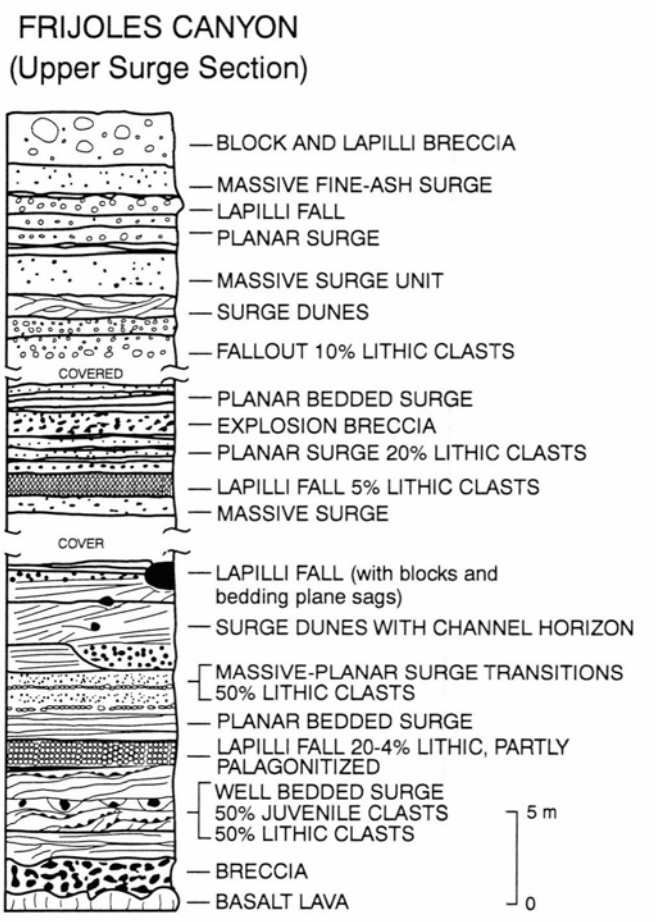

FIGURE W20—Stratigraphic section through the maar volcano at Upper Frijoles Falls, Frijoles Canyon.

When you have reached the Headquarters Visitor Center, enjoy the museum and well-preserved ruins. Ask at the Visitor Center about other geological trail guides.

Frijoles Canyon to Lummis and Alamo Canyons

(17-17.9 km south of Buckman Crossing, west side of the river)

This stretch of canyon consists of mostly basaltic and andesitic lava flows, with some interbedded proximal phreatomagmatic tuffs. These rocks were cut by canyons that were filled by ignimbrites of the Bandelier Tuff; some, but not all, of these canyons have been resurrected by erosion.

Several of the basalt flows of the Cerros del Rio are underlain by the lower member of the Bandelier Tuff (1.4 Ma) and overlain by the upper member of the Bandelier (1.0 Ma).

Arroyo Montoso enters from the east 1 km upstream from Alamo Canyon. There are thick (> 100 m), nearly continuous exposures of coarse phreatomagmatic deposits, dipping dikes, and interlayered basalt flows for 1.5 km up the arroyo from the Rio Grande. The basaltic sequence is capped by approximately 30 m of ignimbrite (lower Bandelier Tuff?), which lie beneath a glassy Cerros del Rio andesite flow.

Quaternary gravel deposits, containing clasts < 4 m in diameter, crop out 30-50 m above the Rio Grande downstream from Alamo Canyon. These gravels are older than 60 ka and may have been deposited after breaching of landslide dams located upstream.

Alamo Canyon to Sanchez Canyon

Along the canyon for 2 km downstream from Alamo Canyon, the river cuts through another maar. Diatomites

are interbedded with the phreatomagmatic deposits east of the canyon. Flows of basaltic andesite and andesite from the Cerros del Rio cap these deposits. West of the river, thick exposures of proximal phreatomagmatic deposits crop out in cliff exposures and lie beneath ignimbrite (Bandelier?) and basalt flows. Interlayered mid-Pliocene cobble gravels and basalt flows lie at water level over much of this reach, and pink arkosic sandstone of the Santa Fe Group is exposed beneath the gravel at several locations.

Between Sanchez Canyon and Rio Chiquito
(22.5 km south of Buckman Crossing)

Faults extending north from the La Bajada fault (and escarpment) cross the canyon through this section. If you drive from Albuquerque to Santa Fe, you climb this escarpment on Interstate Highway 25. These faults and escarpment mark the mouth of White Rock Canyon, where the Rio Grande flows out into the Santo Domingo Basin and opens into the main part of Cochiti Reservoir. There is no evidence for movement along these faults during the Quaternary. Several basaltic vents are located along these faults, but none have been mapped in detail. Scattered patches of distal lower member (Otowi) Bandelier Tuff ignimbrite are interbeddedwith basaltic lavas and tuffs of the Cerros del Rio.

As the Rio Grande turns to the ESE (mouth of the Rio Chiquito), the cliffs on the north bank consist of a 35-m-thick section of hyaloclastite. The deposit consists of orangish-yellow tuffs and highly vesicular bombs. Large bombs increase in number relative to matrix until there is no matrix and the deposit consists of agglutinated bombs that have flowed as rootless lava flows. The largest bombs are 1.3 m x 0.3 m; all are very vesicular, with vesicles up to 1 cm in diameter. Smaller clasts are bomb fragments. The yellow-orange matrix consists of coarse ash, lapilli, and small bombs; bedding plane sags are common. The tuffs are cut by a basaltic dike with an attitude of N10E; this grades upward into a scoria deposit.

Turning toward the south again, the river cuts through another maar deposit consisting of well-bedded pale brown coarse to medium ash and lapilli. Beds are 2-10 cm thick, with ripples, dunes, and bedding plane sags. The well-bedded deposits consist of mostly lithic clasts, including fluvial cobbles and pebbles. Overlying the well-bedded tuffs is 15 m of massive to poorly bedded volcanic breccia, interbedded with yellow tuff.

Boat Ramp, Cochiti Reservoir
(27.5 km south of Buckman Crossing)

From here, it is possible to exit the canyon and river via Cochiti Pueblo, La Bajada escarpment and Interstate Highway 25.

References

Aubele, J., 1978, Geology of the Cerros del Rio volcanic field, *in* J. Hawley (ed.), Guidebook to the Rio Grande rift in New Mexico and Colorado: New Mexico Bureau of Mines and Mineral Resources, Circular 163, pp. 198-201.

Baldridge, W. S., 1979, Petrology and petrogenesis of Plio-Pleistocene rocks from the central Rio Grande rift, New Mexico, and their relation to rift structure; *in* R. Riecker (ed.), Rio Grande rift—tectonics and magmatism: American Geophysics Union, Washington DC, pp. 323-353.

Baldridge, W. S., 1984, Rio Grande rift—problems and perspectives: New Mexico Geological Society, Guidebook 35, pp. 1-12.

Baldridge, W. S., Perry, F. V., Vaniman, D. T, Nealey, L. D., Leavy, B. D., Laughlin, A. W., Kyle, P., Bartov, Y., Steintz, G., Gladney, E. S., 1989, IAVCEI Field Guide, Excursion 8A—Miocene to Quaternary volcanism and extensional tectonics, central Rio Grande rift and southeastern Colorado Plateau, New Mexico and Arizona; *in* Chapin, C. E. and Zidek, J. (eds.), Field excursions to volcanic terranes in the western United States, Volume 1—Southern Rocky Mountain region: New Mexico Bureau of Mines and Mineral Resources, Memior 46, pp. 187-228.

Borton, R. L., 1968, General geology and hydrology of north-central Santa Fe County, New Mexico: *abs in* Guidebook of the San Juan-San Miguel-La Plata region: New Mexico Geological Society, Guidebook 19, pp. 210-211.

Cavazza, W., 1986, Miocene sediment dispersal in the central Espanola Basin, Rio Grande rift, New Mexico, U.S.A.: Sedimentary Geology, v. 51, pp. 119-135.

Chapin, C. E., 1979, Evolution of the Rio Grande rift—a summary; *in* R. Riecker (ed.), Rio Grande rift—tectonics and magmatism: American Geophysics Union, Washington DC, pp. 1-5.

Coons, L. M., and Kelly, T. E., 1984, Regional hydrogeology and the effect of structural control on the flow of ground water in the Rio Grande trough, northern New Mexico: New Mexico Geological Society, Guidebook 35, pp. 241-244.

Dethier, D., (in press), Geology of the White Rock quadrangle, Los Alamos and Santa Fe counties, New Mexico: New Mexico Bureau of Mines and Mineral Resources, Geologic Map 73, scale 1:24,000.

Doell, R. R., Dalrymple, G. B., Smith, R. L., and Bailey, R. A., 1968, Paleomagnetism, potassium-argon ages, and geology of rhyolites and associated rocks of the Valles caldera, New Mexico *in* Coats, R. R., Hay, R. L., and Anderson, C. A. (eds.), Studies in volcanology—a memoir in honor of Howell Williams: Geological Society of America, Memoir 116, pp. 211-248.

Dransfield, B. J., and Gardner, J. N., 1985, Subsurface geology of the Pajarito Plateau, Espanola Basin, New Mexico: Los Alamos National Laboratory Report, LA10455-MS, 15 pp.

Dunker, K. E., 1988, Trace-element geochemistry and stable isotope constraints on the petrogenesis of Cerros del Rio lavas, Jemez Mountains, New Mexico: Unpublished MS thesis, University of Texas (Arlington), 158 pp.

Dungan, M. A., Muehlberger, W. R., Leininger, L., Peterson, C., McMillan, N. J., Gunn, G., Lindstrom, M., and Haskin, L., 1984, Volcanic and sedimentary stratigraphy of the Rio Grande gorge and the late Cenozoic geologic evolution of the southern San Luis Valley: New Mexico Geological Society, Guidebook 35, pp. 157-170.

Fisher, R. V., Heiken, G., Purtymun, W., and Wohletz, K., 1984, Cerros del Rio, New Mexico maars: American Geophysical Union, EOS, Transactions, v. 65, no. 45, p. 1145.

Fisher, R. V., Heiken, G., and Wohletz, K. H, 1986, Base Surges: International Association of Volcanology and Chemistry of the Earth's Interior, International Congress (Abst), American Geophysical Union, p. 101.

Fisher, R. V., and Schmincke, H. U., 1984, Pyroclastic Rocks: Springer-Verlag, New York, 472 pp.

Galusha, T, and Blick, J. C., 1971, Stratigraphy of the Santa Fe Group, New Mexico: American Museum of Natural History, Bulletin 144,127 pp.

Gardner, J. N., Goff, F., Garcia, S., and Hagan, R. C., 1986, Strati-graphic relations and lithologic variations in the Jemez volcanic field, New Mexico: Journal of Geophysical Research, v. 91, no. B2, pp. 1763-1778.

Griggs, R. L., 1964, Geology and ground-water resources of the Los Alamos area, New Mexico: U.S. Geological Survey, Water-supply Paper 1753,104 pp.

Hawley, J. W., 1978, Correlation chart 2—Middle to upper Cenozoic stratigraphic units in selected areas of the Rio Grande rift

in New Mexico *in* J. Hawley (ed.), Guidebook to the Rio Grande rift in New Mexico and Colorado: New Mexico Bureau of Mines and Mineral Resources, Circular 163, pp. 239-241.

Hearne,G. A., 1980, Mathematical model of the Tesuque aquifer system underlying Pojoaque River basin and vicinity, New Mexico: U.S. Geological Survey, Open-file Report 80-1023, 181 pp.

Heiken, G. H., 1971, Tuff rings of the Fort Rock-Christmas Lake Valley Basin, south-central Oregon: Journal of Geophysical Research, v. 76, pp. 5615-5626.

Kelley, V.C., 1978, Geology of the Espanola Basin, New Mexico: New Mexico Bureau of Mines and Mineral Resources, Geologic Map 48, scale 1:24,000.

Machette, M. N., 1978, Geologic map of the San Acacia Quadrangle, Socorro County, New Mexico: U.S. Geological Survey, Geologic Quadrangle Map GQ-1415, scale 1:24,000.

Manley, K., 1976, K-Ar age determinations of Pliocene basalts from the Espanola Basin, New Mexico: Isochron /West, no. 16, pp. 29-30.

Manley, K., 1979, Stratigraphy and structure of the Espanola Basin, Rio Grande rift, New Mexico; *in* R. Riecker (ed.), Rio Grande rift—tectonics and magmatism: American Geophysical Union, Washington DC, pp. 71-86.

Self, S., Kircher, D. E., and Wolff, J. A., 1988, The El Cajete Series, Valles caldera, New Mexico: Journal of Geophysical Research, v. 93, no. B6, pp. 6113-6118.

Smith, R. L., Bailey, R. A., and Ross, C. S., 1970, Geologic map of the Jemez Mountains,New Mexico: U.S. Geological Survey, Miscellaneous Geologic Investigation Map 1-571, scale 1:125,000.

Turbeville, B. N., Waresback, D. B., and Self, S., 1989, Lava-dome growth and explosive volcanism in the Jemez Mountains, New Mexico—evidence from the Plio-Pleistocene Puye alluvial fan: Journal of Volcanology and Geothermal Research, v. 36, no. 4, pp. 267-291.

Waresback, D. B., 1986, The Puye Formation, New Mexico—analysis of a continental rift-filling volcanoclastic alluvial fan sequence: Unpublished MS thesis, University of Texas (Arlington), 225 pp.

Wohletz, K. H. and Sheridan, M. F., 1983, Hydrovolcanic explosions—II, evolution of basaltic tuff rings and tuff cones: American Journal of Science, v. 283, pp. 385-413.

Wohletz, K. H. and McQueen, R., 1984, Experimental studies of hydromagmatic volcanism; *in* Explosive volcanism—inception, evolution, and hazards: National Academic Press, Washington, D. C., pp. 158-169.

Selected conversion factors*

TO CONVERT	MULTIPLY BY	TO OBTAIN
Length		
inches, in	2.540	centimeters, cm
feet, ft	3.048×10^{-1}	meters, m
yards, yds	9.144×10^{-1}	m
statute miles, mi	1.609	kilometers, km
fathoms	1.829	m
angstroms, Å	1.0×10^{-8}	cm
Å	1.0×10^{-4}	micrometers, μm
Area		
in^2	6.452	cm^2
ft^2	9.29×10^{-2}	m^2
yds^2	8.361×10^{-1}	m^2
mi^2	2.590	km^2
acres	4.047×10^{3}	m^2
acres	4.047×10^{-1}	hectares, ha
Volume (wet and dry)		
in^3	1.639×10^{1}	cm^3
ft^3	2.832×10^{-2}	m^3
yds^3	7.646×10^{-1}	m^3
fluid ounces	2.957×10^{-2}	liters, l *or* L
quarts	9.463×10^{-1}	l
U.S. gallons, gal	3.785	l
U.S. gal	3.785×10^{-3}	m^3
acre-ft	1.234×10^{3}	m^3
barrels (oil), bbl	1.589×10^{-1}	m^3
Weight, mass		
ounces avoirdupois, avdp	2.8349×10^{1}	grams, gr
troy ounces, oz	3.1103×10^{1}	gr
pounds, lb	4.536×10^{-1}	kilograms, kg
long tons	1.016	metric tons, mt
short tons	9.078×10^{-1}	mt
oz mt^{-1}	3.43×10^{1}	parts per million, ppm
Velocity		
ft sec^{-1} (= ft/sec)	3.048×10^{-1}	m sec^{-1} (= m/sec)
mi hr^{-1}	1.6093	km hr^{-1}
mi hr^{-1}	4.470×10^{-1}	m sec^{-1}

TO CONVERT	MULTIPLY BY	TO OBTAIN
Pressure, stress		
lb in^{-2} (= lb/in^2), psi	7.03×10^{-2}	kg cm^{-2} (= kg/cm^2)
lb in^{-2}	6.804×10^{-2}	atmospheres, atm
lb in^{-2}	6.895×10^{3}	newtons (N)/m^2, N m^{-2}
atm	1.0333	kg cm^{-2}
atm	7.6×10^{2}	mm of Hg (at 0° C)
inches of Hg (at 0° C)	3.453×10^{-2}	kg cm^{-2}
bars, b	1.020	kg cm^{-2}
b	1.0×10^{6}	dynes cm^{-2}
b	9.869×10^{-1}	atm
b	1.0×10^{-1}	megapascals, MPa
Density		
lb in^{-3} (= lb/in^3)	2.768×10^{1}	gr cm^{-3} (= gr/cm^3)
Viscosity		
poises	1.0	gr cm^{-1} sec^{-1} *or* dynes cm^{-2}
Discharge		
U.S. gal min^{-1}, gpm	6.308×10^{-2}	l sec^{-1}
gpm	6.308×10^{-5}	m^3 sec^{-1}
ft^3 sec^{-1}	2.832×10^{-2}	m^3 sec^{-1}
Hydraulic conductivity		
U.S. gal day^{-1} ft^{-2}	4.720×10^{-7}	m sec^{-1}
Permeability		
darcies	9.870×10^{-13}	m^2
Transmissivity		
U.S. gal day^{-1} ft^{-1}	1.438×10^{-7}	m^2 sec^{-1}
U.S. gal min^{-1} ft^{-1}	2.072×10^{-1}	l sec^{-1} m^{-1}
Magnetic field intensity		
gausses	1.0×10^{5}	gammas
Energy, heat		
British thermal units, BTU	2.52×10^{-1}	calories, cal
BTU	1.0758×10^{2}	kilogram-meters, kgm
BTU lb^{-1}	5.56×10^{-1}	cal kg^{-1}
Temperature		
°C + 273	1.0	°K (Kelvin)
°C + 17.78	1.8	°F (Fahrenheit)
°F − 32	5/9	°C (Celsius)

*_Divide by_ the factor number to reverse conversions.
Exponents: for example 4.047×10^{3} (see acres) = 4,047; 9.29×10^{-2} (see ft^2) = 0.0929.

Editor: *Nancy Gilson*

Typeface: Palatino

Presswork: Miehle Single Color Offset
Harris Single Color Offset

Binding: Smythe-sewn with softbound cover

Paper: Cover on 12-pt. Kivar
Text on 70-lb White Matte

Ink: Cover—PMS, 4-color process
Text—Black

Quantity: 1,000